



U.S. DEPARTMENT OF
ENERGY

PNNL-19135

Prepared for the U.S. Department of Energy
under Contract DE-AC05-76RL01830

Mitigation of Hydrogen Gas Generation from the Reaction of Water with Uranium Metal in K Basin Sludge

SI Sinkov
CH Delegard
AJ Schmidt

January 2010



Pacific Northwest
NATIONAL LABORATORY

*Proudly Operated by **Battelle** Since 1965*

DISCLAIMER

This report was prepared as an account of work sponsored by an agency of the United States Government. Neither the United States Government nor any agency thereof, nor Battelle Memorial Institute, nor any of their employees, makes **any warranty, express or implied, or assumes any legal liability or responsibility for the accuracy, completeness, or usefulness of any information, apparatus, product, or process disclosed, or represents that its use would not infringe privately owned rights.** Reference herein to any specific commercial product, process, or service by trade name, trademark, manufacturer, or otherwise does not necessarily constitute or imply its endorsement, recommendation, or favoring by the United States Government or any agency thereof, or Battelle Memorial Institute. The views and opinions of authors expressed herein do not necessarily state or reflect those of the United States Government or any agency thereof.

PACIFIC NORTHWEST NATIONAL LABORATORY
operated by
BATTELLE
for the
UNITED STATES DEPARTMENT OF ENERGY
under Contract DE-AC05-76RL01830

Printed in the United States of America

**Available to DOE and DOE contractors from the
Office of Scientific and Technical Information,
P.O. Box 62, Oak Ridge, TN 37831-0062;
ph: (865) 576-8401
fax: (865) 576-5728
email: reports@adonis.osti.gov**

**Available to the public from the National Technical Information Service,
U.S. Department of Commerce, 5285 Port Royal Rd., Springfield, VA 22161
ph: (800) 553-6847
fax: (703) 605-6900
email: orders@ntis.fedworld.gov
online ordering: <http://www.ntis.gov/ordering.htm>**

Mitigation of Hydrogen Gas Generation from the Reaction of Water with Uranium Metal in K Basin Sludge

SI Sinkov
CH Delegard
AJ Schmidt

January 2010

Prepared for
the U.S. Department of Energy
under Contract DE-AC05-76RL01830

Pacific Northwest National Laboratory
Richland, WA 99352

Summary

Means to decrease the rate of hydrogen gas generation from the chemical reaction of uranium metal with water were identified by surveying the technical literature. The underlying chemistry and potential side reactions were explored by conducting 61 principal experiments. Several methods achieved significant hydrogen gas generation rate mitigation. Gas-generating side reactions from interactions of organics or sludge constituents with mitigating agents were observed. Further testing is recommended to develop deeper knowledge of the underlying chemistry and to advance the technology maturation level.

Uranium metal reacts with water in K Basin sludge to form uranium hydride (UH_3), uranium dioxide or uraninite (UO_2), and diatomic hydrogen (H_2). Mechanistic studies show that hydrogen radicals ($\text{H}\cdot$) and UH_3 serve as intermediates in the reaction of uranium metal with water to produce H_2 and UO_2 . Because H_2 is flammable, its release into the gas phase above K Basin sludge during sludge storage, processing, immobilization, shipment, and disposal is a concern to the safety of those operations. Findings from the technical literature and from experimental investigations with simple chemical systems (including uranium metal in water), in the presence of individual sludge simulants, with complete sludge simulants, and with actual K Basin sludge are presented in this report.

Based on the literature review and intermediate lab test results, sodium nitrate, sodium nitrite, Nochar Acid Bond N960, disodium hydrogen phosphate, and hexavalent uranium [U(VI)] were tested for their effects in decreasing the rate of hydrogen generation from the reaction of uranium metal with water. Nitrate and nitrite each were effective, decreasing hydrogen generation rates in actual sludge by factors of about 100 to 1000 when used at 0.5 molar (M) concentrations. Higher attenuation factors were achieved in tests with aqueous solutions alone. Nochar N960, a water sorbent, decreased hydrogen generation by no more than a factor of three while disodium phosphate increased the corrosion and hydrogen generation rates slightly. U(VI) showed some promise in attenuating hydrogen but only initial testing was completed.

Uranium metal corrosion rates also were measured. Under many conditions showing high hydrogen gas attenuation, uranium metal continued to corrode at rates approaching those observed without additives. This combination of high hydrogen attenuation with relatively unabated uranium metal corrosion is significant as it provides a means to eliminate uranium metal by its corrosion in water without the accompanying hazards otherwise presented by hydrogen generation.

Objectives

The generation of hydrogen gas through oxidation/corrosion of uranium metal by the reaction with water can potentially create flammable gas atmospheres posing hazards in storage, processing, and disposition of the K Basin sludge. Although hydrogen generation rate reduction is desired to decrease these hazards, specific targets for reduction factors vary because of the variability of uranium metal content in the sludge streams. Process parameters and design features also will affect allowable hydrogen generation rates. For direct disposal of sludge to the Waste Isolation Pilot Plant (WIPP), previous evaluations have shown that reduction factors of ~ 100 would be necessary; for other activities, smaller reduction factors may be adequate.

The objectives of these studies were to:

- identify and evaluate potential methods to reduce the rate of hydrogen gas generation and release from aqueous corrosion of uranium metal in K Basin sludge, and
- determine the underlying chemistry and potential side reactions with K Basin sludge matrices to inform judgments to be made on the technology maturation level.

This report presents results of survey of the technical literature to identify potential methods to decrease the rate of hydrogen gas generation from aqueous corrosion of uranium metal in K Basin sludge. Based on the survey results, tests with simple and more complex chemical systems, including actual K Basin sludge, were performed to evaluate the most promising hydrogen generation mitigation strategies. Results of this laboratory testing are presented in this report. The ultimate goal of these investigations is to provide potential treatment alternatives to mitigate safety issues arising from hydrogen generation from K Basin sludge in its disposition path through storage, on-site transportation, processing, off-site shipment, and disposal.

Survey Results

Four means to decrease the H₂ evolution rate were identified: 1) decreased temperature, 2) reactant isolation (separation of the uranium metal from the water), 3) corrosion inhibition, and 4) hydrogen scavenging.

1. *Decreased Temperature:* Although decreased temperature is applicable to controlled systems, it is not applicable to shipment to WIPP, where transported packages must demonstrate suitably low H₂ generation rates at 60°C.
2. *Reactant Isolation:* Grouting to improve reactant isolation has been shown to decrease H₂ generation rates for simulated sludge by up to a factor of 3. Higher impacts are likely not obtained because appreciable water vapor pressures, which allow reaction of uranium metal with condensing water films, still exist in the grouted products. More effective desiccants such as magnesium and calcium oxide likely would provide better suppression of the uranium metal - water reaction rate. Nochar N960, a commercial water absorbent for nuclear waste applications, also has been proposed as a potential desiccant based on its high capacity to sorb aqueous solutions. However, its desiccant properties have not been described.
3. *Corrosion Inhibition:* In more than 60 years of investigation, the most effective of the inorganic uranium metal corrosion inhibitors in water were found to be nitrite and phosphate salts. The most effective organic corrosion inhibitor decreased corrosion rates by a factor of about 7 but required frequent replenishment. Although dissolved oxygen is known to inhibit the uranium metal corrosion rate, the practical difficulty of maintaining active aeration in dense heterogeneous sludge likely precludes its use under storage and transportation conditions.
4. *Hydrogen Scavenging:* Scavengers of the “nascent” hydrogen that appears in the corrosion of active metals, such as uranium, in water include nitrate, nitrite, permanganate, and chromate. Of these, nitrate and nitrite are the most promising for uranium metal corrosion in terms of compatibility with the K Basin system, Hanford experience, and applicability.

Results from Testing of Hydrogen Generation Mitigation Strategies

Based on the survey findings, seven series of laboratory tests were conducted to determine the effects of nitrate (as NaNO_3), nitrite (as NaNO_2), phosphate (as Na_2HPO_4), Nochar N960, and dissolved U(VI), on the uranium metal corrosion rate and on the generation of H_2 from the reaction of uranium metal with water. The testing approach, hydrogen mitigation by nitrate and nitrite, uranium metal corrosion rate inhibition by nitrate and nitrite, side reactions, comparison of the application of nitrate and nitrite, results from other mitigation approaches, and consideration for future testing and application of this technology are considered in the following sections.

Testing Approach

The tests used nearly spherical high-purity uranium metal beads in water, in aqueous solutions, in the presence of UO_2 , in the presence of simulated K Basin sludge, and in actual K Basin sludge under controlled temperature conditions. The reacting mixture headspace was air for most tests and neon (Ne; an inert gas) for tests with actual sludge. Gas volume changes were monitored in all tests. The final extents of reaction were determined by uranium metal weight loss, analyses of nitrate and nitrite reduction product concentrations, and, for the third series of testing onwards, analyses of the product gas compositions. Nitrate and nitrite reduction products largely were ammonia and accompanying hydroxide. Nitrite was found as a product of nitrate reduction. Gaseous nitric oxide (NO), nitrous oxide (N_2O), and nitrogen (N_2), also were found in certain tests.

Each test series included a control test containing uranium beads plus water to serve as a reference for unmitigated hydrogen generation. The effects of nitrate, nitrite, Nochar, phosphate, and U(VI) on uranium corrosion and gas generation then could be directly compared with the control tests.

Hydrogen Mitigation Results for Nitrate and Nitrite

The effects of added NaNO_3 and NaNO_2 on the H_2 generation rates of uranium metal in aqueous solution at 60°C are shown in Figure S.1 in comparison with the rates observed in the absence of salt in the parallel control tests. The effects are expressed as the H_2 attenuation factor, which is the ratio of the H_2 generation rate in the water/uranium control tests divided by the H_2 generation rate of the test being evaluated. It is seen that the attenuation factors increase with increasing salt concentration. For a given salt concentration, the H_2 attenuation factor in aqueous solution for nitrite is at least a factor of 10 greater than that of nitrate. Some H_2 attenuation factors for nitrite were even greater than a factor of 10, particularly if organic material was present. However, the differences in H_2 attenuation factor between nitrite and nitrate diminish in the presence of UO_2 and in the presence of simulated and genuine sludge. At 0.5 M nitrate or nitrite salt, the attenuation factors for simulated and genuine sludge ranged from about 100 to 1000.

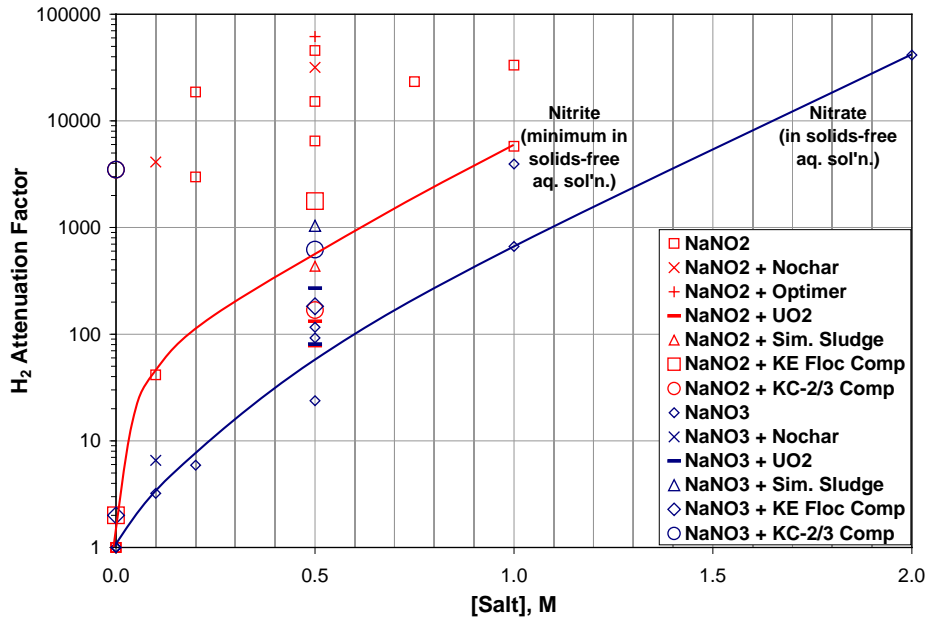


Figure S.1. Effect of NaNO_3 and NaNO_2 Concentrations on Inhibiting Hydrogen Generation from Uranium Metal Corrosion in Aqueous Solution and Simulated and Genuine Sludge at 60°C

The testing showed that Nochar alone, applied at vendor-recommended Nochar:water weight dosages ranging from 0.2:1 to 1:1, decreased H_2 generation rates by factors ranging from 1.3 to 2.6 compared with the control test. Thus, in terms of decreasing the H_2 generation rate from reaction of uranium metal with water, Nochar's performance is roughly equivalent to grouting. Although Nochar had relatively small impact on decreasing H_2 generation rates, Nochar's stickiness and affinity for finely divided uranium oxide particles may make it attractive as an agglomerating agent to reduce the respirable particulate fraction in sludge handling. Uranium oxide particles generated by uranium metal corrosion are well under the 10 micron (μm) diameter that is considered to be respirable by nuclear safety analysis.

Tests of Nochar with 0.1 M NaNO_3 and 0.1 M NaNO_2 gave better attenuation factors than the parallel tests of Nochar alone or salt solution alone. In the tests of mixed Nochar-salt, reaction of the salt with Nochar occurred and produced oxides of nitrogen (NO_x). The effects were more severe for the Nochar test with 0.1 M NaNO_2 , which also produced significant N_2 and N_2O . The gas formation may prohibit the joint use of Nochar with nitrate or nitrite for WIPP purposes, as the mixtures appear to be chemically reactive.

Uranium Corrosion Rate Inhibition by Nitrate and Nitrite

In addition to investigating the effects of salt addition on hydrogen attenuation, the impacts on uranium metal corrosion rate also were determined. The H_2 attenuation factors observed for the control tests and the tests with added nitrate or nitrite as a function of the corrosion rate attenuation factors are plotted in Figure S.2. It is seen that the attenuation of uranium metal corrosion rate was greater for nitrite than for nitrate. For all tests, part of the H_2 attenuation could be attributed to lowered uranium corrosion but the H_2 attenuation factor was always greater than the corresponding corrosion rate attenuation factor. Three tests shown in Figure S.2 had corrosion rate attenuation factors that were greater than 10. Based on

the observed low corrosion rates, it is likely that these tests did not overcome the induction times to reach the anoxic conditions needed to initiate rapid corrosion rates.

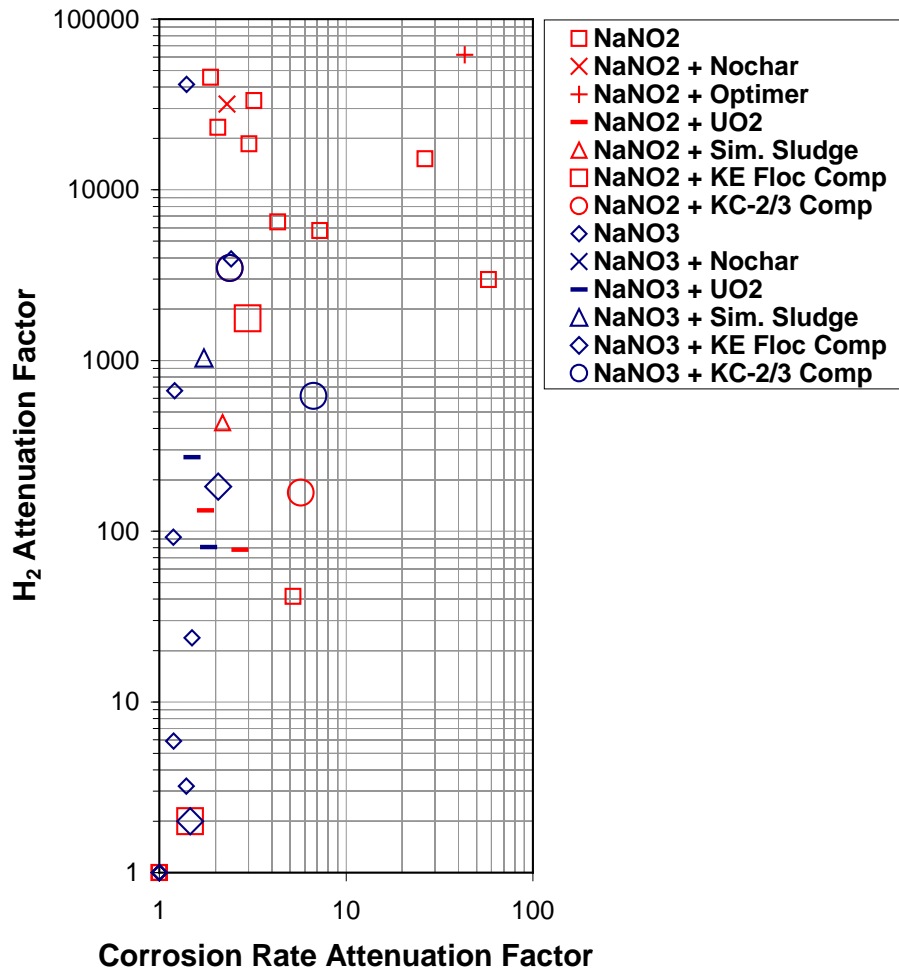


Figure S.2. Hydrogen Attenuation Factors as Functions of Corrosion Rate Attenuation Factors for the Control Tests and Tests with Added Nitrate or Nitrite

Side Reactions of Added Salts with Sludge Components

Tests showed that nitrite reacts with UO₂ while no reaction was observed between nitrate and UO₂. The parasitic reaction of nitrite with UO₂ indicates that additional nitrite may be needed to attain low H₂ generation rates from K Basin sludge. The impact of sorption of nitrate or nitrite onto organic ion exchange resin, known to be present in K Basin sludge, also must be accounted if the addition of these salts to control H₂ generation technique is to be successfully applied.

Tests of full K Basin sludge simulants and actual sludge show that limited quantities (no more than four-times the accompanying sludge volume) of NO are produced when nitrite is used to control H₂ generation. The NO, in turn, reacts with atmospheric oxygen (O₂) and water to produce nitric acid (HNO₃) and can disproportionate in water to produce N₂O and, likely, more nitrite. The production of NO was not observed in parallel tests of simulated or actual sludge in the presence of nitrate.

Comparison of Benefits of Nitrate with Nitrite

The relative benefits of application of nitrate and nitrite to attenuate hydrogen from uranium metal corrosion in anoxic water are shown in Table S.1. Although nitrite provides a greater H₂ attenuation factor than nitrate for a given salt concentration in aqueous solution, the advantage diminishes in genuine sludge. Nitrate generally has less effect on decreasing the uranium metal corrosion rate but the difference in effect between nitrate and nitrite is small in genuine sludge. Disposal pathways for nitrate or nitrite are equivalent. Nitrate offers advantages over nitrite in process behavior (predictability, side reactions), stoichiometric capacity, and safety in handling. Overall, nitrate appears to be a better choice for process application.

Table S.1. Comparison of Nitrate and Nitrite Qualities in Application to Attenuate Hydrogen from Uranium Metal Corrosion

Property	Advantage		Discussion
	Nitrate	Nitrite	
Attenuate H₂			
In water only		✓	~10× higher attenuation coefficients for nitrite than nitrate at equal salt concentrations
With UO ₂	✓		Slightly higher attenuation coefficient for nitrate
In simulated sludge	✓		~2× higher attenuation coefficient for nitrate
In genuine sludge	✓		~4× higher for nitrate in KE canister composite sludge (59 wt% U, dry basis)
		✓	~10× higher for nitrite in KE floor/pit composite sludge (10.3 wt% U, dry basis)
Inhibit U corrosion rate			
In water only	✓		Corrosion rate inhibition factors ~1.1 to 2.4 for nitrate; corrosion rate inhibition factors ~2 to 60 for nitrite
With UO ₂	✓		~20% higher corrosion rate for nitrate than for nitrite
In simulated sludge	✓		~20% higher corrosion rate for nitrate than for nitrite
In genuine sludge	✓		~30% higher corrosion rate for nitrate in KE floor/pit comp. sludge
	≡	≡	Approx. equal corrosion rates in KE canister composite sludge
Stoichiometry/capacity	✓		Nitrate provides 8 equivalents/mole; nitrite provides 6 eq./mole
Predictability of efficacy	✓		Nitrite efficacy in H ₂ attenuation is generally improved by organics but can give significant unwanted corrosion rate inhibition
Side reactions	✓		Nitrite participates in unwanted side reactions (e.g., producing NO in sludge; UO ₂ oxidation) which also increases its consumption
Solubility	≡	≡	Both salts dissolve to >7 M saturated solution at room temperature
Hazard	✓		Both salts are oxidants; nitrite has higher toxicity
Disposal	≡	≡	Both salts are major Hanford underground tank waste components and both may be disposed as low-level waste (LLW)

Results of Other Hydrogen Gas Attenuation Testing

A single test of the effect of phosphate (as 0.07 M Na₂HPO₄) as an inhibitor for uranium metal corrosion in water (and diminish associated hydrogen generation) was performed. The added phosphate increased both uranium corrosion and H₂ generation compared with the control test with water alone. No other tests with phosphate were performed.

As shown in Figure S.1, KC-2/3 Comp sludge (a KE Basin canister sludge) in the absence of any added salt gave an H₂ attenuation factor of 3500. Analyses of the supernatant solution showed the pH to be ~5.5 and the solution to contain 6×10⁻⁴ M U(VI). At this relatively low pH, the U(VI) was present due to dissolution from the abundant metaschoepite (UO₃·2H₂O) present in the sludge. Based on these observations and studies in the technical literature, it appeared that the dissolved U(VI) was an effective hydrogen radical scavenger. The effects of dissolved U(VI) on inhibiting H₂ generation from corroding uranium metal thus were investigated in the seventh test series. In these tests, uranium metal beads were corroded in the presence of metaschoepite that had been adjusted to pH values of ~6.9, 5.1, and 4.3. The U(VI) concentration in these solutions increased with decreasing pH. As expected, the H₂ attenuation factors in these tests increased with decreasing pH and associated increasing U(VI) concentration.

Considerations for Future Testing

Based on the promising findings for hydrogen attenuation by nitrate and nitrite salt and by U(VI), further testing is suggested. Due to nitrate's predictable and adequate H₂ attenuation performance, its lack of extraneous gas formation compared with nitrite (to form NO), and its lack of parasitic loss by oxidation of UO₂ (which was shown by nitrite), further tests into the effects of nitrate concentration on H₂ attenuation should be performed with genuine and simulated sludge. Long-term tests also are required to investigate potential changes in sludge mechanical strength (shear strength, agglomeration) caused by bridging of the sludge particles through precipitation of sodium uranate phases (e.g., Na-compreignacite, clarkeite) formed by the reaction of metaschoepite with sodium ion. Increased sludge strength during storage could complicate sludge retrieval for further processing. The impact of sorption of nitrate onto organic ion exchange resin also must be tested if nitrate is to be added to control H₂ generation.

Tests to study further the performance of dissolved U(VI) as a hydrogen radical scavenger should be performed. As in the proposed tests for nitrate, similar long-term storage tests with dissolved U(VI) should be undertaken to examine the mechanical and chemical property effects. Means to add dissolved U(VI) to sludge streams containing little U(VI) solid phase (e.g., acidification by nitric acid) also should be investigated.

Testing thus far has occurred at ~60°C and 90°C for nitrate and nitrite and only at ~90°C for U(VI). The efficacies of candidate reagents for process use should be tested at the lower temperatures and other conditions prototypic for application (e.g., stainless steel containers, exclusion of light) in trans-site shipment, long-term on-site storage, final treatment and stabilization, and shipment to WIPP. The reagents also should be tested for their potential to diminish radiolytic H₂. If successful in decreasing radiolytic H₂, higher loading in containers during storage and transport could be attained.

The efficacy of the candidate reagents should be tested in proposed final WIPP waste form(s) such as grout or other solidifying matrices. However, if grout is used, U(VI) likely would not be an effective H₂ scavenger because of its low solubility in pH ~11 to 12 cement.

The acceptability of adding nitrate salt in waste forms to be disposed to WIPP must be determined. However, large quantities of pH-neutralized nitric acid materials (effectively sodium nitrate salt) have already been consigned to WIPP from Rocky Flats and the Hanford Site. Depending on the deployment approach, addition of nitrate to sludge could create a nitrate waste solution stream. Therefore, process management of excess nitrate solution and the impact of lower pH caused by sodium ion's reaction with metaschoepite or by intentional pH ~4-5 sludge acidification if U(VI) is used also must be evaluated.

All future testing should be tailored to the target waste stream [e.g., Knock-Out Pot, settler tank, and container sludge; orphan materials in sludge processing; and decommissioning and decontamination rubble] and the particular point of operational insertion (e.g., shipping, storage, or treatment).

Acronyms

ALE	Fitzner-Eberhardt Arid Lands Ecology Reserve
BNFL	British Nuclear Fuels Limited
KE NLOP	K East North Loadout Pit
KW	K (Basin) West
MS	mass spectrometry
OIER	organic ion exchange resin
PNNL	Pacific Northwest National Laboratory
ppm	parts per million
STP	Sludge Treatment Project
TEA	triethanolamine
TI	Test Instruction
UV	ultraviolet
WIPP	Waste Isolation Pilot Plant
XRD	X-ray diffractometry

Chemical Formulas

Al	aluminum	Mg(OH) ₂	magnesium hydroxide
Al(OH) ₃	gibbsite	MgNH ₄ PO ₄ ·6H ₂ O	magnesium ammonium phosphate hexahydrate
Ar	argon		
CaAl ₂ Si ₂ O ₈	anorthite	MO ₄ ²⁻	molybdate
CaO	calcium oxide	N ₂	nitrogen
Ca(OH) ₂	calcium hydroxide	NaAl(OH) ₄	sodium aluminate
CH ₄	methane	Na ₂ Al ₂ Si ₁₀ O ₂₄	mordenite; Zeolon 900
CH ₃ (CH ₂) ₇ CH=CH(CH ₂) ₇ COOH	oleic acid	NaAsO ₂	sodium arsenite
(CH ₃ (CH ₂) ₃ CH(CH ₂ CH ₃)CH ₂ O) ₂ POO ⁻	di-2-ethylhexyl phosphate	NaCl	sodium chloride
		Na ₂ CO ₃	sodium carbonate
C ₂ H ₂	acetylene	Na ₂ Cr ₂ O ₇	sodium dichromate
C ₂ H ₄	ethene	Na ₂ CrO ₄	sodium chromate
C ₂ H ₆	ethane	Na ₂ HPO ₄	disodium hydrogen phosphate
C ₂ H _x	C2 hydrocarbons	NaNO ₂	sodium nitrite
C ₁₆ H ₃₄ O ₄ P ⁻	di-2-ethylhexyl phosphate	NaNO ₃	sodium nitrate
		NaOH	sodium hydroxide
C ₁₈ H ₃₄ O ₂	oleic acid	Na(UO ₂)O(OH)	clarkeite
CO ₂	carbon dioxide	Na ₂ SO ₄	sodium sulfate
CrO ₄ ²⁻	chromate	Na ₂ (UO ₂) ₆ O ₄ (OH) ₆ ·7H ₂ O	sodium compregnacite
Cu ²⁺	copper ion	Ne	neon
Cu(NO ₃) ₂	copper nitrate	NH ₃	ammonia
e _{aq} ⁻	solvated electron	N ₂ H ₄	hydrazine
Fe ²⁺	ferrous	NH ₄ Cl	ammonium chloride
Fe _{0.5185} Al _{0.4185} Ca _{0.466} Na _{0.534} Si ₂ O ₆	aegerine	NH ₄ F	ammonium fluoride
Fe(CN) ₆ ³⁻	ferricyanide	NH ₄ NO ₃	ammonium nitrite
Fe(CN) ₆ ⁴⁻	ferrocyanide	NH ₂ OH	hydroxylamine
Fe(OH) ₃	ferric hydroxide	(NH ₄) ₂ ZrF ₆	ammonium hexafluorozirconate
FeOOH	goethite or lepidocrocite		
Fe ₂ O ₃	hematite	NO	nitric oxide
Fe ₃ O ₄	magnetite	NO ₂ ⁻	nitrite
Fe ₅ O ₇ OH·4H ₂ O	ferrihydrite	NO ₃ ⁻	nitrate
H ⁻	hydrogen radical	N ₂ O	nitrous oxide
H ⁺	hydrogen ion	O ₂	oxygen
H ₂	hydrogen	·OH	hydroxyl radical
HCl	hydrochloric acid	·ONNO ⁻	hyponitrite
HF	hydrogen fluoride	(PO ₃) _x ^{x-}	polyphosphate
H ₂ O	water	PO ₄ ³⁻	phosphate
H ₂ O ⁻	hydrated electron	P ₂ O ₇ ⁴⁻	pyrophosphate
H ₂ O ₂	hydrogen peroxide	SiO ₂	quartz
(HOCH ₂ CH ₂) ₃ N	triethanolamine	SO ₄ ²⁻	sulfate
HONNO ⁻	hyponitrite	U	uranium
HONNOH	hyponitrous acid	UC	uranium carbide
HNO ₃	nitric acid	UH ₃	uranium hydride
HPO ₄ ²⁻	hydrogen phosphate	UO ₂	U(IV) oxide; uranium dioxide;
H ₂ PO ₄ ⁻	dihydrogen phosphate		uraninite
H ₃ PO ₄	phosphoric acid	U ₃ O ₈	uranium octaoxide
KAlSi ₃ O ₈	microcline	U ₄ O ₉ , U ₃ O ₇	uraninite
KFe ₃ (Al _{0.24} Fe _{0.76} Si ₃)O ₁₀ (OH) ₂	mica	UO ₂ Cl ₂	uranyl chloride
KNO ₂	potassium nitrite	UO ₃ ·2H ₂ O	U(VI) oxide hydrate;
Kr	krypton		metaschoepite
Mg _{0.5} Ca _{0.5} CO ₃	dolomite	WO ₄ ²⁻	tungstate
Mg(ClO ₄) ₂	magnesium perchlorate	Xe	xenon
Mg(ClO ₄) ₂ ·3H ₂ O	magnesium perchlorate hydrate	Zn	zinc metal
		Zr	zirconium
MgO	magnesium oxide	ZrF ₃ ⁺	fluorozirconate

Acknowledgments

The authors thank Dan Herting of Washington River Protection Solutions for his chemically insightful suggestion to test nitrate as an agent to diminish hydrogen generation from the reaction of uranium metal with water. The authors also thank Dennis Campbell, Senior Vice President of Nochar, Inc., for providing the Nochar N960 sample and recommending its application dosage. Stan Bos and Pam Berry provided the gas analyses while the X-ray diffraction analyses were provided by Doinita Neiner, all of the Pacific Northwest National Laboratory. The report has been edited by Laura Thierolf and technically reviewed by Susan Jones of the Pacific Northwest National Laboratory.

Contents

Summary	iii
Acronyms	xi
1.0 Uranium Metal Reaction with Water and Means to Decrease H ₂ Generation Rate	1.1
1.1 Overview of Uranium Metal Reaction with Water	1.2
1.2 Isolation of Uranium Metal from Water.....	1.2
1.2.1 Grouting	1.2
1.2.2 Desiccants.....	1.4
1.3 Uranium Metal Corrosion Inhibitors.....	1.5
1.3.1 Phosphates and Uranium Metal Machining Coolant Fluids.....	1.6
1.3.2 Sulfate	1.8
1.3.3 Nitrite	1.8
1.3.4 Dissolved Oxygen	1.9
1.4 Hydrogen Scavengers.....	1.10
1.4.1 Nitrate and Nitrite.....	1.10
1.4.2 Metaschoepite and Ferric Hydroxide	1.16
1.5 Summary of Findings from Review of the Technical Literature	1.17
2.0 Experimental Materials and Methods.....	2.1
2.1 Chemicals and Materials	2.1
2.2 Experimental Apparatus and Experimental Procedures	2.5
2.3 Experimental Matrices	2.10
3.0 Results	3.1
3.1 Effects of Additives on Uranium Metal Corrosion Rates	3.1
3.1.1 Effect of Nochar on Corrosion Rate.....	3.5
3.1.2 Effects of Nitrate, Nitrite, and Phosphate on Corrosion Rate	3.5
3.1.3 Effects of Nitrate and Nitrite with Other Additives and with Sludge Solids on Corrosion Rate.....	3.6
3.2 Effects of Additives on Hydrogen Generation Rate and Gas Composition	3.7
3.2.1 Hydrogen Gas Attenuation.....	3.8
3.2.2 Gas Analysis Results for Series 3.....	3.11
3.2.3 Gas Analysis Results for Series 4.....	3.13
3.2.4 Gas Analysis Results for Series 5.....	3.15
3.2.5 Gas Analysis Results for Series 6.....	3.21
3.2.6 Gas Analysis Results for Series 7.....	3.25
3.3 Nitrate and Nitrite Reduction Products and Material Balance	3.27
3.4 Nitrate and Nitrite Reaction with UO ₂	3.34
3.5 Nochar Properties.....	3.34
3.6 Additional Testing.....	3.35

4.0	Conclusions	4.1
5.0	References	5.1
	Appendix A XRD Analyses of Hanford (ALE) Soil and Ferrihydrite.....	A.1
	Appendix B Initial and Final Gas Volumes and Gas Compositions for Test Series 3, 4, 5, 6, and 7...	B.1

Figures

S.1. Effect of NaNO_3 and NaNO_2 Concentrations on Inhibiting Hydrogen Generation from Uranium Metal Corrosion in Aqueous Solution and Simulated and Genuine Sludge at 60°C	vi
S.2. Hydrogen Attenuation Factors as Functions of Corrosion Rate Attenuation Factors for the Control Tests and Tests with Added Nitrate or Nitrite	vii
1.1. Uranium Metal Corrosion Mechanism in Anoxic Water with Time in the Vertical Axis (liquid or H_2O vapor; rate in H_2O vapor proportional to $[\text{relative humidity}]^{1/2}$)	1.3
1.2. Dehydrothio Orthotoluidine	1.6
1.3. Comparison of Uranium Metal Oxidation Rates in Anoxic Water with Rates in Aerated Water	1.10
1.4. Predicted and Observed Products from Reaction of Aluminum in Alkaline Nitrate Solution (Gresky 1952)	1.12
1.5. Hydrogen Yield from Reaction of Aluminum in NaOH as a Function of NaNO_3 Concentration (Gresky 1952)	1.13
1.6. Relative Radiolytic H_2 Yield Compared with That in Water as a Function of Effective Solute Concentration, $S \times f$ (Meisel et al. 1991)	1.15
2.1. Diagram of Gas Generation Apparatus Used in Testing (A. apparatus used in Series 1; B. apparatus used in all succeeding test series [wider 20-mL vials were used in Series 6 and 7]) ...	2.7
2.2. Apparatus in Heating Blocks Used for Series 1 (left) and Series 2 through 7 (second test series is pictured)	2.7
2.3. UV Absorption Spectra of NaNO_3 and NaNO_2 in 0.1 M NaOH	2.9
3.1. Effect of Nochar:Water Weight Ratio on Inhibiting Uranium Metal Corrosion at 60°C	3.5
3.2. Effect of NaNO_3 and NaNO_2 Concentrations on Inhibiting Uranium Metal Corrosion in Aqueous Salt Solutions at about 60°C and 90°C	3.6
3.3. Effect of NaNO_3 and NaNO_2 Concentrations on Inhibiting Uranium Metal Corrosion in Aqueous Salt Solutions and in the Presence of Additives and Sludge Components at 60°C	3.7
3.4. Hydrogen Attenuation Factors as Functions of Sodium Nitrate or Nitrite Concentrations in Test Series 3, 4, 5, and 6	3.9
3.5. Hydrogen Attenuation Factors as Functions of Corrosion Rate Attenuation Factors for the Control Tests and Tests with Added Nitrate or Nitrite	3.11
3.6. Moles of Gas Produced or Reacted and Moles of Uranium Metal Reacted in Series 3	3.12
3.7. Bottom Views of Vials from Tests with Salt and Nochar in Series 3 Left – Test 10 (0.1 M NaNO_3); right – Test 12 (0.1 M NaNO_2)	3.13
3.8. Moles of Gas Produced or Reacted and Moles of Uranium Metal Reacted in Series 4	3.14
3.9. Moles of Gas Produced or Reacted and Moles of Uranium Metal Reacted in Series 5	3.16
3.10. Appearances of Tests 11, 11S, and 12S Three Days after Mixing ($\sim 2\times$ magnification)	3.17
3.11. Moles of Gas Produced or Reacted and Moles of Uranium Metal Reacted in Series 6	3.22
3.12. Metaschoepite Solubility as a Function of pH	3.26
3.13. Moles of Gas Produced or Reacted and Moles of Uranium Metal Reacted in Series 7	3.27
3.14. <i>cis</i> - and <i>trans</i> -hyponitrite	3.28

3.15. Spectra of 0.1 M NaNO ₃ and Product Solution in Test 7 of Series 3, from Water Condensate on a New Black Rubber Stopper, Water Condensate on a New Silicone Rubber Stopper, and Water Contact with a New Neoprene Rubber Stopper	3.33
3.16. UO ₂ in 0.2 M NaNO ₂ (left two vials; note yellow solids) and in 0.2 M NaNO ₃ (vial on right) after 140 Hours at 84.8°C	3.34
3.17. Immobilized Water Product Expansion at Various Nochar:Water Weight Ratios	3.35

Tables

S.1. Comparison of Nitrate and Nitrite Qualities in Application to Attenuate Hydrogen from Uranium Metal Corrosion	viii
1.1. Reactions of Nitrate and Nitrite with Uranium	1.16
1.2. Gibbs Free Energies of Reaction of Metaschoepite and Ferric Hydroxide with Hydrogen.....	1.17
2.1. Simulated Sludge Composition and Preparation Used in Series 5.....	2.4
2.2. Compositions of K Basin Sludges Used in Testing	2.5
2.3. Gas Permeabilities for Natural, Silicone, and Neoprene Rubber (Speight 2005)	2.8
2.4. Experimental Parameters for the Test Series	2.13
3.1. Uranium Metal Corrosion Rate and Hydrogen Generation Data.....	3.2
3.2. Gas Quantity Calculations	3.8
3.3. Conditions and Results from Series 5 and Supplemental Testing	3.18
3.4. Gas Formation Observations for Mixtures of K Basin Sludge with 0.5 M NaNO ₂	3.19
3.5. U (VI) Concentration and pH in Tests 3, 4, and 5 in Series 7 Experiments	3.25
3.6. Uranium Metal and UO ₂ Oxidation and Water, Oxygen, Nitrate, and Nitrite Reduction Half Reactions.....	3.30
3.7. Chemical Equivalents and Material Balances.....	3.31
4.1. Comparison of Nitrate and Nitrite Qualities in Application to Attenuate Hydrogen from Uranium Metal Corrosion.....	4.3

1.0 Uranium Metal Reaction with Water and Means to Decrease H₂ Generation Rate

Experimental and sludge characterization studies show that reactions to form uranium dioxide (UO₂), uranium hydride (UH₃), and diatomic hydrogen (H₂) occur in uranium metal-bearing K Basin sludge. UO₂ and UH₃, more oxidized uraninites (e.g., U₄O₉, U₃O₇), U₃O₈, and fully oxidized uranium phases (notably metaschoepite, UO₃·2H₂O), have been observed in K Basin sludge by X-ray diffractometry (Makenas et al. 1996, 1997, 1998, 1999). The primary UO₂ particles from U metal aqueous corrosion are exceedingly small, ~6 nanometer (nm), crystallites but also form larger agglomerates (Sinkov et al. 2008). Hydrogen gas has been observed as bubbles rising from sludge in the K Basins, in sludge samples stored in the hot cells for characterization, and in sludge gas generation experiments in closed vessels. Hydrogen gas with krypton (Kr) and xenon (Xe) fission product gases, which are trapped in irradiated uranium metal but released during its corrosion, have been measured in analyses of gases arising from K Basins sludge and irradiated metallic uranium fuel (Makenas et al. 1997, Delegard et al. 2000, Bryan et al. 2004, Schmidt et al. 2003). Uranium metal corrosion rates under anoxic conditions are identical under liquid water or under a condensing water film. The corrosion rate under water vapor decreases with the 0.5 power of the relative humidity (Hilton 1999). The corrosion behavior of uranium metal in water, sludge, and grout was examined in a recent review (Delegard and Schmidt 2008).

Because H₂ is flammable, its release into the gas phase above K Basin sludge during sludge storage, processing, immobilization, shipment, and disposal is a concern to the safety of those operations in the current alternatives and design development activities of the K Basin Sludge Treatment Project (STP). Previous considerations of the disposal of the K Basin sludge to the Waste Isolation Pilot Plant (WIPP) determined that the sludge amount that could be loaded into drums for shipment as remote-handled transuranic waste was limited by the H₂ generation rate (Mellinger et al. 2004). The evaluations showed that the H₂ generation rate is dominated by the H₂ arising from the uranium-water reaction with much lower contributions from radiolytic H₂. The net effect, based on the uranium metal concentrations in sludge streams described in the "Sludge Databook" (Schmidt 2006), is that the anticipated number of drums for certain streams must increase by factors in excess of 100 to accommodate the contained uranium metal, and its associated H₂ generation, compared with the number of drums whose loadings are limited solely by radiolytic H₂ (Mellinger et al. 2004). The suppression, diminution, or complete elimination of the hydrogen gas release therefore is desirable for both operational safety and for compelling economic reasons for the K Basin STP.

The objectives of this report are to provide:

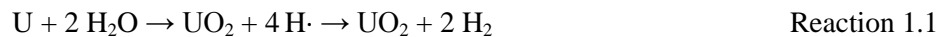
1. Results of a survey of the technical literature to identify methods to decrease the rate of hydrogen gas generation from corrosion of uranium metal in anoxic water.
2. Results from tests performed to evaluate the most promising hydrogen generation mitigation strategies (as identified by the literature study) that can potentially be used by the STP in the development of K Basin sludge management alternatives.

The literature survey identified four means to decrease the hydrogen generation rate from the reaction of uranium metal with water: cooling, isolation of the uranium and water reactants from each other, uranium corrosion inhibitors, and hydrogen scavengers. Although refrigeration at 12° to 15°C has been practiced for the K Basin waters to decrease uranium metal corrosion rates, decreasing the sludge

temperature is not a feasible alternative for on-site sludge management and cannot be considered for shipment of the K Basin sludge to WIPP because the non-refrigerated waste shipment package during transport to the WIPP must have acceptable performance at temperatures as high as 60°C. Information on the effect of temperature on uranium metal corrosion rate in anoxic liquid water has been collected and analyzed (Plys and Schmidt 2006; Delegard and Schmidt 2008). Information on the uranium (U) metal corrosion rate in oxic water is presented in the latter reference and later in the present report.

1.1 Overview of Uranium Metal Reaction with Water

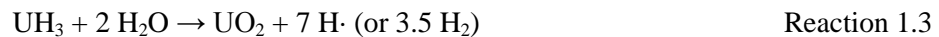
Uranium metal is highly electropositive, reacting with water to produce hydrogen radicals (H·) and UO₂. The reactive hydrogen radicals can combine to form H₂:



The H₂ dissolves in water and, upon water saturation, forms bubbles that are released into the gas phase. The hydrogen radicals or H₂ also can react with uranium metal to form UH₃:



The UH₃ then can react with water to liberate hydrogen radicals or H₂:



The roles of H· and UH₃ as reaction intermediates in the corrosion of U metal in anoxic water to form UO₂ and H₂, the observed associated release of fission product gases (Kr and Xe) in the corrosion of irradiated uranium metal, and the reactant and product material properties are depicted in Figure 1.1.

Results of surveys of the technical literature into the three remaining means to diminish hydrogen generation rate (i.e., by isolation of uranium metal from water, by uranium metal corrosion inhibitors, and by hydrogen scavenging) are presented in Sections 1.2, 1.3, and 1.4, respectively. Guidance on promising avenues of research as determined from review of the technical literature is summarized in Section 1.5.

1.2 Isolation of Uranium Metal from Water

Separation or isolation of the uranium metal from the water would decrease the hydrogen generation rate. Methods that have been tried or may be proposed to effect the uranium-water separation by grouting and by the use of desiccants are considered in sections 1.2.1 and 1.2.2, respectively.

1.2.1 Grouting

Decrease of uranium corrosion by isolating uranium metal from water has been attempted by the use of Portland cement grouts in work at British Nuclear Fuels Limited (BNFL) and the Pacific Northwest National Laboratory (PNNL) and by use of magnesium phosphate grouts at PNNL. Grouting has been used for transuranic waste destined for WIPP disposal because it immobilizes liquid that otherwise would drain from a ruptured container. The overall results of the BNFL and PNNL studies were summarized in Delegard and Schmidt (2008 and references within) and are outlined in the following paragraphs.

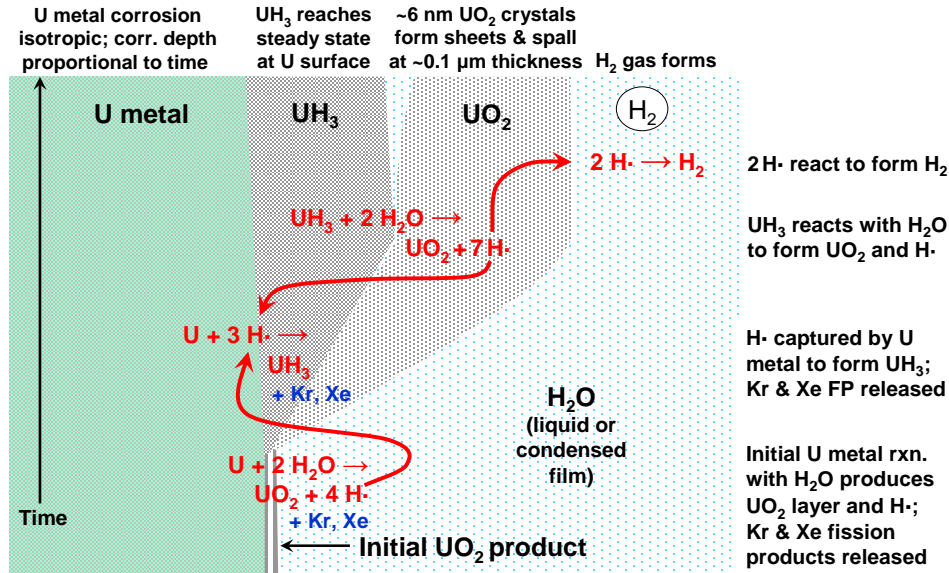


Figure 1.1. Uranium Metal Corrosion Mechanism in Anoxic Water with Time in the Vertical Axis (liquid or H_2O vapor; rate in H_2O vapor proportional to $[\text{relative humidity}]^{1/2}$)

The results of original grout solidification tests of uranium metal performed by BNFL were compiled in a summary report for Fluor Hanford, Inc. (Godfrey et al. 2004). The grouts were composed of varying ratios of blast furnace slag and ordinary Portland cement (Type I, Type II, or Type I/II as known in the United States). The weight ratios of water to cement former (blast furnace slag plus cement) ranged from about 0.4:1 to 0.31:1. These ratios are drier than the $\sim 0.5:1$ ratios used in most Portland cement grouts. Subsequent work performed by BNFL under contract to Fluor Hanford tested drier weight ratios ranging from $\sim 0.21:1$ to $0.31:1$ in water-to-cement former (Butcher et al. 2004). It is known that capillary liquid water is eliminated in completely cured Portland cement products prepared at water:cement ratios at or below about 0.35:1 (Powers 1958) to 0.42:1 (Hansen 1986). The lower water-to-cement ratios were used by BNFL in an effort to decrease the reaction rate of uranium metal with water. Superplasticizers were used to achieve mixability for these low water mixtures. Single tests with cenospheres (spheres from fly ash with gas voids) and barium peroxide also were run to test the effects of these agents that potentially can deliver oxygen to the system and thus impose the slower oxidic reaction of water with uranium metal.¹ Tests were run at $\sim 20^\circ$ to 60°C .

Tests to grout uranium metal in simulated K Basin sludge with four Portland cement and two magnesium phosphate formulations were performed at PNNL (Delegard et al. 2004). Water-to-cement former

¹ A European patent and a U.S. patent application arose from the latter work (Godfrey et al. 2005). The approaches in both the patent and the application are the same as those advanced when the BNFL work was done for Fluor Hanford:

- Use inorganic peroxides to bleed oxygen gas into the grout and avoid the faster corrosion rates under anoxic conditions.
- Use cenospheres to retain oxygenated air in the grout and maintain oxidic conditions (note that cenospheres also are used to produce lightweight cements).
- Use dry grout formulations, with the aid of superplasticizers, to tie up, by cement hydration reactions, the water that causes the uranium metal corrosion.

In addition, air-entraining agents also were proposed in the patent to improve oxygen contact with the uranium metal to retard the more rapid anoxic corrosion.

weight ratios ranged from 0.20 to 0.46 for the four Portland cement preparations and were about 0.13 to 0.14 for the two magnesium phosphate grout compositions. In all but one of the tests (a Portland cement preparation), the amount of water used was limited to that required to make a paste that was just mixable by hand. Superplasticizer was used in one Portland cement test. The magnesium phosphate tests were deficient in the amount of water necessary to produce the $\text{MgNH}_4\text{PO}_4 \cdot 6\text{H}_2\text{O}$ product (i.e., the reaction was water starved), and all but the most dilute Portland cement test were likely water starved. Tests with added bentonite clay were performed for both cement types with the bentonite added to act as a barrier to water diffusion. The uranium metal corrosion rates were measured at $\sim 37^\circ$ to 95°C .

Despite the variety of cement formulations tried and the low amounts of water used to produce the grouts in the BNFL and PNNL testing, hydrogen gas generation rates were decreased no more than a factor of 2 to 3 compared with rates in liquid water alone. Even though liquid water did not exist and thus could not contact uranium metal in most, if not all, of the Portland cement or magnesium phosphate grout tests, the water vapor present in the grouted waste forms evidently was sufficient to condense on the uranium metal and allow significant uranium metal corrosion rates and hydrogen generation.

1.2.2 Desiccants

Uranium metal corrodes in saturated anoxic water vapor at the same rate as in anoxic liquid water. This likely is because at water vapor saturation, a thin film of liquid water collects on the uranium metal surface, essentially creating immersed conditions at the reacting uranium-water interface. However, as noted in a review of uranium metal corrosion (Hilton 2000), the uranium metal corrosion rate in anoxic water vapor decreases in proportion to the square root of the relative humidity. Therefore, use of desiccants to provide low water vapor pressure should decrease uranium metal corrosion rates.

Nochar Acid Bond 660 has been used to absorb aqueous liquids in waste from Rocky Flats destined for WIPP. Acid Bond 660 is a proprietary material and likely is a salt of a low cross-linked polyacrylic acid. Based on application of Acid Bond 660 at Rocky Flats for contact-handled transuranic waste, the Department of Energy Richland Operations Office and the Independent Engineering Review Committee reporting to Fluor Hanford suggested that scoping tests for K Basin sludge be conducted with Nochar Acid Bond N960, the successor to Acid Bond 660. The ability of Nochar to absorb water and keep it from interacting with uranium metal thus might lower hydrogen evolution rates. The ability of Acid Bond N960 to decrease water vapor pressure (i.e., act as a desiccant) was not known.

Conventional desiccants also may be proposed for application to K Basin sludge. Desiccants for use in a spent fuel repository in geologic salt formations were surveyed for use as backfill materials (Simpson 1980). The candidate desiccants were assessed for their abilities and capacities to absorb moisture from air, be chemically compatible with the minerals in geologic salt repositories (e.g., WIPP), to retain absorbed moisture at temperatures above $\sim 200^\circ\text{C}$ (temperatures imposed by the spent fuel radioactive decay heat), to remain solid, and to have low solubility. Based on this survey, magnesium and calcium oxides (MgO and CaO) were recommended individually or in combination as equimolar MgO and CaO from the calcination of dolomite, $\text{Mg}_{0.5}\text{Ca}_{0.5}\text{CO}_3$. With water absorption, MgO and CaO convert to their respective hydroxides, $\text{Mg}(\text{OH})_2$ and $\text{Ca}(\text{OH})_2$. The water vapor pressures in equilibrium with mixtures of $\text{MgO}/\text{Mg}(\text{OH})_2$ and $\text{CaO}/\text{Ca}(\text{OH})_2$ are 0.008 mg H_2O and 0.007 mg H_2O per liter of dried air, respectively at room temperature (Baker 2008), or a relative humidity of $\sim 0.04\%$ for each compound. The affinity of water for the alkaline oxides is strong with $\sim 800^\circ\text{C}$ to 1000°C temperatures needed to

dehydrate the hydroxides. In practice, the water absorption efficacies depend on the natures and preparations of the corresponding oxides. Based on the equilibrium water vapor pressures, the uranium metal corrosion rate in the presence of these desiccants should decrease by a factor of $\sim 0.0004^{1/2}$ (i.e., be about 2% of the rate in liquid water or saturated water vapor at the same temperature).

Bagged anhydrous magnesium perchlorate [$\text{Mg}(\text{ClO}_4)_2$] was applied as a desiccant to retard corrosion for uranium metal fuel plates from the Zero Power Physics Reactor in Idaho (Totemeier et al. 1998). Water vapor pressure in equilibrium with mixtures of $\text{Mg}(\text{ClO}_4)_2$ and its hydrate [$\text{Mg}(\text{ClO}_4)_2 \cdot 3\text{H}_2\text{O}$] are about 0.001 mg H_2O per liter of dried air (Baker 2008) or a relative humidity of about 0.005% to give an expected uranium metal corrosion rate of $\sim 0.7\%$ of that in liquid water or saturated water vapor. In practice, however, the uranium metal corrosion was found to be not inhibited. Although the uranium metal corrosion rate should only be a function of the water vapor pressure, the report authors attributed the lack of effectiveness to the reversibility of the $\text{Mg}(\text{ClO}_4)_2 \leftrightarrow \text{Mg}(\text{ClO}_4)_2 \cdot 3\text{H}_2\text{O}$ hydration reaction, which requires only about 250°C to remove the hydrate water. Use of $\text{Mg}(\text{ClO}_4)_2$, a strong oxidant, as a desiccant for uranium metal, a strong reductant, under dry conditions presents an intrinsic reactivity hazard that likely precludes this particular application for safety reasons.

Silica gel, used as a desiccant in an enclosed DOT 17C shipping container holding 600 kg of iron-clad depleted uranium metal rods that had been stored for $5\frac{1}{2}$ years, was found to be ineffective in stopping uranium corrosion by water vapor. The rods had been shipping with the ends cut so that uranium was exposed to the vapor space. The ineffectiveness of silica gel was shown by corrosion of about 10% of the uranium metal to up to 30 to 40 mm depth in the rod, swelling of the uranium sufficient to split some of the iron cladding, and the presence of 75% nitrogen and 25% hydrogen with depletion of oxygen in the gas space. A low grade explosion sufficient to lift the package lid and a small fire were observed upon opening (Wood et al. 1994). The silica gel was found to contain 3.3% moisture, the pine wood dunnage was dry, and cardboard packing desiccated to the point of brittleness. Water vapor pressure in contact with silica gel should be about 0.03 mg H_2O per liter of dried air (Baker 2008) or a relative humidity of 0.18% to give a uranium corrosion rate about 4% of that in saturated water vapor. In contrast, the silica gel in a parallel package showing no uranium corrosion beyond surface tarnishing had 21% moisture (near the absorptive capacity of silica gel; Baker 2008) and the gas composition was nearly pure air. The difference in behaviors of the two drums was imputed to the differences in the porosity of their gasket materials and to the ineffectiveness of the silica gel desiccant. The gasket examined in the package suffering the high uranium metal corrosion was gas tight while the one having only tarnish of the uranium was porous, maintaining atmospheric oxygen inhibition of the uranium metal corrosion.

1.3 Uranium Metal Corrosion Inhibitors

The production rate of hydrogen gas from the corrosion of uranium metal with water can be decreased if the uranium metal corrosion rate itself is decreased. This corrosion rate decrease might be accomplished by the use of corrosion inhibitors. In anticipation of the planned use of water-cooled uranium metal fueled piles or reactors to produce plutonium, inhibitors of uranium metal corrosion in water were of great experimental interest from the earliest days of the Manhattan Project in the United States and the Tube Alloys program in the United Kingdom.

An early United Kingdom survey explored the effects of 20 different candidate inhibitors on the corrosion of uranium metal in boiling water (Greenwood 1942). The corrosion rate found in boiling

water without inhibitor was 9.0 mm/yr (1.0 $\mu\text{m/hr}$, equivalent to 2.0 $\text{mg/cm}^2\cdot\text{hr}$ and near the STP rate law value of 2.64 $\text{mg/cm}^2\cdot\text{hr}$ in Plys and Schmidt [2006, Appendix G]). Five of the 20 tested inhibitors were inorganic and the other 15 were organic or organic/inorganic mixtures at concentrations ranging from 0.1 to 2 wt%. The inorganic inhibitors tried were 0.5 wt% (0.125 M) sodium hydroxide (NaOH); 0.1 wt% (0.0062 M) sodium chromate (Na_2CrO_4); 0.1 wt% (0.0070 M) disodium phosphate (Na_2HPO_4); 0.1 wt% (0.0077 M) sodium arsenite (NaAsO_2); and a 0.5 wt% silicon ester. Only 4 of the 20 tested inhibitors (all organics) decreased the uranium corrosion rate. According to the report author, this result might be expected because the four successful inhibitors also were known to decrease steel corrosion in acid, which, like uranium, proceeds by hydrogen evolution.

The most effective inhibitor, dehydrothio orthotoluidine (Figure 1.2), decreased the uranium corrosion rate by a factor of ~ 7 , but was found to decompose within 24 hours and thus would require frequent replacement. The other three successful inhibitors decreased the corrosion rate by factors of 2 or less.

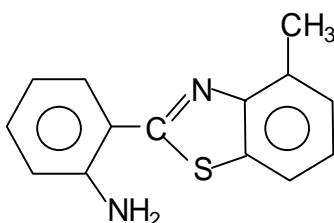


Figure 1.2. Dehydrothio Orthotoluidine

1.3.1 Phosphates and Uranium Metal Machining Coolant Fluids

Further testing of phosphate as a uranium metal corrosion inhibitor was performed in subsequent Manhattan Project work (Draley and English 1944). The corrosion rate in 70°C water containing 167 parts per million (ppm) phosphate at pH ~ 2 to 5.5 was about half of that observed in water alone. At this pH range, the phosphate solution species and concentration would have been 0.0018 M H_2PO_4^- rather than the 0.0077 M HPO_4^{2-} (at pH ~ 7 to 12) used in the test by Greenwood (1942), which showed a \sim two-fold corrosion rate increase at 100°C. Together, these separate tests indicate that phosphate at these low concentrations had little if any effect on uranium metal corrosion.

A later extensive series of experiments performed to identify corrosion inhibitors for water-based cooling fluids used to machine uranium metal showed phosphates to be effective (Sprague et al. 1964). The test program was specifically undertaken to discover ways to overcome uranium pitting corrosion caused by chloride ion, Cl^- , which arose from handling the metal pieces and from cooling fluid breakdown. In the first set of experiments, twelve different water-based commercial cutting fluids/coolants, most of which contained triethanolamine [TEA, $(\text{HOCH}_2\text{CH}_2)_3\text{N}$], were investigated as additives. The commercial coolant concentrations were usually present at about 1% concentration in water. Most of the coolants contained nitrite, NO_2^- , and a few also contained copper ion, Cu^{2+} . In comparative tests, nitrite, at about 0.02 to 0.04 M in the 1% coolant solutions, provided significant inhibition against pitting corrosion by chloride. Because the nitrite was found to air-oxidize to nitrate, NO_3^- , the effects of nitrate also were investigated and shown to increase pitting attack rate in the presence of chloride. Copper increased the corrosion rate slightly under similar conditions. Carbonate or bicarbonate, whose

concentrations increased with time due to atmospheric carbon dioxide uptake, also increased uranium corrosion rates in the presence of chloride.

Besides uranium metal corrosion protection, a suitable coolant must have favorable low foaming properties, low cost, and high stability. Because none of the commercial fluids gave overall satisfactory performance, additional uranium metal corrosion tests were performed for simple aqueous solutions with and without TEA (Sprague et al. 1964). The aqueous solutions tested were sodium salts of:

- chromate (CrO_4^{2-})
- molybdate (MoO_4^{2-})
- tungstate (WO_4^{2-})
- ferrocyanide [$\text{Fe}(\text{CN})_6^{4-}$]
- ferricyanide [$\text{Fe}(\text{CN})_6^{3-}$]
- oleic acid [$\text{CH}_3(\text{CH}_2)_7\text{CH}=\text{CH}(\text{CH}_2)_7\text{COOH}$]
- hydrogen phosphate (HPO_4^{2-})
- phosphate (PO_4^{3-})
- metaphosphate [$(\text{PO}_3)_x^{x-}$]
- pyrophosphate ($\text{P}_2\text{O}_7^{4-}$)
- di-2-ethylhexyl phosphate [$(\text{CH}_3(\text{CH}_2)_3\text{CH}(\text{CH}_2\text{CH}_3)\text{CH}_2\text{O})_2\text{POO}^-$].

The solutions generally contained 100 ppm (0.0028 M) chloride as an intentional contaminant.

When used in sufficient concentration, the most effective additives were found to be HPO_4^{2-} and PO_4^{3-} . The corrosion rates were found to be $<0.00012 \text{ mg/cm}^2\cdot\text{hr}$ for 25°C TEA-free coolants contaminated with 100 ppm chloride that contained 5 to 10 g of Na_2HPO_4 per liter (0.035 to 0.070 M). This rate is $<0.25\%$ of the rate, $0.048 \text{ mg/cm}^2\cdot\text{hr}$, observed with 2 g Na_2HPO_4 /liter under similar conditions. The rate in anoxic water at 25°C is $0.0104 \text{ mg/cm}^2\cdot\text{hr}$ according to the STP rate law (Plys and Schmidt 2006). Further tests showed that varying pH in the range 8.4 to 12.2 had negligible effect in $\text{HPO}_4^{2-}/\text{PO}_4^{3-}$ solutions; at pH 7.2, the corrosion rates were not measurable but a light metal tarnish was observed. In contrast, the phosphate concentrations in the tests with the magnesium phosphate grouts (Delegard et al. 2004) evidently were not sufficient to provide corrosion attenuation of the magnitude observed in the solution tests of Sprague et al. (1964).

A thin blue film formed on the uranium metal surface in the presence of phosphate was credited with providing the corrosion protection. The film, determined to be UO_2 and $(\text{UO}_2)_3(\text{PO}_4)_2\cdot 4\text{H}_2\text{O}$ by X-ray diffraction, was found to be self-healing such that if it was scratched, it would re-form if the specimen was again immersed in a phosphate solution even containing chloride. Sprague et al. (1964) concluded:

Twelve commercial coolants and numerous other solutions known for their corrosion protection were tested at the 100-ppm chloride level with uranium; however, none were found to be as effective as the orthophosphate system.

Although not applicable to present considerations of uranium metal corrosion inhibition in K Basin sludge, the protection afforded by phosphate even extends to acid conditions. Thus, the uranium metal corrosion rate observed in concentrated phosphoric acid (14.6 M H₃PO₄) at 80°C is ~0.08 µm/hr or ~0.15 mg/cm²·hr (Delegard et al. 2008), a factor of five lower than the 0.76 mg/cm²·hr corrosion rate expected in anoxic water at 80°C according to the STP rate law (Plys and Schmidt 2006). In contrast, the uranium metal corrosion (dissolution) rate in 80°C concentrated nitric acid (15.6 M HNO₃) is about 90 mg/cm²·hr (extrapolated from the data of Lacher et al. 1961), a factor of 600 higher than observed in concentrated H₃PO₄.

1.3.2 Sulfate

Inhibition of uranium metal corrosion in water by added sulfate was observed in Manhattan Project research (Draley and English 1944). In tests at 70°C, the rate in 695 ppm SO₄²⁻ (~0.0072 M) was 0.082 mg/cm²·hr or about 21% of that observed in water according to the STP rate law (Plys and Schmidt 2006).

1.3.3 Nitrite

Nitrite, chromate, tungstate, and molybdate, added at concentrations ranging from 10⁻³ to 10⁻⁵ M, were reported to be “moderately effective” in inhibiting uranium metal corrosion in water with nitrite providing the best performance (Waber 1956, p. 39). However, quantitative data on the inhibition magnitudes were not provided.

As noted in Section 1.3.1, commercial metal machining coolants containing 0.02 to 0.04 M nitrite (generally as sodium nitrite [NaNO₂]) inhibit uranium metal pitting corrosion in the presence of aerated chloride solutions much better than coolants containing no nitrite (Sprague et al. 1964). Sodium nitrite at 1 g per liter (~0.0145 M) in 50/50% water/propylene glycol coolant has been used to provide corrosion resistance in machining uranium metal (Hinton et al. 1986). Nitrite, at 1000 ppm (about 0.022 M), also is mentioned as a uranium metal corrosion inhibitor for an aqueous propylene glycol machining coolant (Cristy et al. 1986). Quantitative data on the efficacies of nitrite in inhibiting corrosion are not described in either report.

Nitrite, as ~500 ppm potassium nitrite (0.0059 M KNO₂), reportedly was added as a uranium metal corrosion inhibitor for the fuel contained in closed K West (KW) Basin canisters (page 61 of IAEA 1998). This rationale for KNO₂ addition to the closed KW fuel storage canisters is repeated in other reports (Johnson et al. 1994; Johnson and Burke 1995, pp. 3-4 to 3-5). Attribution of uranium corrosion inhibition efficacy to KNO₂ is based on the recollection of an engineer who formerly worked on K Basin spent fuel storage (Johnson et al. 1994; Johnson and Burke 1995). However, despite extensive investigation, no published accounts of original research to qualify the use of KNO₂ to mitigate uranium metal corrosion were found nor were reports on the effects of KNO₂ on uranium metal corrosion in Hanford fuels identified. The investigation included searching of technical letters and reports in this topic at Hanford Central Files, Hanford office collections, Process Aids, surveys of Hanford Site literature through the Integrated Document Management System, surveys of open source literature, and interviews of active and retired personnel familiar with the K Basin fuel storage operations who might have been

able to recall or direct attention towards such reports.² The only germane information found was the report on the design of the fuel encapsulation program, which noted that the KNO_2 was added to the KW fuel storage canisters for aluminum canister material corrosion control and that the effect of the KNO_2 addition on uranium metal corrosion was not known (Hanson and Brouns 1980, pp. 25 and 44, respectively).

A later report noted that nitrite was suspected to react with dissolved oxygen in the closed canisters to form nitrate (Trimble 1996). However, if oxygen consumption by nitrite did occur and was the controlling factor in uranium corrosion, uranium corrosion rates might be expected to be higher than if nitrite were absent because uranium corrosion rates are higher in anoxic water than in oxic water.

1.3.4 Dissolved Oxygen

As noted in Section 1.1, dissolved oxygen inhibits uranium metal corrosion in water. General and specific aspects of this topic are discussed in a prior STP report (Section 2.3 of Delegard and Schmidt 2008). The temperature dependence of the rate of uranium metal corrosion in aerated water is steeper than that shown in anoxic water. Although the rates in oxic and anoxic water are nearly equal at $\sim 100^\circ\text{C}$, the rate is lower by about a factor of 100 in oxic (aerated) 25°C water than the rate in 25°C anoxic water. Uranium corrosion rates in aerated and anoxic water are compared in Figure 1.3.

Fewer experimental data exist for the aerated uranium metal corrosion system than for the anoxic system because maintenance of stable oxic conditions is difficult. Oxic conditions vary over the duration of the experiment by oxygen consumption through reaction with uranium metal and with UO_2 , metallic iron, and organic species, by decreasing oxygen solubility in water with increased temperature, and by oxygen formation through radiolysis. Oxygen concentrations also vary within the heterogeneous solid-liquid system. Thus, anoxic regions form by differential aeration in crevices and other occluded regions due to local oxygen depletion while oxygenation is higher near the air-liquid interface. Differential aeration cells arise and are manifest by greater uranium metal corrosion rates in the occluded oxygen-starved regions. Finally, the lower uranium metal corrosion rates observed under oxic conditions give way with time to anoxic conditions and correspondingly higher corrosion rates at rates accelerated by higher temperatures. The practical difficulty of maintaining active aeration in dense heterogeneous sludge likely precludes its use under storage and transportation conditions.

² The experts consulted on Hanford irradiated fuel storage were SP Burke, AB Johnson, Jr., BB Emory, AP Larrick, DB Bechtold, DH Shuford, and PL Koehmstedt.

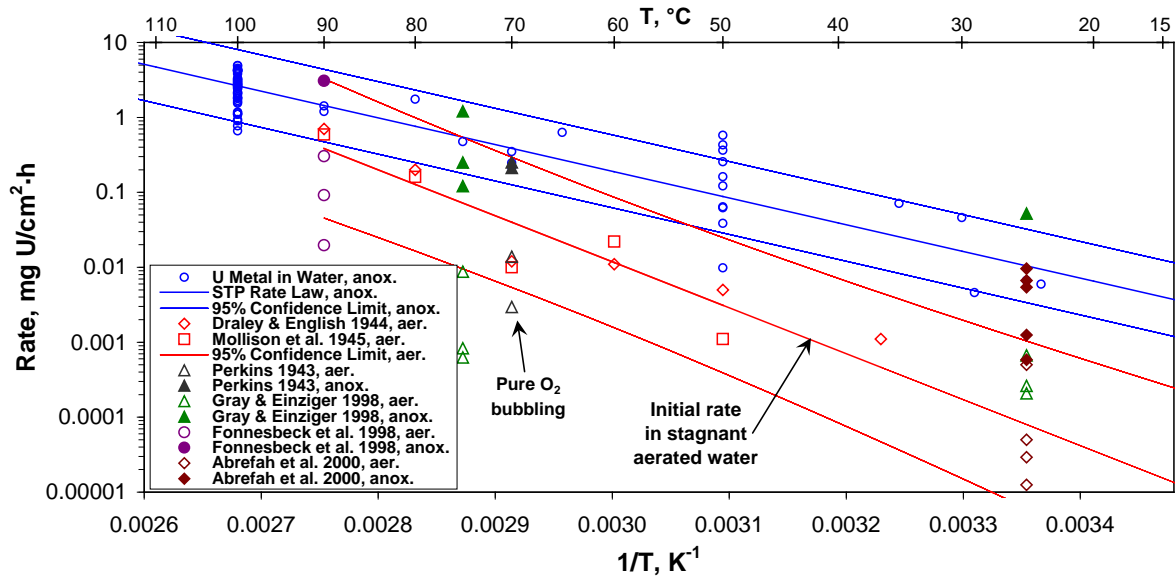


Figure 1.3. Comparison of Uranium Metal Oxidation Rates in Anoxic Water with Rates in Aerated Water

1.4 Hydrogen Scavengers

The generation of hydrogen from corrosion of uranium metal in K Basin sludge may be attenuated by use of materials that react with (scavenge) the hydrogen. In the chemical production of hydrogen by reaction of water with active metals, such as the aqueous corrosion of uranium metal, the hydrogen initially forms in the atomic state as hydrogen radicals, $H\cdot$, in an excited high energy state of H_2 (page 246 of Wiberg 2001), or perhaps as diatomic hydrogen (H_2) activated on the product oxide surface. In any event, at the moment of production (*in statu nascendi*), the newly formed hydrogen is much more reactive than is the H_2 that dissolves in solution and then appears in the gaseous state. Because the freshly generated hydrogen is more reactive, it is more susceptible to scavenging by an appropriate dissolved oxidant than the H_2 that ultimately reports to the solution and then escapes to the gas phase.³

1.4.1 Nitrate and Nitrite

One potential method to decrease or eliminate hydrogen is through the reaction of “nascent hydrogen” with nitrate, NO_3^- . Referring to nitrate salt solutions, Wiberg (2001, p. 672) states:

In aqueous solution, however, they are only able to oxidize strong reducing agents, such as nascent hydrogen. They are then even reduced to ammonia; this reaction is utilized in analytical chemistry for both qualitative and quantitative determination of nitrates, by boiling the alkaline solution with Zn, Al, or Devarda’s alloy = Cu/Al/Zn.

³ Alternatively, the purported hydrogen radical scavenging agent may react directly with the metal to become the metal oxidant in place of water. The existence of “nascent hydrogen” as the water reduction product formed by active metals recently has been challenged on mechanistic (Meija and D’Ulivo 2008) and thermodynamic (Laborda et al. 2002) bases. Nevertheless, the term “nascent hydrogen” will be used where appropriate in these discussions to maintain consistency with the cited literature.

In a similar fashion, the chemical denitration (or denitrification) of water containing trace nitrate has been accomplished through chemical reduction by exposing the waters to active metals. Active metals that have been tested for water denitration include magnesium, iron, and aluminum (Fanning 2000; Kumar and Chakraborty 2006; Choe et al. 2004 and references therein).

Removal of nitrate and nitrite contamination from groundwaters by reaction with dissolved atmospheric pressure H_2 gas over metallic catalysts is described as nitrate (or nitrite) hydrogenation (Marchesini et al. 2008). The metallic catalysts generally are noble metals (e.g., platinum, palladium, or their alloys) on porous ceramic oxide supports. The noble metals serve to make the hydrogen reactive; no reaction of dissolved hydrogen with nitrate or nitrite occurs in the absence of catalyst. The nitrogen reduction products observed in catalyzed hydrogenation include nitrite (from nitrate), which then is reduced to nitrogen gas (N_2) and ammonia (NH_3). The observed reduction products depend on site selectivity and environmental conditions. Nitrous oxide (N_2O) also may be observed in small concentrations.

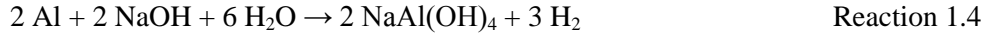
Iron or steel parts can be polished by tumbling with abrasives and water in a closed vessel. In such systems, H_2 often is observed to accumulate due to the reaction of the fresh metal surfaces with water. It has been found that oxidizing salts (ammonium, lithium, sodium, and potassium salts of nitrate, nitrite, permanganate, and chromate) added to the water react with the “nascent hydrogen” to prevent H_2 accumulation (Burroughs 1959). According to this patent, the presence of at least 0.79 M sodium nitrate ($NaNO_3$) or 0.87 M $NaNO_2$ in the aqueous solution is sufficient to oxidize the H_2 to water and eliminate H_2 accumulation. With nitrate, the principal reduction product is ammonia and nitrite is formed as an intermediate transitory product of low concentration. Burroughs (1959) observed nitrite to be more reactive than nitrate such that the initial reduction products from nitrite are more readily scavenged by the excess nitrite than the initial nitrate reduction products are scavenged by excess nitrate. As a result, nitrite forms a wider variety of intermediate products than does nitrate. Nitrite first forms hyponitrite, $ONNO^-$, which then hydrolyzes to form N_2O gas autogenously or can react further with $H\cdot$ to form N_2 gas and ammonia. The N_2O and N_2 gases, however, largely escape from solution to pressurize the metal polishing container and, furthermore, are not available to scavenge $H\cdot$. Because of these losses of intermediates to the gas phase, nitrate is more chemically efficient than nitrite.

Reactions of active metals with water to produce hydrogen gas, and the influence of nitrate on these reactions, are considered for aluminum and zinc in alkaline solution (Section 1.4.1.1) and zirconium in fluoride solution (Section 1.4.1.2). Nitrate and nitrite reaction rates and efficiencies are discussed in Section 1.4.1.3 and reaction stoichiometries are described in Section 1.4.1.4.

1.4.1.1 Aluminum and Zinc

As noted by Wiberg (2001, p. 672), reaction of Al with nitrate in alkaline solution produces ammonia. This reaction was exploited in dissolving the Al cladding from single-pass reactor fuel in the Hanford Site Bismuth Phosphate (202-T and 202-B), REDOX (202-S), and PUREX (202-A) reprocessing plants where the Al fuel slug jackets were dissolved chemically in NaOH solution.

The reaction of aluminum with NaOH solution without nitrate produces sodium aluminate [$NaAl(OH)_4$] solution and H_2 :



The evolution of H₂ was moderated by the addition of NaNO₃ to the cladding removal solution to form ammonia. The chemical reduction of the nitrate to ammonia occurs by the following stoichiometry:



With higher sodium nitrate concentrations, ammonia decreases and NaNO₂ is favored:



Systematic study of the effects of NaOH concentration and the NaNO₃:Al ratio were undertaken to optimize the cladding removal process to minimize H₂ release and decrease the unwanted production of NH₃ (Gresky 1952). The reactions showed reasonable adherence to stoichiometry, as the NaNO₃:Al ratio was varied, particularly at lower ratios. However, as shown in Figure 1.4, the release of NH₃ could not be completely supplanted by NaNO₂, even at high NaNO₃:Al mole ratios.

Testing also showed that NaNO₃ concentrations above ~1 M (85 g NaNO₃/liter) had little further effect in decreasing the H₂ yield (Figure 1.5). At high NaNO₃ concentrations, the H₂ yield was ~2 mL of gas (~8.3×10⁻⁵ moles) per gram (3.7×10⁻² moles) of aluminum or 2.2×10⁻³ moles of H₂ per mole of Al. This is about 0.15% of the 1.5 moles H₂ per mole of Al yield that would have occurred in nitrate-free alkaline solution or an attenuation factor of 1/0.0015 (~670).

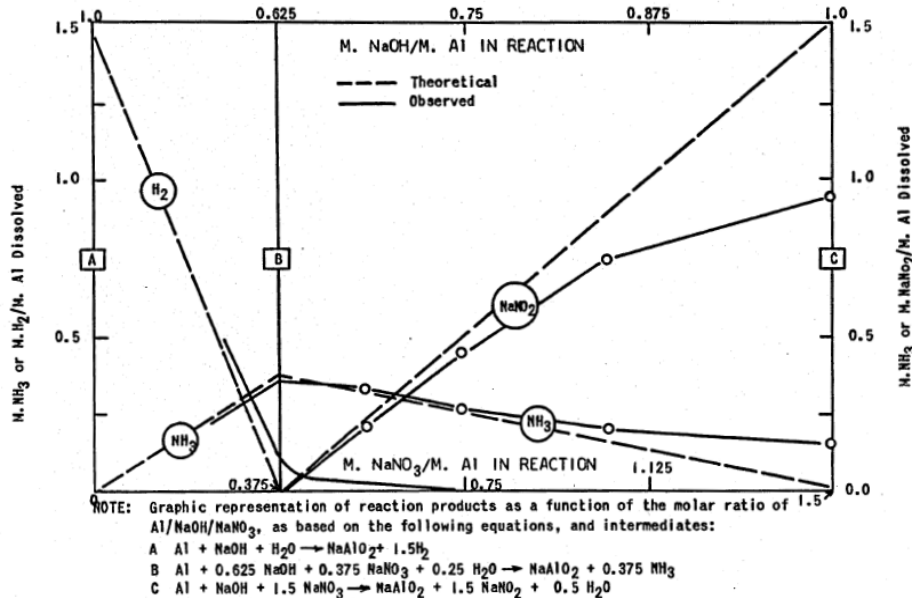


Figure 1.4. Predicted and Observed Products from Reaction of Aluminum in Alkaline Nitrate Solution (Gresky 1952)

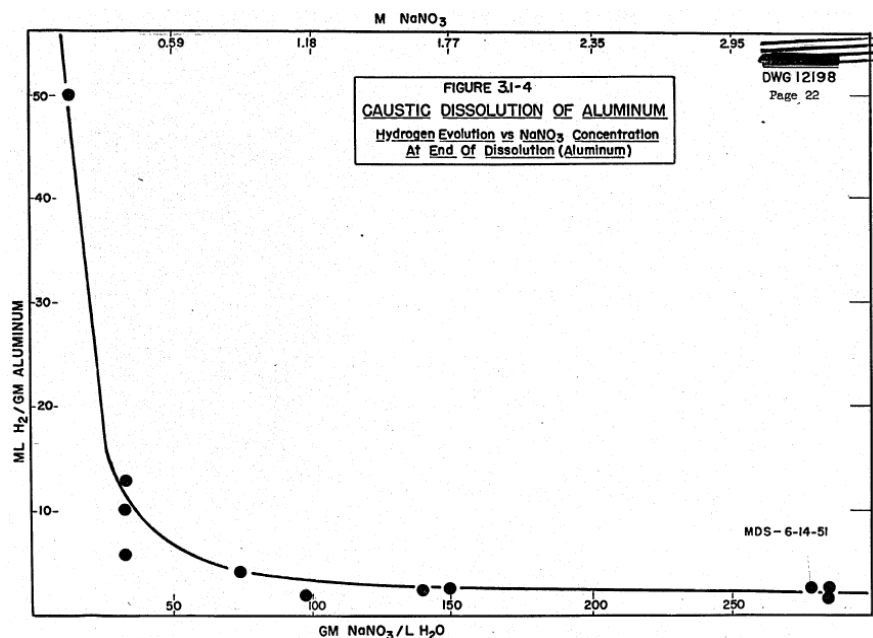


Figure 1.5. Hydrogen Yield from Reaction of Aluminum in NaOH as a Function of NaNO₃ Concentration (Gresky 1952)

The joint evolutions of H₂ and NH₃ were found to be at a practical minimum under plant conditions when the nitrate and aluminum mole quantities were nearly equal (Gresky 1952):



Based on these studies, H₂ evolution also can be decreased by the addition of NaNO₂ to the alkaline aluminum digestion solution. However, in this case, NH₃ would be the favored reduced nitrogen product.

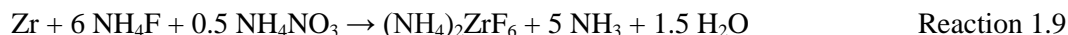
Zinc metal (Zn) reacts analogously to aluminum in NaOH solution to give H₂. Like Al, the H₂ may be supplanted by NH₃ in strongly alkaline solution if nitrite or nitrate is present (Pourbaix 1966).

1.4.1.2 Zirconium

Zirconium dissolves readily in hydrofluoric acid, HF, to produce H₂ and the fluorozirconate complex, ZrF₃⁺:



The zirconium can be dissolved with decreased H₂ evolution if nitrate is added at near-neutral pH with ammonium fluoride (NH₄F) as the fluoride source and ammonium nitrate (NH₄NO₃) as the nitrate source (Swanson 1958). The Zirflex process to remove the Zircaloy cladding from Hanford N Reactor fuel in the Hanford Site REDOX and PUREX reprocessing plants exploited this chemistry. Ammonia forms from nitrate reduction by zirconium metal according to the following ideal reaction:



The reaction stoichiometry under plant conditions (boiling 5.5 M NH₄F/0.5 M NH₄NO₃) was found to be:



with the H_2 yield about 6% of what it would have been in HF solution containing no added nitrate. The hydrogen attenuation factor thus was $1/0.06 \cong 17$ (Moore et al. 1980).

1.4.1.3 Nitrate and Nitrite Reaction Kinetics and Efficiencies

Radiolysis decomposes water to radical and ionized species including the solvated electron, e^-_{aq} (functionally, H_2O^-), the hydrogen radical ($\text{H}\cdot$), the hydroxyl radical ($\cdot\text{OH}$), the hydrogen ion (H^+), and the hydroxide ion (OH^-):



Diatomic hydrogen can form by combination of various radiolysis products according to the following three reactions:



The Reaction 1.13 rate constant is about five times greater than that of either Reaction 1.12 or Reaction 1.14. Because the radiolytic yield of $\text{H}\cdot$ is about 20% of that of H_2O^- , the H_2 yield by Reaction 1.14 is much lower than those of Reactions 1.12 and 1.13 (Hayon and Moreau 1965). Overall, Reactions 1.12 and 1.13 predominate.

Nitrate is known to be a very efficient scavenger of solvated electrons and thus should diminish H_2 produced by interaction of primary water radiolysis products according to Reactions 1.12 and 1.13. Nitrite, meanwhile, is an effective $\text{H}\cdot$ and $\cdot\text{OH}$ scavenger and thus should be effective against H_2 production by Reactions 1.13 and 1.14 (Meisel et al. 1991). This is confirmed in comparative studies that show that the reaction rate of $\text{H}\cdot$ with nitrite is about 300 times greater than the rate of $\text{H}\cdot$ with nitrate at 25°C (Mezyk and Bartels 1997). Together, these rate data indicate that nitrate, because it is effective against the solvated electron implicated in both of the dominant Reactions 1.12 and 1.13, should be more efficient in suppressing radiolytic hydrogen than is nitrite, which is effective only against the $\text{H}\cdot$ implicated in Reaction 1.13 and the minor Reaction 1.14.

The radiolytic hydrogen attenuations provided by KNO_2 and NaNO_3 (and other solutes) are given in Figure 1.6 as functions of effective solute concentrations (Meisel et al. 1991). It is seen that for a given concentration, NaNO_3 is about 2.4 times as effective as KNO_2 is decreasing the radiolytic yield of H_2 .

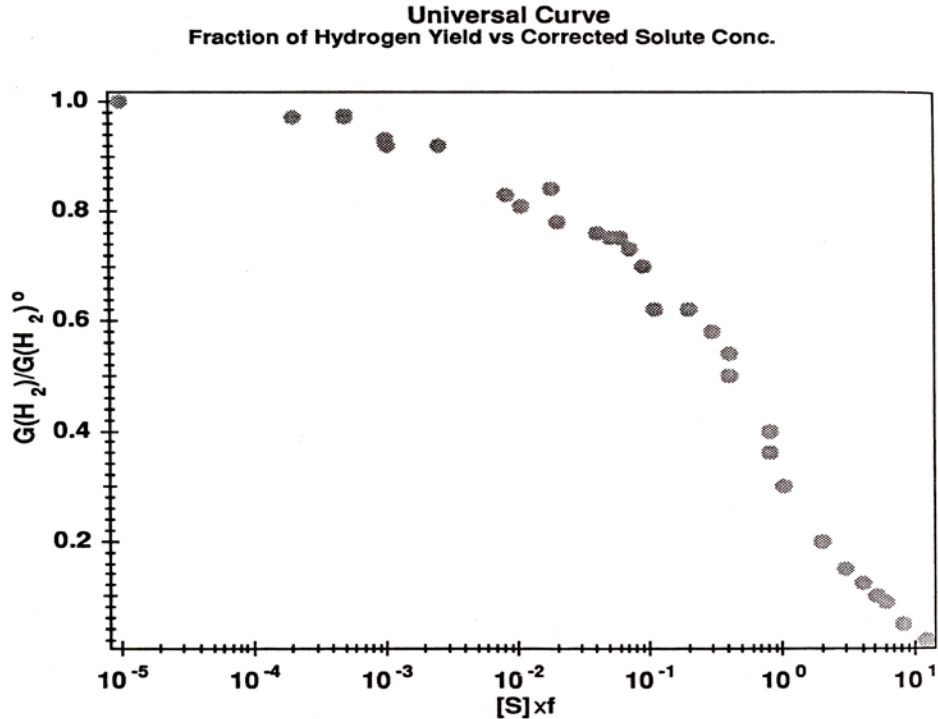


Figure 1: The ratio of H₂ yield, $G(H_2)$, in the presence of the solute concentration $[S]$ to the yield of H₂ in the absence of solute, $G(H_2)^0$. From reference 28. The concentration correction factor, f , for the solutes tested are: KNO₂, 1.0; NaNO₃, 2.4; H₂O₂, 2.5; acrylamide, 4.0; Na₂Cr₂O₇, 8.2; Cu(NO₃)₂, 10.

Figure 1.6. Relative Radiolytic H₂ Yield Compared with That in Water as a Function of Effective Solute Concentration, $S \times f$ (Meisel et al. 1991). The correction factors, f , for solute concentration, S , for the solutes tested are KNO₂ – 1.0, NaNO₃ – 2.4, H₂O₂ – 2.5, acrylamide – 4.0, Na₂Cr₂O₇ – 8.2, and Cu(NO₃)₂ – 10 (Meisel et al. 1991).

Based on these findings, adding either nitrate or nitrite to the K Basin sludge would be expected to decrease the H₂ yield from water radiolysis and, at a specified concentration, nitrate would be more effective than nitrite by a factor of about 2.4. According to Figure 1.6, 1 M NaNO₂ (based on the findings for KNO₂) would decrease radiolytic hydrogen yield by a factor of ~5 while 0.4 M NaNO₃ would have the same effect. However, it is not known that, if nitrate or nitrite were added to the K Basin sludge prepared for WIPP disposal, WIPP authorities would credit the expected decrease in radiolytic hydrogen yield for waste package transportation or storage purposes.

The radiolysis studies also show that nitrite likely would be a better scavenger for the hydrogen radical, the probable form of active hydrogen created during aqueous uranium metal corrosion, than would nitrate at the same concentration (Meisel et al. 1991; Mezyk and Bartels 1997).

1.4.1.4 Hypothetical Reactions of Nitrate and Nitrite in Aqueous Corrosion of Uranium Metal

The postulated net reactions and their enthalpies to form nitrite, nitrous oxide, nitrogen, and ammonia from sodium nitrate in the reaction of uranium metal in aqueous solution are summarized and compared with the simple reaction of uranium metal with anoxic water in Table 1.1. Potential reactions of NaNO₂ with uranium metal in water also are shown in the table.

Table 1.1. Reactions of Nitrate and Nitrite with Uranium

Reaction	ΔH_{rxn} , kJ/mole U	N Oxn. State Change	Mole Ratios		
			NO_3^- or NO_2^- /U	Gas/U	NaOH/U
$\text{U} + 2 \text{H}_2\text{O} \rightarrow \text{UO}_2 + 2 \text{H}_2$	-513.24	NA	0.0	2.0	0.0
<i>With nitrate</i>					
$\text{U} + 2 \text{NaNO}_3 \rightarrow \text{UO}_2 + 2 \text{NaNO}_2$	-879.61	2	2.0	0.0	0.0
$2 \text{U} + 2 \text{NaNO}_3 + \text{H}_2\text{O} \rightarrow 2 \text{UO}_2 + \text{N}_2\text{O} + 2 \text{NaOH}$	-922.40	4	1.0	0.5	1.0
$5 \text{U} + 4 \text{NaNO}_3 + 2 \text{H}_2\text{O} \rightarrow 5 \text{UO}_2 + 2 \text{N}_2 + 4 \text{NaOH}$	-987.72	5	0.8	0.4	0.8
$2 \text{U} + \text{NaNO}_3 + 2 \text{H}_2\text{O} \rightarrow 2 \text{UO}_2 + \text{NH}_3 + \text{NaOH}$	-849.89	8	0.5	0.0	0.5
<i>With nitrite</i>					
$\text{U} + 2 \text{NaNO}_2 + \text{H}_2\text{O} \rightarrow \text{UO}_2 + \text{N}_2\text{O} + 2 \text{NaOH}$	-965.19	2	2.0	1.0	2.0
$3 \text{U} + 4 \text{NaNO}_2 + 2 \text{H}_2\text{O} \rightarrow 3 \text{UO}_2 + 2 \text{N}_2 + 4 \text{NaOH}$	-1059.79	3	1.33	0.67	1.33
$3 \text{U} + 2 \text{NaNO}_2 + 4 \text{H}_2\text{O} \rightarrow 3 \text{UO}_2 + 2 \text{NH}_3 + 2 \text{NaOH}$	-839.98	6	0.67	0.0	0.67
ΔH_{rxn} based on H_f^0 (enthalpy of formation) data from Wagman et al. (1982).					

Both nitrate and nitrite reductions to N_2 , N_2O , and NH_3 produce NaOH as a byproduct. The amounts of NaOH produced, and the amounts of NaNO_3 or NaNO_2 required, per mole of uranium decrease with increasing change in nitrogen oxidation state. It is also seen that all listed nitrate and nitrite reactions are 1.6- to 2.0-times more energetic, per mole of uranium metal, than the anoxic reaction of uranium metal with water.

1.4.2 Metaschoepite and Ferric Hydroxide

Both metaschoepite ($\text{UO}_3 \cdot 2\text{H}_2\text{O}$) and ferric hydroxide [$\text{Fe}(\text{OH})_3$] are found in K Basin sludge and are thermodynamically capable of reacting with hydrogen. Metaschoepite potentially can react with hydrogen to form UO_2 while ferric hydroxide can react with hydrogen to form magnetite (Fe_3O_4) (Table 1.2).

It has been postulated that metaschoepite or other U(VI) phases may have been responsible for the shortfall in hydrogen production, compared with release of fission product gases krypton and xenon, observed for irradiated uranium metal fuel corrosion in gas generation tests of K Basin sludge (Bryan et al. 2004; Delegard and Schmidt 2008). Such shortfall also might be attributed to scavenging of hydrogen by iron(III) phases to form magnetite. However, the observed shortfall only occurred for sludges containing <5 wt% uranium metal and did not attenuate hydrogen generation rates to the same degree or at all for all tests. The efficacies of solid phase metaschoepite and ferric hydroxide also may be kinetically limited due to their inability to diffuse near the hydrogen radical source at the uranium metal surface. Therefore, even though the postulated reactions are feasible thermodynamically, they may not occur reliably at any concentration and to a great enough degree to affect hydrogen generation rates in genuine sludge.

Table 1.2. Gibbs Free Energies of Reaction of Metaschoepite and Ferric Hydroxide with Hydrogen

<i>Metaschoepite Reduction to Form Uraninite</i>	
$\text{UO}_3 \cdot 2\text{H}_2\text{O} + \text{H}_2 \rightarrow \text{UO}_2 + 3 \text{H}_2\text{O}$	$\Delta_f G^\circ \text{UO}_3 \cdot 2\text{H}_2\text{O} = -1630.8 \text{ kJ/mol}$
	$\Delta_f G^\circ \text{UO}_2 = -1031.7 \text{ kJ/mol}$
	$\Delta_f G^\circ \text{H}_2\text{O} = -237.129 \text{ kJ/mol}$
$\Delta G_{\text{rxn.}} = +[-1031.7 + 3 \times (-237.129)] - [-1630.8] = -112.3 \text{ kJ/mol}$	
<i>Ferric Hydroxide Reduction to Form Magnetite</i>	
$6 \text{Fe}(\text{OH})_3 + \text{H}_2 \rightarrow 2 \text{Fe}_3\text{O}_4 + 10 \text{H}_2\text{O}$	$\Delta_f G^\circ \text{Fe}(\text{OH})_3 = -696.5 \text{ kJ/mol}$
	$\Delta_f G^\circ \text{Fe}_3\text{O}_4 = -1015.4 \text{ kJ/mol}$
	$\Delta_f G^\circ \text{H}_2\text{O} = -237.129 \text{ kJ/mol}$
$\Delta G_{\text{rxn.}} = +[2 \times (-1015.4) + 10 \times (-237.129)] - [6 \times (-696.5)] = -223.1 \text{ kJ/mol}$	
Thermodynamic data from Wagman et al. (1982).	

1.5 Summary of Findings from Review of the Technical Literature

The survey of the technical literature in sections 1.2 through 1.4 identified three general approaches to decrease H_2 generation rates from the reaction of uranium metal with water. The three methods are isolating the water from the metal by sequestration, such as by reaction, absorption, or with desiccants, using uranium metal corrosion inhibitors, and using hydrogen scavenging agents. A fourth method, temperature decrease, was judged to be impractical for sludge storage and not feasible for transportation.

Grouts based on Portland cement and on magnesium phosphate have been investigated in prior tests for their abilities to diminish uranium metal corrosion rates by chemically combining or absorbing water. However, neither grout type decreased rates more than a factor of 2 to 3 even with high relative amounts of cement former. The marginal rate decreases likely were because of small decreases in the relative humidities in these waste forms. More effective desiccants, such as MgO or CaO , might provide lower humidity and correspondingly lower uranium metal corrosion rates. The uranium metal corrosion rates are known to decrease in proportion to the square root of the relative humidity. Nochar N660 is an organic polymeric absorbent that has been applied to immobilizing aqueous liquids in wastes destined for WIPP disposal. Based on this application, Nochar N960, a chemically similar successor absorbent, has been proposed as a material that might be used to limit water reaction with uranium metal by its ability to absorb water. Nochar N960 was tested at a number of ratios in the present experimentation to decrease the reaction rate of uranium metal with water and thus the hydrogen generation rate. Based on perceived promise, MgO and CaO as desiccant material may merit testing in future experiments.

Numerous uranium metal corrosion inhibitors in water have been investigated as described in the technical literature. Dissolved oxygen inhibits corrosion but the practical difficulty of maintaining active aeration in dense heterogeneous sludge likely precludes its use under storage and transportation conditions. Of the tested corrosion inhibitors, neutral to alkaline phosphate solutions, such as $>0.04 \text{ M Na}_2\text{HPO}_4$, seem to be the most promising. Nitrite also has been investigated as a uranium corrosion inhibitor. However, as a constituent in coolant solutions used in uranium metal machining, nitrite's effect in decreasing uranium metal corrosion rate is not as marked as that of phosphate. Based on the findings

from the technical literature, phosphate was tested in the present experimentation for its effect in inhibiting uranium corrosion in water.

“Nascent hydrogen,” such as the hydrogen radical, likely is the initial water reduction product from corrosion of active metals in aqueous solution. Nitrate, nitrite, permanganate, and chromate have been investigated as “nascent hydrogen” scavengers with most work focusing on nitrate and nitrite. Based on the results of the literature survey, nitrate and nitrite were investigated in the present testing for their abilities to decrease hydrogen gas generation from corrosion of uranium metal in water.

In K Basins sludge, metaschoepite and ferric hydroxide also might act as hydrogen radical scavengers based on favorable thermodynamics (negative Gibbs free energies of reaction) but their efficacies likely suffer due to their inability to diffuse near the hydrogen radical source at the uranium metal surface. However, in performing experiments for the present set of investigations, it was discovered that a genuine sludge sample, having relatively low pH (~5.5) and correspondingly high U(VI) solution concentration ($\sim 6 \times 10^{-4}$ M), attenuated hydrogen gas generation by a large factor. Based on these findings, dissolved U(VI) was tested in the present investigations for its ability to decrease hydrogen gas generation from uranium metal corrosion in water.

2.0 Experimental Materials and Methods

Experiments were performed to determine the effects of nitrate, nitrite, phosphate, and Nochar Acid Bond N960 on the reaction of uranium metal with water in the presence of aqueous solutions alone, with added UO_2 , with simulated sludge, and with genuine sludge. The tests were undertaken in six test series. The simulated sludge components included U metal, UO_2 , metaschoepite ($\text{UO}_3 \cdot 2\text{H}_2\text{O}$), ferrihydrite ($\text{Fe}_5\text{O}_7\text{OH} \cdot 4\text{H}_2\text{O}$; or $\text{Fe}_2\text{O}_3 \cdot 1.8\text{H}_2\text{O}$), gibbsite [$\text{Al}(\text{OH})_3$], mordenite inorganic ion exchanger, mixed bed (cation/anion) organic ion exchange resin (OIER), Hanford blow sand, and Optimer 7194 Plus, a flocculating agent that has been used to settle solids in K Basin sludge handling operations. A seventh test series was performed to determine the effects of U(VI) as a scavenger of hydrogen from the reaction of water with uranium metal.

The materials used in the testing are described in Section 2.1, the uranium corrosion experiments are described in Section 2.2, and the analytical methods are outlined in Section 2.3.

2.1 Chemicals and Materials

The nitrate, nitrite, phosphate, and chloride used in the testing were the reagent grade sodium salts, NaNO_3 , NaNO_2 , Na_2HPO_4 , and NaCl respectively. Hydrochloric acid used for pH adjustment and for partial dissolution of metaschoepite also was reagent grade. Solutions were prepared with distilled and deionized (DI) water.

The Nochar N960 for the testing is a near white granular material that was used as received from the vendor. The individual granules are rough and irregular in shape, like crushed rock. According to manufacturer's data, particle diameters range from 0.3 to 1 mm and the particle density is 0.8 g/cm^3 . The composition of Nochar N960 is a trade secret. However, Nochar N960 likely is a salt of a polyacrylic acid superabsorbent polymer given its high affinity for water uptake, its appearance, and its faint amine or ammonia odor.

The uranium metal used in the testing is of natural enrichment and in the form of nearly spherical beads. Prior energy dispersive spectroscopy showed aluminum and iron present in small but non-quantified concentrations. Analyses by spectrophotometry of a solution produced by quantitatively dissolving a portion of the metal in nitric acid showed the uranium concentration in the metal to be 99.7 wt%. Carbon also is present at about 73 parts per million parts of uranium (Delegard et al. 2004). Subsequent analyses of the dissolved metal by kinetic phosphorescence for the purpose of using this material as a uranium metal standard in analyses of K Basin sludge under an internal PNNL procedure⁴ showed the uranium concentration in the beads to be $100 \pm 1\%$.

⁴ Jones SA. 2009. *Sample Preparation for Determination of Uranium Metal Concentration in Sludge*, RPG-CMC-107, Pacific Northwest National Laboratory, Richland, Washington.

Prior to use in the experiments, the uranium metal beads were cleaned of uranium oxide surface corrosion. This was done by immersing the beads in either 2 M sodium carbonate (Na_2CO_3) solution containing 1% hydrogen peroxide (H_2O_2) or in ~6 M HNO_3 at room temperature until visibly shiny. The chemicals used in the cleaning were reagent grade. The cleaning solutions in each case were discarded and the cleaned beads rinsed with DI water and air-dried. In all but one of the present experiments, 30 beads were used. The beads were individually selected for roundness and size such that the 30 beads weighed ~0.10 to 0.11 grams in total. Based on 19.1 g/cm^3 uranium metal density, the average bead diameter was about 700 μm . A single uranium metal bead was used in the single remaining test.

Uranium dioxide (UO_2) was prepared under PNNL direction by an outside vendor by reaction of high-purity (99.96 wt%) uranium metal turnings in ~60°C water. The source uranium metal was 0.19% ^{235}U (i.e., of depleted enrichment). The UO_2 has been stored underwater in a closed jar since preparation. Prior characterization showed this material to be nearly stoichiometric UO_2 and to have nominal 6 nm diameter particle size with larger agglomerates (Sinkov et al. 2008).

The metaschoepite was prepared by oxidation of UO_2 with a pure oxygen gas purge in aqueous suspension (Sinkov et al. 2008). The residual UO_2 comprised 1% or less of the total uranium based on spectrophotometric analysis of the dissolved oxide.

The ferrihydrite, identified as ferric oxide hydroxide by the vendor (Shepherd Chemical Company), was found by X-ray diffractometry (XRD) to contain significant 6-line ferrihydrite when synthesized in 2004 whereas XRD analysis by PNNL in 2009 found only hematite ($\alpha\text{-Fe}_2\text{O}_3$ or Fe_2O_3 ; ~64%) and goethite ($\alpha\text{-FeOOH}$ or FeOOH ; ~36%) according to Rietveld analysis of the diffraction pattern (Appendix A). Because, as observed elsewhere (Jambor and Dutrizac 1998), the poorly crystalline hematite and goethite phases arose from slow room-temperature transformation of ferrihydrite, the material used in testing will be referred to a ferrihydrite. The aluminum hydroxide was reagent grade (JT Baker, now Mallinckrodt Baker, Inc.) and identified to be gibbsite by prior XRD analyses.

The mordenite used in the testing was sodium mordenite LZM-5 from UOP, LLC. This material was selected to substitute for the Norton Zeolon 900 mordenite used to removal radioactive cesium from the K Basins. The Norton Zeolon 900 was no longer available for testing. Dry LZM-5 is nominally $\text{Na}_6\text{Al}_6\text{Si}_{42}\text{O}_{96}$, equivalent to $\text{NaAlSi}_7\text{O}_{16}$, for a Si:Al mole ratio of 7.0 (Ramachandran et al. 2005). The chemical composition of Zeolon 900 (containing 98% mordenite) is reported to have the formula $\text{Na}_2\text{Al}_2\text{Si}_{10}\text{O}_{24}$ for a Si:Al mole ratio of 5.0⁵ and, for Zeolon 900H (the hydrogen form of Zeolon 900), as 32.1 wt% Si and 6.9 wt% Al for Si:Al mole ratio of 4.5.⁶

⁵ Hastings TW. 1997. FAX communication to I Papp, May 19, 1997, Zeolyst International, Valley Forge, PA.

⁶ Pool KH, CH Delegard, AJ Schmidt, and KL Silvers. 1998. "Results from Test 1, 'Acid Digestion of Zeolite and Hydrated Iron Oxide in Proportions Representative of Analyzed Sludge Materials'." Letter report 28510-04 to Duke Engineering & Services, Hanford. January 1998, Pacific Northwest National Laboratory, Richland, WA.

The OIER used in the testing was Purolite NRW37, a 40:60 (by volume) mixture of strong acid cation (NRW100) and strong base anion (NRW200) resin. This is the same resin that was used to control water quality in the K Basins. Nitrate, nitrite, and phosphate can absorb onto anion exchange resin. Therefore, if used to attenuate hydrogen generation, their absorptions must be accounted to determine what additional nitrate, nitrite, or phosphate might be required to satisfy uptake on the OIER present in the sludge.⁷

The finely granular to powdery Hanford blow sand collected from the Fitzner-Eberhardt Arid Lands Ecology (ALE) Reserve in July 2007 between mileposts 9 and 10 on the south side of State Highway 240 contained quartz (SiO_2), anorthite ($\text{CaAl}_2\text{Si}_2\text{O}_8$), mica [$\text{KFe}_3(\text{Al}_{0.24}\text{Fe}_{0.76}\text{Si}_3)\text{O}_{10}(\text{OH})_2$], aegerine [$\text{Fe}_{0.5185}\text{Al}_{0.4185}\text{Ca}_{0.466}\text{Na}_{0.534}\text{Si}_2\text{O}_6$], and microcline (KAlSi_3O_8) according to XRD. See Appendix A. Non-crystalline or glassy phases found in basalt ubiquitous in the Hanford soils are not seen by XRD. The observed mineral distribution is similar to the quartz, feldspar (e.g., albite and anorthite), basalt, mica (muscovite, biotite), clay (chlorite, smectite), and accompanying calcite (CaCO_3) constituents typical of Hanford soils (Serne et al. 2002, and references therein; Schmidt et al. 1999; Zachara et al. 2002).

The Optimer 7194 Plus flocculating agent was obtained from the Nalco manufacturer distributor as a concentrate. A 0.5 wt% dispersion in water of the Optimer agent was prepared. The diluted Optimer was introduced to simulated water-suspended sludge solids, without the uranium metal beads, according to manufacturer's recommendations and in amounts corresponding to the concentrations used in K Basin operations. The basis, material quantities, and preparation of the simulated sludge used in each of the two tests in the Series 5 are described in Table 2.1.

Scoping tests of the reactions of the KE NLOP, KC-4 Whole, KE Floc Comp, and KC-2/3 Comp sludges with 0.5 M NaNO_2 were done within Series 5. These sludges broadly represent the sludges now present in containers and settler tubes in the KW Basin. The KC-2/3 Comp and KE Floc Comp archive sludges used in the Series 6 were selected to represent, respectively, the expected compositions of the uranium-rich settler tube sludge and the flocculated floor, pit, and canister sludges now containerized in the KW Basin. The sludge compositions are shown in Table 2.2.

⁷ The OIER used in the K Basins, mixed bed cation/anion resin Purolite NRW37, is composed of 60 vol% anion resin NRW400 and 40 vol% NRW100 cation resin (Purolite 2007). These resins were designed to withstand high radiation doses for power reactor water decontamination. Therefore, ion exchange capacity loss due to radiolytic or chemical degradation is unlikely. However, some ion exchange capacity for OIER in the containerized sludge present in the KW Basin likely is occupied by calcium, sodium, and carbonate (and chemically trace radionuclides such as cesium-137 and strontium-90) from prior treatment of the K Basin waters and subsequent water exposure.

It is conservatively estimated that a single sludge batch several cubic meters in volume may include up to 20 vol% OIER. Because settled sludge is nominally ~75 vol% water, 20 vol% OIER constitutes 80% of the total solids inventory. The 20 vol% OIER in settled sludge is 3 to 4 times the nominal ~5.7 vol% OIER concentration in containerized sludge (1.05 m³ of OIER is present in 18 m³ of total containerized sludge). Vendor specifications show that the anion exchange capacity of pure NRW400 resin is 1.0 eq/L on a wet volume basis (Purolite 2007). Because NRW400 is 60 vol% of the NRW37 mixed bed resin used in the K Basins, the anion uptake capacity of pure mixed resin is 0.6 eq/L. Therefore, 20 vol% OIER in the settled sludge (but 80% of the settled solids volume) provides 0.48 equivalents of anion capacity per liter of settled sludge. Equivalents are equal to moles for nitrate or nitrite but are twice the number of moles for the doubly charged hydrogen phosphate, HPO_4^{2-} . Because settled sludge typically is ~75 vol% water, an interstitial solution concentration of 0.64 anion equivalents per liter will match the capacity of the associated OIER in settled sludge. Based on this calculation and assuming total nitrate or nitrite uptake, at most 0.64 M nitrate or nitrite in the interstitial water might need to be sacrificed to satisfy the OIER in settled sludge. If supernatant solution is present, a lower sacrificial concentration is required to satisfy the OIER exchange sites.

Table 2.1. Simulated Sludge Composition and Preparation Used in Series 5

Physical/Chemical Based on the memo, G MacLean to R Lokken, "K-Basin Sludge Simulants," 08/07/2008, Fluor, Richland, WA.		Uranium, OIER, and Mordenite Components Added			Component Quantities to Prepare 3.264 mL of Settled Sludge Simulant ^(a)	
Material	Amt., wt%	Material	Amt., wt%	Amt., g/mL	Material	Amt., g
FeOOH or Fe(OH) ₃	21.9	Ferrihydrite	21.9	0.186	Ferrihydrite	0.608
Al(OH) ₃	7.8	Al(OH) ₃	7.8	0.066	Al(OH) ₃	0.217
Sand	14.7	ALE sand ^(b)	27.6	0.235	ALE sand	0.767
Aggregate	16.9	OIER ^(c)	2.0	0.017	OIER	0.055
		Mordenite ^(d)	2.0	0.017	Mordenite	0.056
CeO ₂ or equiv.	30.9	UO ₂ ^(e)	16.0	0.136	Wet UO ₂ ^(f)	0.684
Steel grit or equiv.	4.2	UO ₃ ·2H ₂ O ^(e)	19.1	0.162	Wet UO ₃ ·2H ₂ O ^(f)	2.092
Dense metal or alloy	3.6	U metal	3.6	0.0306	U metal	0.100
Total	100.0	Total	100.0	0.851	Total	4.579
Added water ^(g)						6.459
Flocculating agent – 0.5 wt% Optimer 7194 Plus ^(h)						1.740
<p>(a) Target 3.264 mL of settled sludge simulant used in each test requires 0.100 g of U metal beads, corresponding to the amounts of U metal used in prior tests.</p> <p>(b) ALE sand weight corresponds to the amount of Sand in the Physical/Chemical simulant plus the Aggregate left over after deducting the OIER and Mordenite weights.</p> <p>(c) The relative OIER amount corresponds to the amount in KE Basin sludge (1.05 m³ OIER/18.4 m³ total sludge) based on the density of OIER (Purolite 2007), the assumption that the OIER ratio in KW Basin sludge is the same as that in KE Basin sludge, and the assumption that the volume fractions water in settled OIER and settled sludge are equal.</p> <p>(d) The relative mordenite amount is based on the amount in KE Basin sludge (20 ft³, or 0.566 m³, of mordenite in 18.4 m³ total sludge), the assumption that the mordenite ratio in KW Basin sludge is the same as that in KE Basin sludge, and the assumption that the volume fractions water in settled mordenite and settled sludge are equal.</p> <p>(e) The UO₂ and UO₃·2H₂O combined weights correspond to the sum of CeO₂ (or equivalent) and steel grit (or equivalent) weights where CeO₂ and steel grit are physical representations of particulate and agglomerated uranium oxide, respectively. The distribution of UO₂ to UO₃·2H₂O is 50/50 mole% U(IV) and U(VI).</p> <p>(f) The wet, settled solids, quantities of UO₂ and UO₃·2H₂O slurries are based on the uranium compound densities (2.443 and 1.255 g/mL) and concentrations (65.1 and 25.3 wt%) determined in prior testing (Sinkov et al. 2008).</p> <p>(g) Water in wet UO₂, 0.239 g, in UO₃·2H₂O, 1.562 g, and in flocculating agent, 1.740 g, with 6.459 g of added water totals 10.000 g.</p> <p>(h) A 0.5 wt% dispersion of Optimer 7194 Plus is prepared. From this dispersion, 1.740 g (or mL) is added to the sludge solid components [UO₂, UO₃·2H₂O, ferrihydrite, ALE sand, OIER, Al(OH)₃, and mordenite; but not U metal] suspended in 10.0 mL of water. The amount of flocculent is provided by Moore and Duncan (2005) projections but adjusted downward based on later actual flocculent usage and losses. The 0.5 wt% dispersion is added slowly below the solution surface to allow coating of the suspended sludge particles.</p>						

The actual sludges used had been kept as archive in hot cells (under water cover in glass jars at ambient hot cell temperatures ranging from ~31°C to 38°C) after prior characterization testing. The KE NLOP sludge was taken in 2003; all other sludges were obtained in 1999. As shown in Table 2.2, the phases previously observed by XRD and the more recently analyzed distributions of U(IV) and U(VI) in the uranium indicate that significant oxidation has occurred during the ~10 years of hot cell storage since the sludge was sampled. These sludges have no measurable residual U metal.

Table 2.2. Compositions of K Basin Sludges Used in Testing⁸

Sludge	KE NLOP	KC-4 Whole	KE Floc Comp	KC-2/3 Comp
Dry Basis				
Element	Concentration, wt%			
Al	3.93	6.82	7.70	5.16
Ca	0.937	1.04	0.945	0.134
Fe	6.83	24.3	24.2	1.84
Mg	0.122	0.33	0.230	0.0462
Na	Below detection	0.36	0.365	0.24
Si	36.3	4.91	3.57	0.752
U	2.51	16.6	10.3	59.0
Compound ^(a)	108.0	101.7	92.6	94.8
Radionuc.	Concentration, $\mu\text{Ci/g}$			
⁶⁰ Co	0.280	1.08	1.02	0.441
¹³⁷ Cs	34.6	1680	783	860
¹⁵⁴ Eu	0.542	2.6	1.68	8.14
²³⁸ Pu	0.280	4.91	3.22	16.2
^{239/240} Pu	9.00	39.2	23.9	114
²⁴¹ Am	7.82	29.2	18.9	90.5
Settled Sludge Basis				
Element / H₂O	Concentration, wt%			
Al	0.562	3.83	2.53	3.04
Ca	0.134	0.584	0.310	0.0791
Fe	0.977	13.7	7.92	1.09
Mg	0.0174	0.185	0.0755	0.0273
Na	Below detection	0.202	0.120	0.142
Si	5.19	2.76	1.17	0.444
U	0.359	9.33	3.37	34.8
H ₂ O	85.7	43.8	67.2	41.0
Radionuc.	Concentration, $\mu\text{Ci/g}$			
⁶⁰ Co	0.0400	0.607	0.334	0.260
¹³⁷ Cs	4.95	944	257	507
¹⁵⁴ Eu	0.0775	1.46	0.552	4.80
²³⁸ Pu	0.0400	2.76	1.06	9.56
^{239/240} Pu	1.29	22.0	7.84	67.3
²⁴¹ Am	1.12	16.4	6.20	53.4
Density	Density, g/cm³			
	1.08	1.60	1.25	2.03
Date	Phases ^(b)			
Initial analysis	Q	Not determined	F, Q; not det'd.	U, M, G
2007	M, C, F	B, M, NaU	USi, M, NaU, B	M
Date	Solution Oxidation State, %U(VI); Sinkov et al. 2008			
2008	96.2	Not determined	97.6	Not determined
(a) Total compound weights as representative oxides, hydroxides, and carbonates.				
(b) B = becquerelite [Ca(UO ₂) ₆ O ₄ (OH) ₆ (H ₂ O) ₈]; C = cristobalite [SiO ₂]; F = FeOOH; G = gibbsite [Al(OH) ₃]; M = metaschoepite [UO ₃ ·2H ₂ O]; NaU = [Na ₂ (UO ₂) ₆ O ₄ (OH) ₆ ·8H ₂ O]; Q = quartz [SiO ₂]; U = uraninite [UO ₂]; USi = uranophane [Ca(H ₃ O) ₂ (UO ₂) ₂ (SiO ₄) ₂ (H ₂ O) ₂]				

2.2 Experimental Apparatus and Experimental Procedures

The apparatus used in the gas generation testing was designed to hold the reacting water and uranium metal, in the presence of various additives, sludge components, or simulated or actual sludge, at constant

⁸ Delegard, CH, AJ Schmidt, and JW Chenault. 2007. "Characteristics of KE Basin Sludge Samples Archived in the RPL – 2007." Letter report 53451-RPT01. Pacific Northwest National Laboratory, Richland, WA.

temperature and allow gas collection and measurement of the gas volume. The test apparatus used in the initial testing to investigate addition of nitrate and nitrite salt is sketched in Figure 2.1 (A). The gas volumes changes occurring as the uranium metal corroded were registered in the water-gas levels observed in the plastic syringe. In Series 1, the gas volume collected in the control test containing only uranium metal and water was found to be lower than expected based on the measured amounts of uranium mass reacted. Subsequent monitoring of a similar apparatus holding hydrogen showed decrease of gas volume with time, indicating that hydrogen likely was diffusing through the plastic tubing or gas collection syringe.

Because of the gas leakage, the apparatus was modified to use stainless steel tubing and a glass gas collection vessel (an inverted centrifuge tube). The modified apparatus, shown to be gas-tight by holding hydrogen gas during monitoring over four days, was used in most of the subsequent testing [Figure 2.1 (B)]. Like the original apparatus, the modified apparatus also allowed measurement of gas volume changes by registering the observed water-gas levels but in the centrifuge tube rather than the syringe. Photographs of both apparatus types, including placement in the heating blocks, are given in Figure 2.2.

Ordinary black rubber stoppers were used in the first five test series. The black rubber stoppers available in existing laboratory supply were used in the first three test series. Additional new black rubber stoppers were purchased for use in the fourth and fifth test series. The new stoppers were more pliable than the old stoppers, likely improving the gas tightness of the apparatus. However, it was found that the black rubber stoppers imparted an artifact in the ultraviolet (UV) absorbance spectrum of the test solution, interfering with the spectrophotometric analysis of nitrate and particularly nitrite. Therefore, in the sixth test series, new silicone stoppers were acquired and used. It was discovered that the silicone stoppers had high gas permeability. Neoprene stoppers, which are about as gas-tight as black rubber but impart little to the UV absorbance, were used in the seventh test series.

No provisions were made to control the cover gas in the first five and in the seventh test series. Therefore, the initial gas present in these tests was air. The cover gas used in the sixth test series was 99.999% neon. The neon was introduced by purging of the assembled apparatus through an aperture in each of the test vials' silicone stoppers.

In each experiment, the cleaned and weighed uranium metal beads were loaded into the test vials with the appropriate test solution, salt, and other components. The first five test series used 16-mL vials approximately 7 cm tall and 1.7 cm inner diameter. The sixth and seventh test series used 20-mL vials about 5 cm tall and 2.2 cm inner diameter. The larger vials were used to simplify introduction of the archive sludge materials to the test vials in Series 6. This sludge loading was done in hot cell facilities using remote manipulators.

For the tests with 0.8 g and larger amounts of added Nochar (in Series 3), efforts were made to disperse the uranium metal beads evenly throughout the Nochar by rotating the vial holding the dry beads and dry Nochar granules while the water or salt solution was slowly added to the solids mixture. As the Nochar absorbed the liquid, the rotation continued with the effect that the uranium metal beads became supported in the moist and swelling Nochar. If the water or solution had simply been added to the uranium metal beads and Nochar, the high metal bead density would have caused them to remain together at the bottom of the test vial and not be well dispersed within the Nochar. The water-gas levels in the gas measurement vessels (10-mL plastic syringe in the initial test series, 15-mL glass centrifuge tube in most

tests in subsequent series, 50-mL glass centrifuge tubes in a few tests in the sixth series, and all of the tests in the seventh series) were adjusted to be about 3 mL at the beginning of each test.

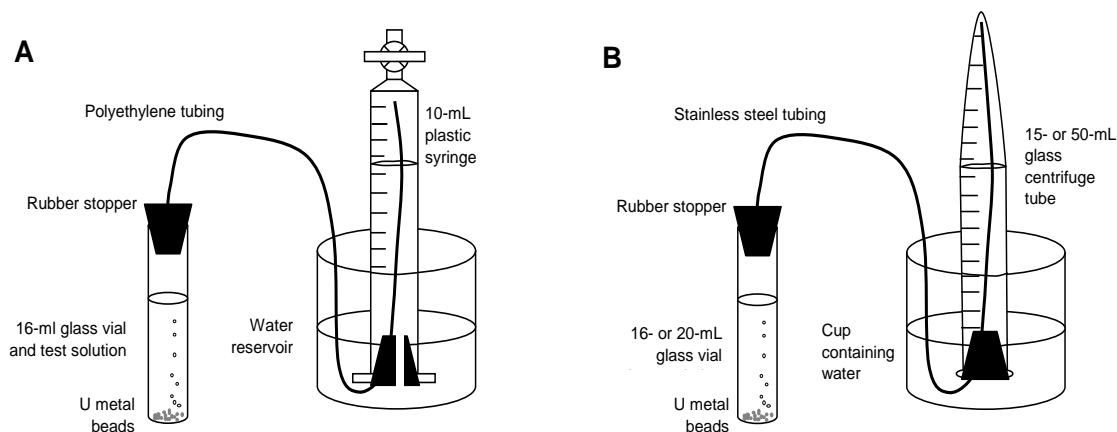


Figure 2.1. Diagram of Gas Generation Apparatus Used in Testing (A. apparatus used in Series 1; B. apparatus used in all succeeding test series [wider 20-mL vials were used in Series 6 and 7])



Figure 2.2. Apparatus in Heating Blocks Used for Series 1 (left) and Series 2 through 7 (second test series is pictured)

The test apparatus were kept in radiological fume hoods for contamination control. The test vials and contents were held at the selected test temperature by placement into aluminum heating blocks kept under feedback thermostat control. The test temperature was registered by a calibrated thermocouple held in similar test vials without the associated gas measurement hardware or held in the heating block. Because of active air flow in the fume hoods, the gas measurement vessels were at ambient laboratory temperature (generally $\sim 21^\circ\text{C}$). Heating expanded the gas (air or neon plus product gases) contained in the test vials. The gas volumes were measured at least once each working day for the seven test series. The gas

volumes fluctuated due to on/off cycling of the heating block and due to room temperature cycling, making point-by-point volume measurements erratic. Therefore, the more reliable differences in gas volumes between the beginning and final readings at room temperature are provided in this report.

Gas leakage from the test apparatus compromised gas volume measurements in the first and sixth test series. The first test series used plastic tubing to connect the test vial and the gas collection syringe (Figure 2.2) while silicone rubber stoppers were used in the sixth test series. Both the plastic tubing and the silicone stoppers leaked measureable amounts of air. Black rubber stoppers, which have much lower gas permeability, were used in the first five test series and neoprene (polychloroprene) rubber stoppers were used in the seventh test series. The gas permeabilities of natural, silicone, and neoprene rubber are compared in Table 2.3 and show how the silicone is much more susceptible to gas leakage.

Table 2.3. Gas Permeabilities for Natural, Silicone, and Neoprene Rubber (Speight 2005)

Material	Gas Permeability, $s^{-1}cm_{Hg}^{-1}$					
	Ne	Ar	N ₂	O ₂	CO ₂	H ₂
Natural rubber; 25°C			9.43	23.3	15.3	52.0
Silicone rubber; 0°C	191	550	227	489		233
Neoprene (polychloroprene); 25°C		3.79	1.2	4.0	25.8	13.6

The first five and the seventh test series were begun with air in the apparatus gas spaces. Gases were sampled and analyzed by mass spectrometry at the conclusion of 60°C heating for the third and all ensuing test series. Gases were not sampled and analyzed in the first two test series. Because of the starting air cover in the third, fourth, fifth, and seventh test series, gases found at the conclusion included atmospheric nitrogen (N₂), oxygen (O₂), argon (Ar), and carbon dioxide (CO₂). The initial cover gas in the sixth test series was neon (Ne). The 99.999% Ne was introduced by purging of the apparatus before commencement of heating. Despite the use of Ne cover gas, significant air contamination was found at the conclusion of the sixth series tests due to the relatively high gas permeability of the silicone rubber stoppers used. At the conclusion of heating, the vessels were returned to room temperature.

In the third and subsequent test series, the contained gas was sampled for analysis by inserting a hollow needle into the stopper and withdrawing a 1-mL sample through small diameter tubing into a gas-tight syringe (Dynatech Precision Sampling Corporation, Model A-2). The sampling syringe was purged before sampling by withdrawing some contained gas through the sampling needle and tubing and then discharging the gas from the syringe. Occasionally, duplicate gas samples were taken. The gas samples were analyzed individually using a Finnigan MAT-271 mass spectrometer according to a routine technical procedure.⁹ The sensitivity of the instrument was checked daily prior to use with high purity nitrogen, N₂, and two air standards were analyzed weekly to assure correct instrument operation.

For tests having solutes such as NaNO₃ or NaNO₂ in the test media, the solutions were adjusted to their initial volumes or weights with DI water addition at the conclusion of the tests to compensate for evaporative water losses to the gas collection system.

⁹ Bos SJ, *Quantitative Gas Mass Spectrometry*, PNNL-98523-284, Pacific Northwest National Laboratory, Richland, Washington, November 30, 2007.

Solution samples were taken at the conclusion of testing and also at the beginning of testing in the sixth and seventh test series. Nitrate and nitrite concentrations for test series one through six were analyzed by absorption spectrophotometry. Spectrophotometry also was used to measure uranium solution concentrations. Spectrophotometric analyses could not be done for the experiments with Nochar because of solution uptake. For nitrate, the absorption peak maximum is at 302 nm (molar extinction coefficient, $\epsilon_{301.7} = 7.7$ L/mol-cm); the nitrite peak is at 355 nm ($\epsilon_{354.9} = 24.7$ L/mol-cm). The nitrate and nitrite absorption spectra measured in the present testing (Figure 2.3) are consistent with published spectra (Wetters and Uglum 1970). However, as will be discussed in more detail in Section 3.3, the black rubber stoppers also contributed to the UV spectrum, complicating the analyses.

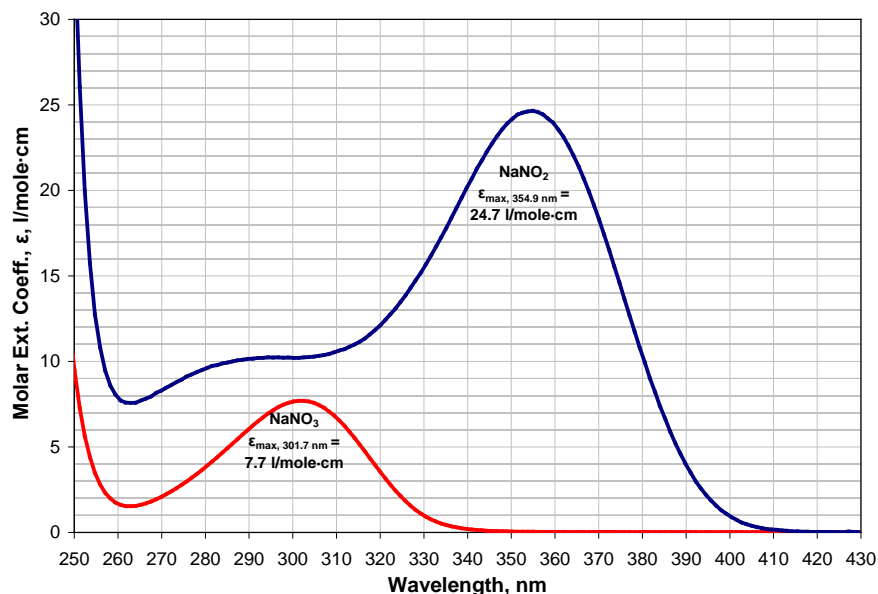


Figure 2.3. UV Absorption Spectra of NaNO₃ and NaNO₂ in 0.1 M NaOH

The chemical reductions of nitrite and the reductions of nitrate to anything but nitrite produce sodium hydroxide (Table 1.1). The sodium hydroxide quantities evolved in testing were determined by measurement of the solution pH and correlation of the pH with the pH found for similar NaNO₃ or NaNO₂ solutions containing known added NaOH concentrations.

The concentrations of ammonia produced by chemical reduction of nitrate and nitrite were measured by ion selective electrode using reagent ammonium chloride (NH₄Cl) for calibration. The method of standard additions was used to determine NH₃ solution concentrations.

The weights of the residual uranium metal beads were determined by retrieving the beads from the test matrix, rinsing the matrix away, and then cleaning the beads of their UO₂ corrosion layers by heating to ~80°C in concentrated H₃PO₄ containing 0.14 M Na₂SO₄. This solution dissolves UO₂ rapidly but attacks uranium metal slowly (Delegard et al. 2008). For tests with UO₂, simulated sludge, or actual sludge, the same process was used but considerably more solids material had to be handled. The residual beads then were rinsed with water, air dried, and weighed. The uranium corrosion rates in the various test matrices were determined based on the initial and final uranium bead weights, the average uranium metal bead diameters based on spherical shape and the known uranium metal density, and the time the beads spent at the test temperature.

Dissolution of Nochar by the concentrated H_3PO_4 / 0.14 M Na_2SO_4 reagent was not attempted. Instead, mechanical means were used to separate the residual uranium metal from the Nochar. Retrieval of the residual uranium metal beads from the tests with Nochar was difficult owing to the adhesiveness of the Nochar, the small size of the uranium metal beads, and the significant expansion that occurs when water is added to Nochar. The most effective way to separate the uranium metal after the corrosion testing was to excise the black regions (indicating product UO_2) from the off-white Nochar using forceps and pointed tools and feeling for the hard uranium metal in the pliable surrounding Nochar. The beads with accompanying Nochar then were placed in water. The Nochar washed away, but with difficulty. To ensure that bead recoveries were maximized, all of the Nochar ultimately was added to water. The recovery procedure involved water dilution of each sample in a beaker to produce a gel sufficiently fluidic to allow, with stirring, gravity settling of the remaining uranium metal beads to the bottom. The uranium metal beads were retrieved by use of magnifying glasses and a transfer pipette.

Nochar's stickiness and affinity for finely divided UO_2 indicate that it may function well as an agglomerating agent for sludge. Particles below 10 μm are treated as respirable material in nuclear safety analysis. Uranium oxide particles generated by uranium metal corrosion in sludge are well under 10 μm diameter (Makenas et al. 1996, 1997, 1998, 1999). The intrinsic UO_2 particle size from U metal corrosion in water is 6 nm (Sinkov et al. 2008).

Measurements of the physical swelling of Nochar mixtures with water and NaNO_3 and NaNO_2 solution were performed by preparing weighed mixtures, allowing the swelling to occur, centrifuging the products, and noting the final centrifuged volumes. The water uptake of Nochar from water-saturated 60°C air also was measured by exposing weighed Nochar portions to water vapor in closed 60°C humidors and periodically reweighing the Nochar.

2.3 Experimental Matrices

Seven uranium metal corrosion test series were performed by executing seven separate approved Test Instructions (TIs).¹⁰ As noted in Section 2.1, each test but one (in Series 7) used 30 uranium metal beads of total weight ranging from 0.10 to 0.11 grams. The beads were approximately spherical in shape and of visibly similar size (about 700 μm diameter given the uranium metal density of 19.1 g/cm^3). A parallel control test with water plus uranium was performed in each test series to provide data for direct comparison with the remaining tests. The tests in Series 1, 2, and 7 were run at 90°C and lasted four or five days. The tests in Series 3, 4, 5, and 6 were run at about 60°C and lasted about four weeks. All tests run at 60°C began with brief (several hour) intervals at 90°C to help overcome the induction times observed in prior tests of uranium corrosion at 60°C (e.g., the tests of uranium metal corrosion in water, simulated sludge, and simulated sludge with grout; Delegard et al. 2004). The test durations at ~60°C and 90°C resulted in about 70 μm corrosion penetration, according to the nominal STP rate of uranium corrosion in the anoxic liquid water control tests, and corroded about half of the starting uranium weight. The uranium metal corrosion rates could be readily calculated by measuring weight losses over the time spans of the corrosion tests because the beads were spherical and of uniform size. Except for the third test series (described further below), all tests used ~10 mL of water or aqueous solution.

¹⁰ Seven TIs were executed under the current revision at the time of the procedure, *Routine Research Operations*, RPL-OP-001, Pacific Northwest National Laboratory, Richland, Washington:

- *Attenuation of Hydrogen Generation Rate in the Process of U Metal Corrosion in Water by Use of Nitrate*

The goal of the work under the first test series (53451-TI10) was to determine the effects of 1, 3, and 6 M NaNO₃ and of 6 M NaNO₂ on the gas generation rate from corrosion of uranium metal beads at 90°C. Although gas volumes and uranium corrosion quantities were measured, no gas sampling or analysis was performed in this test series.

The goal of the work in the second test series (53451-TI11) was to determine the effects of 0.1, 1, and 3 M NaNO₂ and reinvestigate 6 M NaNO₃ effects on uranium metal bead corrosion at ~90°C. The effects of 0.2 M NaNO₃ and 0.2 M NaNO₂ on UO₂ at 90°C (e.g., potential oxidation of UO₂ by nitrate or nitrite) also were studied under the second test series. In these latter two tests, no uranium metal beads were added. Accordingly, the vials were only capped and the testing was done without the gas collection apparatus.

The third test series (under 53451-TI12) had several goals. One goal was to determine the effects of Nochar N960 on uranium metal corrosion in water at various manufacturer-recommended loadings. Loadings ranged from 0.2:1 to 1:1 Nochar:water weight ratio. Another goal was to determine the effects of 1 M NaNO₂, 0.1 M NaNO₂, and 0.1 M NaNO₃ on uranium metal corrosion. The third objective was to determine the effects on uranium metal corrosion of mixing Nochar (at 0.2:1 Nochar:solution weight ratio) with 1 M NaNO₂, 0.1 M NaNO₂, and 0.1 M NaNO₃. The gases at the completions of these tests were sampled and the sample compositions measured by mass spectrometry. Because Nochar had not been used in prior testing, the volume changes and densities of mixtures of Nochar with water and with the salt solutions were measured to obtain information on these important process parameters. Because the potential effect of Nochar on decreasing uranium metal corrosion rate likely would hinge on Nochar's affinity for water, the water uptake on Nochar in saturated water vapor at 60°C was measured as well. Each gas generation test in the third series used 30 uranium metal beads weighing ~0.1 g total and used 4.0 mL of solution. The solution volume had to be decreased to accommodate the swollen Nochar product of many of the tests.

The goals of the fourth test series under 53451-TI13 were to examine in more detail the effects of NaNO₃ and NaNO₂ concentrations (0 to 2 M and 0 to 1 M, respectively) on attenuating hydrogen gas from the reaction of uranium metal with water. New black rubber stoppers were acquired and used in this test series because the existing laboratory supply was exhausted. A single test to determine the effect of phosphate, as 0.07 M Na₂HPO₄, on uranium corrosion was run. Finally, tests of uranium corrosion in 0.5 M NaNO₃ and 0.5 M NaNO₂ under an overburden of 1 mL UO₂ slurry were performed.

and Nitrite as the Hydrogen Scavengers, 53451-TI10, SI Sinkov, PNNL, Richland, Washington (July 2008).

- *Hydrogen Attenuation from U Metal Corrosion by Nitrate and Nitrite*, 53451-TI11, CH Delegard, PNNL, Richland, Washington (August 2008).
- *Hydrogen Attenuation from U Metal Corrosion by Nochar, Nitrate, and Nitrite at 60°C*, 53451-TI12, CH Delegard, PNNL, Richland, Washington (September 2008).
- *Hydrogen Attenuation from U Metal Corrosion by Nitrate, Nitrite, and Phosphate at 60°C*, 53451-TI13, CH Delegard, PNNL, Richland, Washington (November 2008).
- *Attenuation of Hydrogen Generation from Uranium Metal Corrosion by Nitrate and Nitrite with and without K Basin Sludge Components*, 53451-TI15, CH Delegard, PNNL, Richland, Washington (February 2009).
- *Attenuation of Hydrogen Generation from U Metal Corrosion by Nitrate and Nitrite in K Basin Sludge*, 53451-TI18, CH Delegard, PNNL, Richland, Washington (April 2009).
- *Attenuation of Hydrogen Generation from Uranium Metal Corrosion by Dissolved U(VI)*, 53451-TI19, CH Delegard, PNNL, Richland, Washington (August 2009).

The fifth test series (under 53451-TI15) was performed to confirm results of prior studies of the effects of NaNO_3 and NaNO_2 concentration, to determine the effects of addition of small amounts of Nochar and Optimer 7194 Plus to 0.5 M NaNO_2 solution, and to determine the effects of 0.5 M NaNO_3 and 0.5 M NaNO_2 in the full K Basin sludge simulant at 60°C. The composition of the full sludge simulant is given in Table 2.1. New black rubber stoppers and initial air cover gas were used in all tests in this series.

Gas was evolved upon mixing the 0.5 M NaNO_2 with the full sludge simulant in Series 5. Gassing was not observed in the parallel test with 0.5 M NaNO_3 with the full sludge simulant nor had similar immediate gassing been observed in any test in the prior test series. Therefore, nine additional scoping tests were performed to determine which sludge components or component combinations were responsible for the immediate gas formation in the presence of NaNO_2 . Because mass spectrometric analyses showed that the gas was nitric oxide, NO, nitrite reduction reactions were suspected. Therefore, the supplemental testing focused on redox-active sludge components (e.g., UO_2 , $\text{UO}_3 \cdot 2\text{H}_2\text{O}$, ferrihydrite, Optimer 7194 Plus, and Hanford sand). Further scoping tests also were performed to observe if gassing occurred upon mixing samples of actual sludge with 0.5 M NaNO_2 . The actual sludges (KC-2/3 Comp, KE Floc Comp, KC-4, and KE NLOP) were tested in hot cell containment under a separate TI.¹¹ The sludge compositions are given in Table 2.2.

Tests with two archive actual sludges, KE Floc Comp and KC-2/3 Comp, were performed in the sixth test series (under 53451-TI18). Parallel tests in the absence of sludge also were performed. For each set, tests were run in water only, in 0.5 M NaNO_3 , and in 0.5 M NaNO_2 . All tests were run at 60°C and were performed in a fume hood after retrieval of the sludge samples from aliquots taken from hot cell storage. Because the water exposed to new black rubber stoppers contained spectral absorbances that interfered with the nitrate and nitrite spectra, silicone stoppers were used in all experiments of the sixth test series. Each test was run under a 99.999% neon cover gas introduced to the closed test apparatus by five to ten minutes of purging. The neon entered through an aperture in the stopper at the top of the test vial, continued through the stainless steel tube to the gas collection tube, and then was vented to the air.

Significant air in-leakage occurred in all Series 6 tests. The in-leakage was due to the high gas permeability of the silicone stoppers used in this test series. Therefore, neoprene rubber stoppers were used in the Series 7 tests. Despite the gas leakage in the sixth test series, it was discovered that significant hydrogen attenuation was obtained for the test of KC-2/3 Comp in the absence of salt additives. The solution pH for this test was low (~5.5) and relatively high hexavalent uranium [6×10^{-4} M U(VI)] concentrations were in solution. The high U(VI) concentrations were caused by dissolution of the metaschoepite contained in the KC-2/3 Comp sludge at the relatively low pH. It was surmised that the U(VI) might itself have acted as a hydrogen radical scavenger.

Based on the Series 6 test results, tests to determine the effects of dissolved U(VI) as a potential hydrogen radical scavenger from corrosion of uranium metal in water were performed in the seventh test series (under 53451-TI19). A single control test with uranium metal in water only was performed as in all of the other test series. The U(VI) concentrations in three of the tests were varied by varying the pH of metaschoepite suspensions using dilute hydrochloric acid (HCl). The pH levels selected were 6.9

¹¹ *K Basin Sludge Aliquoting and Testing of Nitrate and Nitrite*, 53451-TI16, CH Delegard, PNNL, Richland, Washington (March 2009). The TI was executed under the current revision at the time of the procedure, *Routine Research Operations*, RPL-OP-001, Pacific Northwest National Laboratory, Richland, Washington.

(metaschoepite in the absence of added HCl), 5.1 and 4.3. A test with 0.05 M NaCl was run to determine separately the effect of chloride. The sixth test was conducted with a single uranium metal bead in the presence of 6×10^{-4} M UO_2Cl_2 solution to determine if dissolved U(VI), in the absence of $\text{UO}_3 \cdot 2\text{H}_2\text{O}$ solids, is removed from solution to form relatively insoluble UO_2 by its reaction with hydrogen radicals produced in the corrosion of the single U metal bead. All tests were run at nominally 90°C under air cover gas.

The experimental parameters for the seven gas generation test series are summarized in Table 2.4.

Table 2.4. Experimental Parameters for the Test Series

Test	T, °C	[NaNO ₃], M	[NaNO ₂], M	Other Materials	Solution Vol., mL	Stopper Material ^(a)	Initial Cover Gas
<i>Test Series 1, 53451-TII0</i>							
1	90	0.0	0.0	None – control	10.0	Old BR	Air
2	90	1.0	0.0	None	10.0	Old BR	Air
3	90	3.0	0.0	None	10.0	Old BR	Air
4	90	6.0	0.0	None	10.0	Old BR	Air
5	90	0.0	6.0	None	10.0	Old BR	Air
<i>Test Series 2, 53451-TIII</i>							
1	90	0.0	0.0	None – control	10.0	Old BR	Air
2	90	0.0	0.1	None	10.0	Old BR	Air
3	90	0.0	1.0	None	10.0	Old BR	Air
4	90	0.0	3.0	None	10.0	Old BR	Air
5	90	6.0	0.0	None	10.0	Old BR	Air
6	90	0.2	0	UO ₂ ; no U metal beads	10.0	Plastic cap	Air
7	90	0	0.2	UO ₂ ; no U metal beads	10.0	Plastic cap	Air
8	90	0	0.2	UO ₂ ; no U metal beads	10.0	Plastic cap	Air
<i>Test Series 3, 53451-TII2</i>							
1	60	0.0	0.0	None – control	4.0	Old BR	Air
2	60	0.0	0.0	0.8 g Nochar	4.0	Old BR	Air
3	60	0.0	0.0	0.8 g Nochar	4.0	Old BR	Air
4	60	0.0	0.0	2.0 g Nochar	4.0	Old BR	Air
5	60	0.0	0.0	2.0 g Nochar	4.0	Old BR	Air
6	60	0.0	0.0	4.0 g Nochar	4.0	Old BR	Air
7	60	0.1	0.0	None	4.0	Old BR	Air
8	60	0.0	1.0	None	4.0	Old BR	Air
9	60	0.0	0.1	None	4.0	Old BR	Air
10	60	0.1	0.0	0.8 g Nochar	4.0	Old BR	Air
11 ^(b)	60	0.0	1.0	0.8 g Nochar	4.0	Old BR	Air
12	60	0.0	0.1	0.8 g Nochar	4.0	Old BR	Air
<i>Test Series 4, 53451-TII3</i>							
1	60	0.0	0.0	None – control	10.0	New BR	Air
2	60	0.2	0.0	None	10.0	New BR	Air
3	60	0.5	0.0	None	10.0	New BR	Air
4	60	1.0	0.0	None	10.0	New BR	Air
5	60	2.0	0.0	None	10.0	New BR	Air
6	60	0.0	0.2	None	10.0	New BR	Air

Table 2.4. Experimental Parameters for the Test Series (Cont.)

Test	T, °C	[NaNO ₃], M	[NaNO ₂], M	Other Materials	Solution Vol., mL	Stopper Material ^(a)	Initial Cover Gas
8	60	0.0	0.75	None	10.0	New BR	Air
9	60	0.0	1.0	None	10.0	New BR	Air
10	60	0.5	0.0	1 mL settled UO ₂	10.0	New BR	Air
11	60	0.0	0.5	1 mL settled UO ₂	10.0	New BR	Air
12	60	0.0	0.0	0.07 M Na ₂ HPO ₄	10.0	New BR	Air
<i>Test Series 5, 53451-TII5</i>							
1	60	0.0	0.0	None – control	10.0	New BR	Air
2	60	0.0	0.2	None	10.0	New BR	Air
3	60	0.0	0.5	None	10.0	New BR	Air
4	60	0.0	0.75	None	10.0	New BR	Air
5	60	0.5	0.0	None	10.0	New BR	Air
6	60	1.0	0.0	None	10.0	New BR	Air
7	60	0.0	0.5	1 mL settled UO ₂	10.0	New BR	Air
8	60	0.5	0.0	1 mL settled UO ₂	10.0	New BR	Air
9	60	0.0	0.5	0.01 g Nochar	10.0	New BR	Air
10	60	0.0	0.5	0.0087 g Optimizer 7194 Plus	10.0	New BR	Air
11	60	0.0	0.5	3.264 mL sim. sludge	10.0	New BR	Air
12	60	0.5	0.0	3.264 mL sim. sludge	10.0	New BR	Air
<i>Test Series 6, 53451-TII8</i>							
1	60	0.0	0.0	None – control	10.0	Silicone	Ne
2	60	0.5	0.0	None	10.0	Silicone	Ne
3	60	0.0	0.5	None	10.0	Silicone	Ne
4	60	0.0	0.0	~0.5 mL KE Floc Comp	9.2	Silicone	Ne
5	60	0.5	0.0	~1.2 mL KE Floc Comp	10.2	Silicone	Ne
6	60	0.0	0.5	~1.5 mL KE Floc Comp	10.0	Silicone	Ne
7	60	0.0	0.0	~2.0 mL KC-2/3 Comp	9.5	Silicone	Ne
8	60	0.5	0.0	~1.8 mL KC-2/3 Comp	10.5	Silicone	Ne
9	60	0.0	0.5	~1.8 mL KC-2/3 Comp	10.2	Silicone	Ne
<i>Test Series 7, 53451-TII9</i>							
1	90	0.0	0.0	None – control	10.0	Neoprene	Air
2	90	0.0	0.0	0.05 M NaCl	10.0	Neoprene	Air
3	90	0.0	0.0	2 mL MS ^(c) slurry; pH ~6	10.0	Neoprene	Air
4	90	0.0	0.0	2 mL MS slurry; pH ~5	10.0	Neoprene	Air
5	90	0.0	0.0	2 mL MS slurry; pH ~4	10.0	Neoprene	Air
6	90	0.0	0.0	0.6 mM UO ₂ ²⁺ as UO ₂ Cl ₂ , single U metal bead	10.0	Neoprene	Air
Unless otherwise noted, each test used 30 uranium metal beads weighing ~0.1 g in total.							
(a) BR is black rubber.							
(b) Test not performed because of marked room temperature reaction of Nochar with 1 M NaNO ₂ solution in parallel test without added uranium metal.							
(c) MS is metaschoepite.							

3.0 Results

The results from experiments to determine the effects of sodium nitrate, sodium nitrite, Nochar Acid Bond N960, sodium hydrogen phosphate, and hexavalent uranium additives on the reaction of uranium metal with water in aqueous solutions, in UO_2 , and in simulated and actual sludge are summarized in Table 3.1. The effects of these additives on the uranium metal corrosion rates are described in more detail in Section 3.1. Section 3.2 describes the effects of the additives on the hydrogen gas generation rates. The product gas compositions also are described in Section 3.2. Findings from analyses of the product solutions (nitrate, nitrite, hydroxide, and ammonia) are examined in light of the uranium metal corrosion and gas products to arrive, where possible, at material balances in Section 3.3. The effects of NaNO_3 and NaNO_2 on UO_2 are discussed in Section 3.4. The physical properties of mixtures of Nochar with water and solutions of NaNO_3 and NaNO_2 and the water uptake of Nochar from water-saturated 60°C air are described in Section 3.5. The scope of further proposed testing is outlined in Section 3.6.

3.1 Effects of Additives on Uranium Metal Corrosion Rates

The uranium corrosion rates in each test were determined by measuring the starting and ending masses of the 30 uranium metal beads, calculating the average diameters of the beads at the beginning and end of each test (assuming identical size and spherical shape, based on uranium metal density of 19.1 g/cm^3), determining the difference in diameters, dividing by two to obtain linear penetration, and dividing by the time at reaction temperature. The uranium corrosion data are summarized in Table 3.1.

The nominal test temperatures were determined by averaging the temperatures logged manually over the durations of each test series. The times at temperature likewise were determined based on manually logged values with standard deviations at 1σ of $<2^\circ\text{C}$ (generally $<1^\circ\text{C}$) for all average temperatures reported. Significant heating intervals at about 90°C were imposed in the third through sixth test series to overcome the lengthy and unknown induction time that would have been required had the experiments been run entirely at the target 60°C . The induction time at 90°C was expected to be negligible according to prior studies (Delegard and Schmidt 2008, Delegard et al. 2000). Based on the STP rate law (Plys and Schmidt 2006, Appendix G), the uranium metal corrosion rate at 90°C is about 7-times faster than at 60°C . Therefore, the higher corrosion rates for times at the elevated temperatures (e.g., 90°C) were accounted in determining the total amount of corrosion expected based on the STP rate law.

Test 1 in each test series was a control test with U metal beads and water only (i.e., containing no additive or sludge solid). The uranium metal corrosion rates expected at the test temperatures, based on the STP rate equation, are presented in Table 3.1 for comparison with the observed corrosion rate. For example, in the first test series, the uranium metal corrosion rate observed at 91.4°C was $0.642 \mu\text{m/h}$, 78% of the $0.821 \mu\text{m/h}$ rate expected by the STP equation. It is seen that the observed uranium metal corrosion rates in water ranged from about 53 to 125% of the expected rate (average $84\% \pm 26\%$ at one standard deviation).

Table 3.1. Uranium Metal Corrosion Rate and Hydrogen Generation Data

Test	[NaNO ₃]/ [NaNO ₂], M	Other Materials	U Bead wt., mg		Corrosion Rate, μm/h	Corr. Rate Relative to Control	Corr. Rate Attenuation Factor ^(a)	H ₂ Produced, moles	H ₂ Relative to Control	H ₂ Attenuation Factor ^(a)
			Initial	Final						
<i>Test Series 1</i> – Rate at 91.4°C average temperature = 0.821 μm/h ^(b)										
1	0.0/0.0	None	114.07	69.92	0.642	1.0	1.0	Not measured.		
2	1.0/0.0	None	104.14	72.87	0.464	0.72	1.4	Not measured.		
3	3.0/0.0	None	101.45	81.01	0.296	0.46	2.2	Not measured.		
4	6.0/0.0	None	116.43	97.68	0.244	0.38	2.6	Not measured.		
5	0.0/6.0	None	103.61	94.92	0.119	0.19	5.4	Not measured.		
<i>Test Series 2</i> – Rate at 84.8°C average temperature = 0.774 μm/h ^(b)										
1	0.0/0.0	None	101.09	55.27	0.451	1.0	1.0	Not measured.		
2	0.0/0.1	None	109.26	85.25	0.201	0.45	2.2	Not measured.		
3	0.0/1.0	None	95.07	80.11	0.134	0.30	3.4	Not measured.		
4	0.0/3.0	None	111.55	97.82	0.109	0.24	4.1	Not measured.		
5	6.0/0.0	None	106.68	85.66	0.178	0.39	2.5	Not measured.		
<i>Test Series 3</i> – Rate at 60.9°C average temperature = 0.106 μm/h ^(b)										
1	0.0/0.0	None	112.39	45.73	0.119	1.0	1.0	0.276	1.00	1.0
2	0.0/0.0	0.2 g Nochar/g solution	108.53	49.17 ^(c)	0.105	0.89	1.1	0.197	0.71	1.4
3	0.0/0.0	0.2 g Nochar/g solution	108.18	50.70 ^(c)	0.101	0.85	1.2	0.218	0.79	1.3
4	0.0/0.0	0.5 g Nochar/g solution	101.38	50.08 ^(c)	0.0926	0.78	1.3	0.126	0.46	2.2
5	0.0/0.0	0.5 g Nochar/g solution	107.37	58.86 ^(c)	0.0818	0.69	1.4	0.104	0.38	2.6
6	0.0/0.0	1.0 g Nochar/g solution	107.01	58.19	0.0827	0.70	1.4	0.150	0.54	1.8
7	0.1/0.0	None	108.08	57.84	0.0850	0.72	1.4	0.0859	0.31	3.2
8	0.0/1.0	None	103.12	92.13	0.0164	0.14	7.2	0.0000479	0.00017	5800
9	0.0/0.1	None	113.15	97.12	0.0228	0.19	5.2	0.00664	0.024	42
10	0.1/0.0	0.2 g Nochar/g solution	107.29	Remaining beads were not recovered. ^(d)				0.0421	0.15	6.6
11	0.0/1.0	0.2 g Nochar/g solution	Test not performed.							
12	0.0/0.1	0.2 g Nochar/g solution	105.79	Remaining beads were not recovered. ^(d)				0.0000672	0.00024	4100

Table 3.1. Uranium Metal Corrosion Rate and Hydrogen Generation Data (Cont.)

Test	[NaNO ₃]/ [NaNO ₂], M	Other Materials	U Bead wt., mg		Corrosion Rate, μm/h	Corr. Rate Relative to Control	Corr. Rate Attenuation Factor ^(a)	H ₂ Produced, mmoles	H ₂ Relative to Control	H ₂ Attenuation Factor ^(a)
			Initial	Final						
<i>Test Series 4 – Rate at 62.6°C average temperature = 0.120 μm/h^(b)</i>										
1	0.0/0.0	None	99.38	61.71	0.0831	1.0	1.0	0.281	1.00	1.0
2	0.2/0.0	None	99.81	67.33	0.0697	0.84	1.2	0.0472	0.17	6.0
3	0.5/0.0	None	105.24	77.70	0.0555	0.67	1.5	0.0117	0.042	24
4	1.0/0.0	None	100.91	68.53	0.0689	0.83	1.2	0.000416	0.0015	670
5	2.0/0.0	None	100.69	72.31	0.0594	0.71	1.4	0.00000655	0.000023	43000
6	0.0/0.2	None	101.05	87.09	0.0275	0.33	3.0	0.0000148	0.000053	19000
7	0.0/0.5	None	106.19	83.72	0.0441	0.53	1.9	0.00000613	0.000022	46000
8	0.0/0.75	None	102.69	82.43	0.0404	0.49	2.1	0.0000117	0.000042	24000
9	0.0/1.0	None	102.81	89.48	0.0259	0.31	3.2	0.00000821	0.000029	34000
10	0.5/0.0	UO ₂	104.07	76.69	0.0556	0.67	1.5	0.00102	0.0036	270
11	0.0/0.5	UO ₂	104.30	80.72	0.0471	0.57	1.8	0.00210	0.0075	130
12	0.0/0.0	0.07 M Na ₂ HPO ₄	104.60	44.43	0.194	2.3	0.43	0.530	1.88	0.53
<i>Test Series 5 – Rate at 61.4°C average temperature = 0.109 μm/h^(b)</i>										
1	0.0/0.0	None	96.17	61.38	0.0736	1.0	1.0	0.228	1.00	1.0
2	0.0/0.2	None	104.59	103.86	0.00127	0.017	58	0.0000766	0.00034	3000
3	0.0/0.5	None	100.12	98.57	0.00278	0.038	26	0.0000150	0.000066	15000
4	0.0/0.75	None	102.82	99.76	0.00542	0.074	14	Gas sample lost.		
5	0.5/0.0	None	98.64	68.17	0.0619	0.84	1.2	0.00247	0.011	92
6	1.0/0.0	None	103.15	86.77	0.0304	0.41	2.4	0.0000578	0.00025	3900
7	0.0/0.5	UO ₂	99.22	87.77 ^(c)	0.0214	0.29	3.4	0.00292	0.013	78
8	0.5/0.0	UO ₂	103.12	81.87	0.0401	0.55	1.8	0.00282	0.012	81
9	0.0/0.5	0.01 g Nochar	98.89	82.21	0.0319	0.43	2.3	0.00000717	0.000031	32000
10	0.0/0.5	0.0087 g Optimer 7194 Plus	96.87	95.94	0.00170	0.023	43	0.00000369	0.000016	62000
11	0.0/0.5	3.264 mL sim. sludge	96.37	79.12	0.0337	0.46	2.2	0.000527	0.0023	430
12	0.5/0.0	3.264 mL sim. sludge	102.38	86.47	0.0425	0.58	1.7	0.000220	0.00096	1000

Table 3.1. Uranium Metal Corrosion Rate and Hydrogen Generation Data (Cont.)

Test	[NaNO ₃]/ [NaNO ₂], M	Other Materials	U Bead wt., mg		Corrosion Rate, μm/h	Corr. Rate Relative to Control	Corr. Rate Attenuation Factor ^(a)	H ₂ Produced, mmoles	H ₂ Relative to Control	H ₂ Attenuation Factor ^(a)
			Initial	Final						
<i>Test Series 6 – Rate at 61.3°C average temperature = 0.109 μm/h^(b)</i>										
1	0.0/0.0	None	105.39	72.72	0.0576	1.0	1.0	0.0471	1.00	1.0
2	0.5/0.0	None	105.63	60.16	0.0847	1.5	0.68	0.000405	0.0086	120
3	0.0/0.5	None	104.97	96.68	0.0134	0.23	4.3	0.0000728	0.00015	6500
4	0.0/0.0	~0.5 mL KE Flocc Comp	102.86	80.03	0.0394	0.68	1.5	0.0235	0.50	2.0
5	0.5/0.0	~1.2 mL KE Flocc Comp	104.32	87.63	0.0278	0.48	2.1	0.000258	0.0055	180
6	0.0/0.5	~1.5 mL KE Flocc Comp	104.92	93.08	0.0193	0.34	3.0	0.0000267	0.00057	1800
7	0.0/0.0	~2.0 mL KC-2/3 Comp	106.22	91.45	0.0241	0.42	2.4	0.0000135	0.00029	3500
8	0.5/0.0	~1.8 mL KC-2/3 Comp	102.17	96.89	0.00858	0.15	6.7	0.0000760	0.0016	620
9	0.0/0.5	~1.8 mL KC-2/3 Comp	103.59	97.37	0.0100	0.17	5.7	0.000280	0.0060	170
<i>Test Series 7 – Rate at ~90.3°C average temperature = 0.771 μm/h^(b)</i>										
1	0.0/0.0	None	96.73	43.18	0.963	1.00	1.0	0.352	1.00	1.0
2	0.0/0.0	0.05 M NaCl	99.29	35.12	1.21	1.25	0.80	0.459	1.3	0.77
3	0.0/0.0	2 mL MS ^(c) slurry; pH 6.9	101.82	42.42	1.05	1.09	0.92	0.405	1.6	0.87
4	0.0/0.0	2 mL MS slurry; pH 5.1	101.65	68.39	0.514	0.53	1.9	0.135	0.38	2.6
5	0.0/0.0	2 mL MS slurry; pH 4.3	102.49	32.15	1.33	1.4	0.72	0.0833	0.24	4.2
6	0.0/0.0	0.6 mM UO ₂ ²⁺ as UO ₂ Cl ₂	1.36	0.15	2.59	2.7	0.37	Not measured.		
<p>(a) Attenuation factor = (Corrosion rate or amount of H₂ in experiment)/(Corrosion rate or amount of H₂ in control test 1 in each respective series).</p> <p>(b) Corrosion rate at average test temperature based on the STP rate law (Appendix G of Plys and Schmidt 2006).</p> <p>(c) 22, 23, 27, and 28 beads recovered, respectively, in Tests 2, 3, 4, and 5 of Series 3 and 29 beads in Test 7 of Series 5; final bead weights were pro-rated by factors of 30/22, 30/23, 30/27, 30/28, and 30/29, respectively. All 30 beads were recovered in the other tests except Tests 10 and 12 in the third test series.</p> <p>(d) Uranium metal beads were not recovered in these tests because of the difficulty in separating the residual beads from Nochar and because the Nochar-salt mixtures showed high reactivity precluding its applicability and acceptability for WIPP. See Section 3.2.</p> <p>(e) MS is metaschoepite.</p>										

3.1.1 Effect of Nochar on Corrosion Rate

The effect of Nochar in inhibiting the uranium metal corrosion rate at 60°C as a function of the Nochar:water weight ratio are shown in Figure 3.1. The corrosion rate decrease for Nochar at the highest recommended loading (where the Nochar weight matches that of the water) is about 30%.

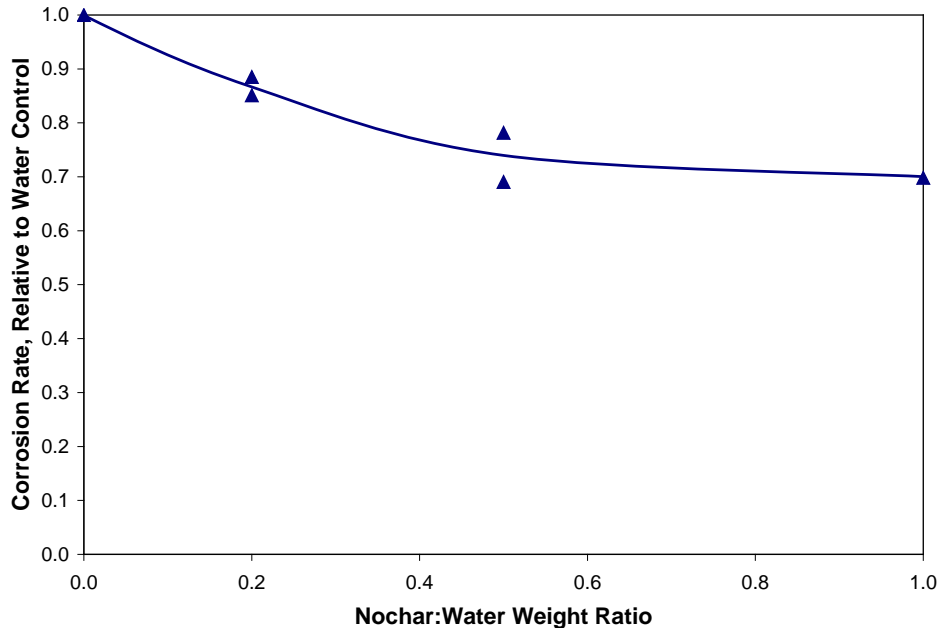


Figure 3.1. Effect of Nochar:Water Weight Ratio on Inhibiting Uranium Metal Corrosion at 60°C

3.1.2 Effects of Nitrate, Nitrite, and Phosphate on Corrosion Rate

A single test was performed to determine if phosphate, in the form of 0.07 M Na_2HPO_4 , would be effective in decreasing hydrogen generation. As shown in Table 3.1, for Test 12 in Series 4, phosphate actually increased the uranium metal corrosion rate by a factor of about 2.3. Further tests with phosphate were not performed.

Thirty-two tests (including the six control tests with water and U metal beads only) were conducted to determine the effects of varying NaNO_3 and NaNO_2 aqueous solution concentration on uranium metal corrosion rate and hydrogen generation. The dependence of uranium corrosion rate on NaNO_3 and NaNO_2 concentration at the nominal 90°C and 60°C test temperatures are plotted in Figure 3.2. It is seen that in 90°C solution and at each concentration, NaNO_2 is about twice as effective as NaNO_3 in decreasing the uranium metal corrosion rate. The maximum corrosion rate decrease, about a factor of 5, is shown for 6 M NaNO_2 while 6 M NaNO_3 decreases the corrosion rate about a factor of 2.5. Although the data at 60°C are more scattered, NaNO_2 is generally more effective than NaNO_3 in decreasing the corrosion rate.

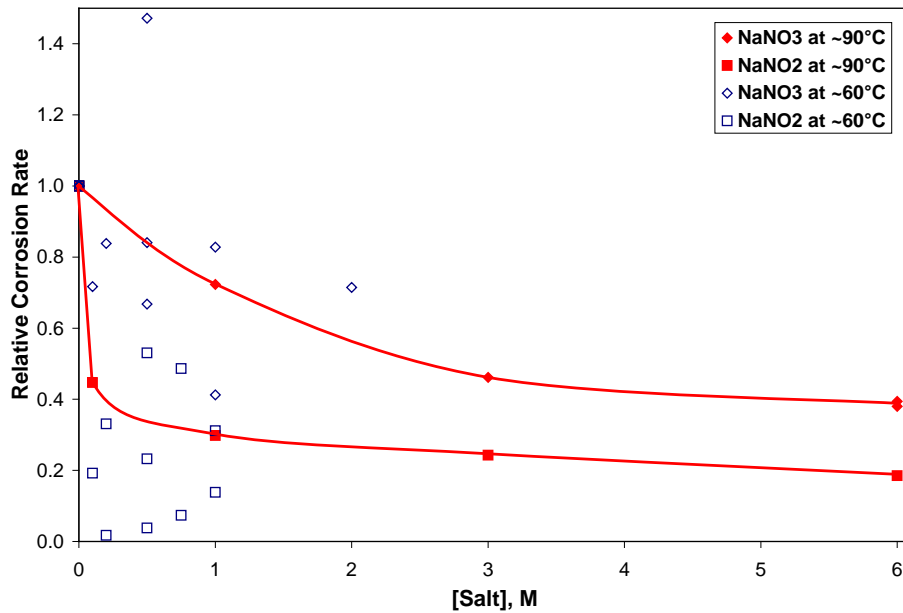


Figure 3.2. Effect of NaNO_3 and NaNO_2 Concentrations on Inhibiting Uranium Metal Corrosion in Aqueous Salt Solutions at about 60°C and 90°C

3.1.3 Effects of Nitrate and Nitrite with Other Additives and with Sludge Solids on Corrosion Rate

Experiments were performed to determine the effectiveness of nitrate and nitrite in the presence of individual sludge components (Optimer 7194 Plus flocculating agent, for a single nitrite test, and UO_2), additives (Nochar Acid Bond 960), a simulated sludge, and two actual sludge materials. The corrosion rate attenuation factor, which is the ratio of the corrosion rate observed in the control test for a particular test series divided by the corrosion rate observed in the presence of the nitrate or nitrite with and without additive or sludge material, was calculated for each experiment (Table 3.1). The data are plotted in Figure 3.3.

Overall, the corrosion rate attenuations for tests with nitrate were lower than those with nitrite. Except for one test with actual sludge KC-2/3 Comp, where the attenuation factor was 6.7, the corrosion rate attenuation factors with nitrate were 2.4 or less. The corrosion rate attenuation factors in the presence of nitrite range from 1.8 to 58; most corrosion rate attenuation factors for nitrite were ~2 to 5.

For the simulated sludge, which contained equal uranium mole amounts of U(IV) and U(VI) solid phases (uraninite and metaschoepite, respectively), the corrosion rate attenuation factors were 1.7 and 2.7, respectively, for 0.5 M nitrate and nitrite. For the actual sludge sample, KE Floc Comp, the corrosion rate attenuation factors were about the same as for the simulated sludge, 1.5 and 2.4, respectively. The corrosion rate attenuation factors for the actual sludge sample KC-2/3 Comp, were 6.7 and 5.7, respectively, for 0.5 M nitrate and nitrite.

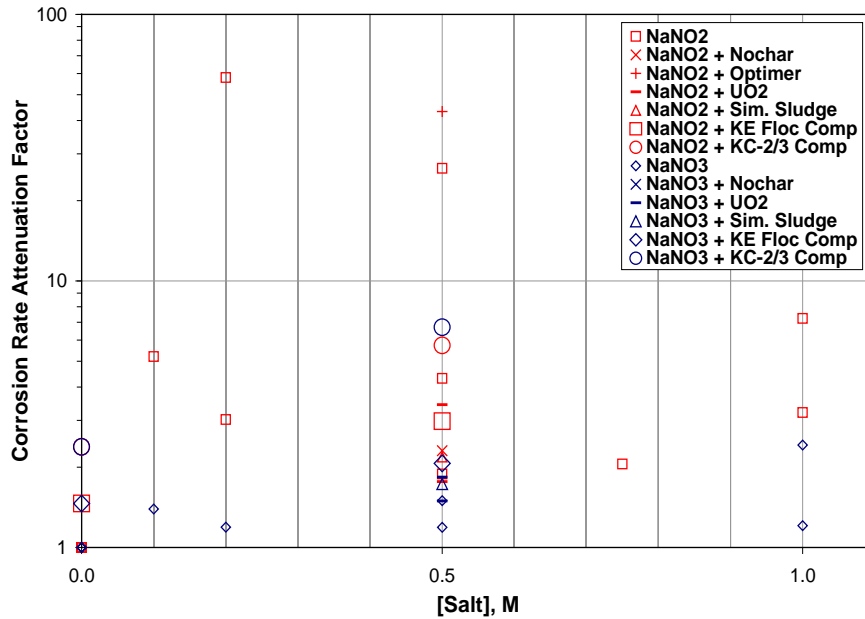


Figure 3.3. Effect of NaNO_3 and NaNO_2 Concentrations on Inhibiting Uranium Metal Corrosion in Aqueous Salt Solutions and in the Presence of Additives and Sludge Components at 60°C

3.2 Effects of Additives on Hydrogen Generation Rate and Gas Composition

Gas volumes and compositions for tests in Series 3 through 7 are shown in Appendix B. Hydrogen, from the corrosion of uranium metal in water, was found in all tests. Because Ar is inert to chemical reaction, the observed O_2 :Ar and N_2 :Ar ratios give evidence of any reaction that might have produced or consumed O_2 and N_2 . For Series 6, however, gas ratio interpretations were partially compromised by the high and varied permeability of silicone to atmospheric Ar, O_2 , and N_2 . Oxygen was consumed in all tests in Series 3, 4, and 5 based on O_2 :Ar ratios and likely was consumed in all tests in Series 6 as well. Oxygen consumption from the air cover gas caused overall gas volume decrease in many tests in Series 3, 4, and 5. Methane, CH_4 , produced by the reaction with water of uranium carbide (UC) present in the uranium metal (Bradley and Ferris 1962 and 1964), was observed in many of the tests and C_2H_x (i.e., ethane, ethylene, acetylene), also from hydrolysis of UC, was observed in many tests. Methane and C_2H_x were observed in gas analyses of prior gas generation tests of K Basin sludge (Delegard et al. 2000), metallic uranium fuel (Schmidt et al. 2004), and uranium metal beads (from the same source as used in the present tests; Delegard et al. 2004).

The volumes of O_2 and N_2 in the gas space at the beginning of each experiment were determined based on the initial gas volume at room temperature and the O_2 and N_2 concentrations in normal air. For example, the initial gas (air) volume in Test 1 of Series 3 was 13.15 mL and air is 20.946 mole% (and vol%) O_2 . Therefore, the initial O_2 volume is 2.75 mL. The O_2 and N_2 quantities in the gas space at the end of each experiment in Series 3, 4, 5, and 7 were determined based on the initial gas volumes, the known concentrations of Ar, O_2 , and N_2 in air, and the Ar, O_2 , and N_2 concentrations measured in the gas samples taken at the end of each test. Because Ar does not react and is not produced in any of the tests, the Ar concentration indicates whether O_2 and N_2 concentrations increase or decrease in the sampled gas

space. The H₂ quantities at the end of each experiment were determined based on the total final room temperature gas volume and the measured H₂ concentration in the gas sample at the end of each test. Similar calculations were made for other gases such as N₂O and NO_x ordinarily found in negligible atmospheric concentrations. Although trace minor gas concentrations are found in air, initial H₂, CH₄, C₂H_x (i.e., ethane, ethylene, and acetylene, C₂H₆, C₂H₄, and C₂H₂, respectively), N₂O, and NO_x (or NO) concentrations were assumed to be zero in each test.

The gas quantities expressed in volumes may be converted to moles using the Ideal Gas Law. The gas quantity calculations are shown in Table 3.2. Note the differences in the calculations used for Series 3, 4, 5, and 7, which began with air cover gas and used relatively leak-tight rubber stoppers, and Series 6, which began with neon cover gas and using silicone stoppers having high gas permeability.

Table 3.2. Gas Quantity Calculations

Value	Gases Measured	Example Equation
Initial individual gas volume; Series 3, 4, 5, and 7	O ₂ , N ₂	$V_{O_2, \text{initial}} = V_{\text{total, initial}} \times [O_2]_{\text{air}}$
Initial individual gas volume; Series 6	Ne	$V_{\text{Ne, initial}} = V_{\text{total, initial}}$
Final individual gas volume; Series 3, 4, 5, and 7	O ₂ , N ₂	$V_{O_2, \text{final}} = V_{\text{total, initial}} \times \frac{[Ar]_{\text{air}}}{[Ar]_{\text{final}}} [O_2]_{\text{final}}$
	All but O ₂ and N ₂	$V_{H_2, \text{final}} = V_{\text{total, final}} \times [H_2]_{\text{final}}$
Final individual gas volume; Series 6	All	$V_{O_2, \text{final}} = V_{\text{total, final}} \times [O_2]_{\text{final}}$
Moles of gas were calculated based on the Ideal Gas Law at 21°C (294) lab temperature:		
$\text{Moles of gas} = \frac{PV}{RT} = \frac{1 \text{ atm} \times V \text{ (liters)}}{\frac{0.082058 \text{ liter} \cdot \text{atm}}{\text{mole} \cdot \text{deg}} \times 294 \text{ deg}} = \frac{V \text{ (mL)}}{24,125 \text{ mL / mole}}$		

3.2.1 Hydrogen Gas Attenuation

As noted in Section 1.0, the suppression, diminution, or complete elimination of the H₂ gas evolution from K Basin sludge is desired for both operational safety and compelling economic reasons. Therefore, the experimental outcome of most interest to the STP is determination of the degree to which the tested additives; nitrate, nitrite, phosphate, Nochar Acid Bond N960, and U(VI); affect the rate of H₂ generation from the reaction of uranium metal with water. To obtain basic understanding, most of the tests were with U metal beads in aqueous solution alone. The H₂ attenuation factor is used to assess the effectiveness of the various additives. As shown in the footnotes to Table 3.1, the attenuation factor for a particular test is the ratio of the amount of H₂ produced in the control test containing water alone to the amount of H₂ gas produced by the test in question.

Based on data for Series 3 given in Table 3.1, Nochar was found to be only marginally effective in decreasing H₂ generation rates with the H₂; the attenuation factors range from about 1.3 to 2.6 as the dry

Nochar to water weight ratio varied from 0.2 to 1.0. However, Nochar enhanced the H_2 suppression effect of nitrite. In a single test, it was seen that phosphate actually increased the U corrosion and H_2 generation rates. U(VI) in genuine sludge was suspected to be responsible for high hydrogen attenuation. Most of the remaining studies focused on nitrate and nitrite in aqueous solution in the presence of added Nochar, sludge components (Optimer 7194 Plus and UO_2), simulated sludge, and genuine sludge. Initial tests of the effects of U(VI) in aqueous solution, with and without U(VI) solid phase present as metaschoepite, also were performed.

The H_2 attenuation factors for the experiments in Series 3, 4, 5, 6, and 7 (i.e., all experiments for which gases were analyzed) are summarized in Table 3.1. The results for tests with no added salts and the tests with sodium nitrate and sodium nitrite are plotted as functions of salt concentration in Figure 3.4.

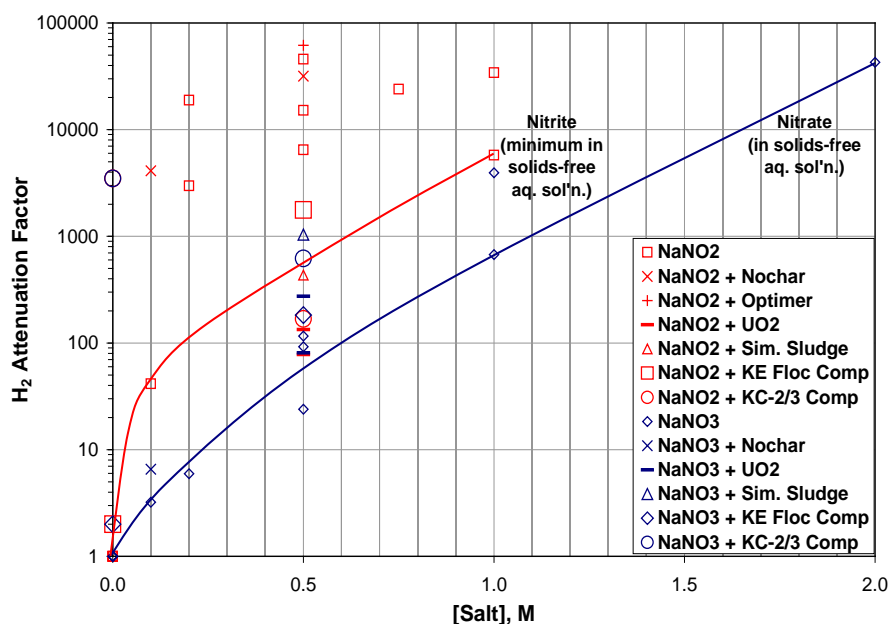


Figure 3.4. Hydrogen Attenuation Factors as Functions of Sodium Nitrate or Nitrite Concentrations in Test Series 3, 4, 5, and 6

It is seen that both nitrate and nitrite strongly attenuated H_2 release with the effectiveness increasing with increasing salt concentration. For nitrate solutions, attenuation factors rose from about 3 at 0.1 M $NaNO_3$ to about 60 at 0.5 M $NaNO_3$ and then to about 600 at 1 M $NaNO_3$. At comparable concentrations, nitrite was at least ten-times more effective than nitrate (i.e., the H_2 attenuation factor was ten-times higher and the amount of H_2 produced was ten-times lower for nitrite than nitrate).

A number of the tests with nitrite in aqueous solution alone showed H_2 attenuation factors even greater than the minimum indicated by the upper curved line in Figure 3.4. For example, it is seen that the addition of Nochar to nitrite solution increased the H_2 attenuation factor by about a factor of 100 compared to the minimum attenuation factor observed for nitrite in the absence of Nochar. In contrast, Nochar had little effect on nitrate in the single test performed. A single test of 0.5 M nitrite with the flocculating agent Optimer 7194 Plus also enhanced the H_2 attenuation factor. However, other nitrite tests without the Nochar or Optimer 7194 Plus organic additives also showed H_2 attenuation factors, ranging from ~3,000 to 50,000 between 0.2 and 1 M $NaNO_2$, markedly higher than the minimum ~100 to

6,000 observed over the same concentration range. The enhanced H₂ attenuation may have been due to trace organics or other agents released by the new rubber stoppers used in Series 4 and 5. In any event, the H₂ attenuation factors for nitrite in simple aqueous solution were at least ten-times higher than those of nitrate at the same concentration.

The differences between nitrate and nitrite performance narrowed in the presence of UO₂, with the H₂ attenuation factors increasing for nitrate and decreasing for nitrite compared with the factors observed in the aqueous solution alone. Thus, in separate experiments in 0.5 M NaNO₃, H₂ attenuation factors of 130 and 78 were observed while in 0.5 M NaNO₂, H₂ attenuation factors were 270 and 81. Without UO₂, the expected H₂ attenuation factor in 0.5 M NaNO₃ would be ~50 while the minimum H₂ attenuation factor in 0.5 M NaNO₂ would be ~500.

With simulated sludge and 0.5 M salt, H₂ attenuation factors were 1,000 for nitrate and 430 for nitrite as determined in Series 5 tests while H₂ attenuation factors were measured in Series 6 for two different actual archive sludge materials. Tests with actual sludge were done in water, 0.5 M NaNO₃, and 0.5 M NaNO₂ solution. The two archive sludge materials were KE Floc Comp, a flocculated floor, pit, and canister sludge composite similar to containerized sludge, and KC-2/3 Comp, a uranium-rich composite of canister sludge representative of sludge in the settler tanks. Because both sludge composites have been kept in archive for ~10 years, much of the original UO₂ has oxidized to U(VI) phases such as metaschoepite (see Table 2.2).

The H₂ attenuation factor for KE Floc Comp sludge in water alone was 2.0. This level of inhibition is similar to that observed to be imposed by sludge overburden in prior gas generation testing (Delegard et al. 2004). With 0.5 M NaNO₃, the H₂ attenuation coefficient was 180 and in 0.5 M NaNO₂ was 1800. These values are of the same magnitude, though in opposite order, as those observed for the simulated sludge.

The H₂ attenuation factor for KC-2/3 Comp sludge in water alone (no added salt) was 6500. As shown by the U metal corrosion results, however, corrosion still occurred. Therefore, the drastically attenuated H₂ rate in this test was not caused by corrosion inhibition but must have occurred by hydrogen scavenging. The H₂ attenuation factors for KC-2/3 Comp were 620 in 0.5 M NaNO₃ and 170 in 0.5 M NaNO₂. Further discussion on the unusual behavior of the KC-2/3 Comp sludge will be provided later in this report.

The H₂ attenuations observed for the control tests and the tests with added nitrate or nitrite as a function of the corrosion rate attenuation factors are plotted in Figure 3.5. It is seen that for several tests, part of the H₂ attenuation could be attributed to low uranium corrosion (i.e., high corrosion rate attenuation factors). Three tests in particular; Tests 2, 3, and 10 in Series 5; had corrosion rate attenuation factors that were greater than 10. Test 4 in Series 5 also had a corrosion rate attenuation factor greater than 10 (it was 14) but was not plotted in Figure 3.5 because the gas sample was lost. Three of these four tests contained NaNO₂ in aqueous solution at concentrations ranging from 0.2 to 0.75 M; one of the tests contained 0.5 M NaNO₂ with Optimer 7194 Plus. Based on the observed low corrosion rates, it appears that these samples did not overcome the induction times to reach the anoxic conditions needed for high corrosion rates to occur.

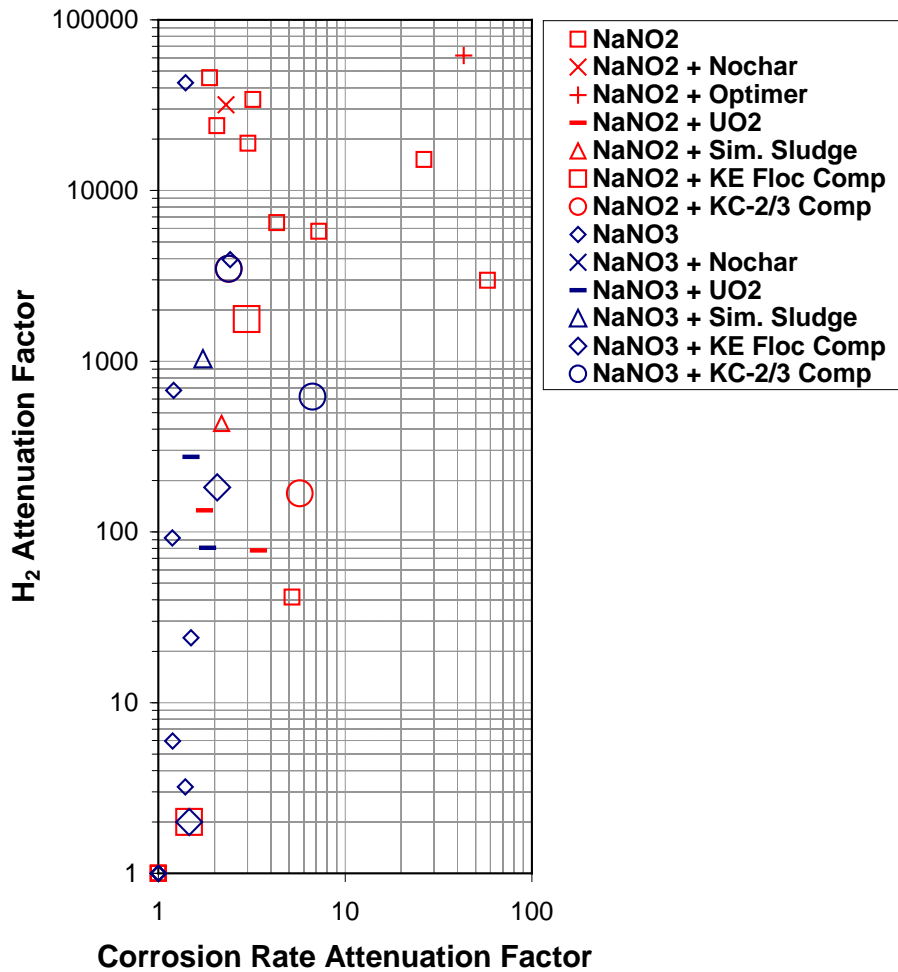


Figure 3.5. Hydrogen Attenuation Factors as Functions of Corrosion Rate Attenuation Factors for the Control Tests and Tests with Added Nitrate or Nitrite

The data plotted in Figure 3.5 also demonstrate that, overall, corrosion rates were less attenuated for nitrate than for nitrite. With one exception (Test 7 in Series 6; 0.5 M NaNO₃ + KC-2/3 Comp; with a corrosion rate attenuation factor of 6.7), the corrosion rate attenuation factors for systems containing nitrate were 2.4 or lower.

3.2.2 Gas Analysis Results for Series 3

Test Series 3 was performed to examine the influence of nitrate, nitrite, and Nochar Acid Bond 960 on the corrosion of uranium metal in water. Eight of the twelve tests were with Nochar or with Nochar plus nitrate or nitrite. One of the planned tests (Test 11), which had 1 M NaNO₂ solution added to Nochar, was not performed when a parallel test lacking the uranium metal beads showed rapid discoloration (yellowing) and noticeable immediate gassing at room temperature.

The molar quantities of H₂, O₂, and N₂ produced or consumed in tests from Series 3 are compared with the molar quantities of corroded uranium metal in Figure 3.6 and its associated table. Hydrogen was produced in each test in Series 3 but in vastly different quantities. It is seen that increasing amounts of

Nochar decreased H₂ production by about a factor of two. However, nitrate and especially nitrite (Tests 7, 8, and 9) as well as the Nochar and 0.1 M nitrate or nitrite mixtures (Tests 10 and 12, respectively) decreased H₂ generation strongly compared with the control Test 1. It is important to note that the H₂ generated for 0.1 M nitrate test in the presence of Nochar (Test 10) was about half that observed in the parallel test without Nochar (Test 7) while the H₂ generated in the 0.1 M nitrite test with Nochar (Test 12) was about 1% of that found in the parallel test without Nochar (Test 9).

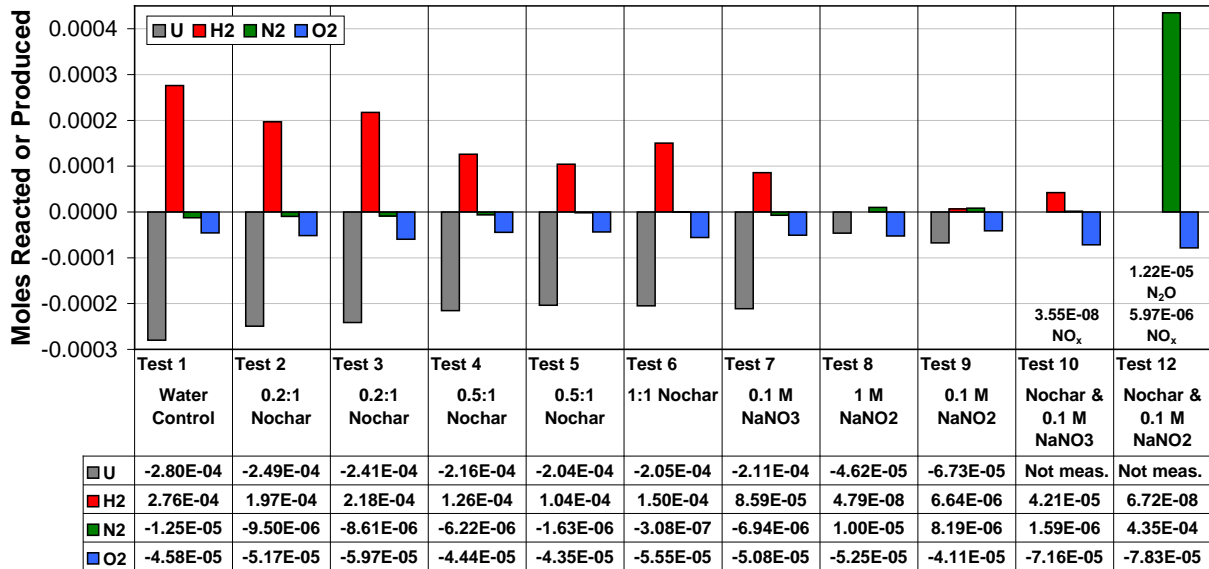


Figure 3.6. Moles of Gas Produced or Reacted and Moles of Uranium Metal Reacted in Series 3

The gas analyses also showed that O₂ was consumed in each test. Nitrogen changes generally were small; N₂ was consumed in the water control, Test 1, in all tests with Nochar and water without salt, and in Test 7 with 0.1 M NaNO₃. The greatest amount of N₂ consumption, 1.25×10⁻⁵ moles, was for the Test 1 control. Nitrogen consumption in Test 1 is supported by the observed decreased N₂:Ar mole ratio, 81.1, compared with the N₂:Ar mole ratio found for the original air cover gas of 83.6. The chemical reduction of N₂ by U metal to form NH₃ was postulated to occur in prior gas generation testing (Delegard et al. 2000) and may have occurred in Test 1 and the experiments with Nochar in the Series 3 testing.

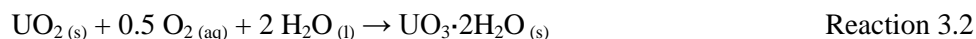
Test 12 in Series 3 containing Nochar and NaNO₂ produced large amounts of N₂. Nitrous oxide, N₂O, was produced in one test (again, Test 12) and trace amounts of NO_x were found in two tests (Tests 10 and 12 with Nochar and added NaNO₃ and NaNO₂, respectively). CH₄ was found in each test and undifferentiated C₂ hydrocarbons (C₂H_x) were found in three of the tests.

The quantities of O₂ reacted for all tests were remarkably consistent, ranging from 4.09×10⁻⁵ moles to 7.81×10⁻⁵ moles. If the two tests with Nochar and added nitrate or nitrite salt, and their likely Nochar oxidation reactions, are neglected (Tests 10 and 12), the range of O₂ consumption, 4.09×10⁻⁵ to 5.95×10⁻⁵ moles [(4.92±0.61)×10⁻⁵], is much tighter.

The dissolved O₂ could have reacted with the uranium metal beads to form UO₂ while the solution was becoming anoxic:



Alternatively, the O₂ could have reacted with the fresh UO₂ product, from anoxic aqueous corrosion of uranium metal, to form metaschoepite, UO₃·2H₂O:



The consistency of the amounts of O₂ consumed for Tests 1 through 9 and the consistency of the uranium metal amounts and surface areas used in each test suggest that the O₂ consumption was by reaction with uranium metal and not by reaction with the variable amounts of UO₂ produced. The reaction of uranium metal with O₂ is not likely to have been affected by the added Nochar, NaNO₃, or NaNO₂.

The 4.56×10⁻⁵ moles of O₂ reacted in Test 1 is about 16% of the 2.80×10⁻⁴ moles of uranium metal that corroded to form UO₂. The number of moles of H₂ that should have formed in Test 1 is two times the difference between the total reacted uranium metal and the reacted O₂, or 4.69×10⁻⁴ moles H₂. As seen in Figure 3.6, only 2.76×10⁻⁴ moles of H₂ was found in the gas phase, a yield of 59%. Thus, about 41% of the H₂ evidently was lost from the apparatus. Further considerations of the reaction stoichiometry are provided in Section 3.3.

Both Tests 10 and 12 used Nochar with added salt; Test 10 had 0.1 M NaNO₃ and Test 12 had 0.1 M NaNO₂. The Nochar in Test 12, which had been heated to 60°C and for limited time at 90°C, yellowed to a degree similar to that observed for Nochar with 1 M NaNO₂ at room temperature. Test 10 also showed some yellowing (Figure 3.7). Oxygen consumption for both tests was greater than in any other test in Series 3. Test 12, having 0.1 M NaNO₂, showed greater O₂ consumption than the parallel 0.1 M NaNO₃ test. Negligible N₂ was formed in Test 10 with NaNO₃ but significant N₂ was produced in Test 12 with NaNO₂. Test 12 also produced N₂O. Tests 10 and 12 both produced small amounts of NO_x.

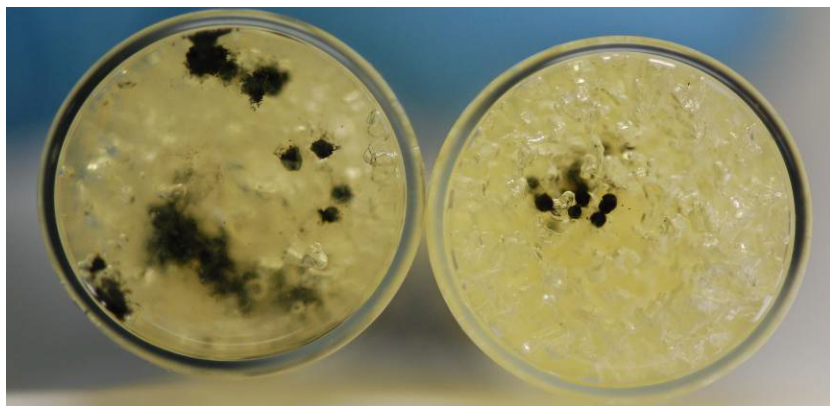


Figure 3.7. Bottom Views of Vials from Tests with Salt and Nochar in Series 3
Left – Test 10 (0.1 M NaNO₃); right – Test 12 (0.1 M NaNO₂)

3.2.3 Gas Analysis Results for Series 4

Test Series 4 was performed to determine the effects of varying nitrate and nitrite concentration on the reaction of uranium metal with water. Tests of the effects of 0.5 M nitrate and 0.5 M nitrite in the presence of added UO₂ on uranium metal corrosion were performed. A single test to determine the effects of added phosphate (as 0.07 M Na₂HPO₄) also was performed.

The molar quantities of H₂, O₂, N₂, and N₂O produced or consumed and the molar quantities of U metal corroded in the Series 4 tests are shown in Figure 3.8 and its associated table. As in Series 3, H₂ was produced in widely varying quantities in the Series 4 tests. The greatest amount of H₂ production was for the test with 0.07 M Na₂HPO₄ (Test 12). Its H₂ production was almost 2-times that of the parallel control Test 1 with water alone. In the control Test 1, H₂ and O₂ accounted for 1.59×10⁻⁴ moles (101%) of the 1.58×10⁻⁴ moles of observed U metal oxidation. In Test 12, with phosphate, H₂ and O₂ accounted for 3.07×10⁻⁴ moles (121%) of the 2.53×10⁻⁴ moles of observed U metal oxidation. Some of the O₂ consumption in either test could have come from oxidation of UO₂ to UO₃·2H₂O. Both nitrate and nitrite decreased H₂ production with nitrite being more effective than nitrate. The H₂ evolution decreased with increasing nitrate concentration but was very low and constant over the 0.2 to 1.0 M nitrite concentration range tested.

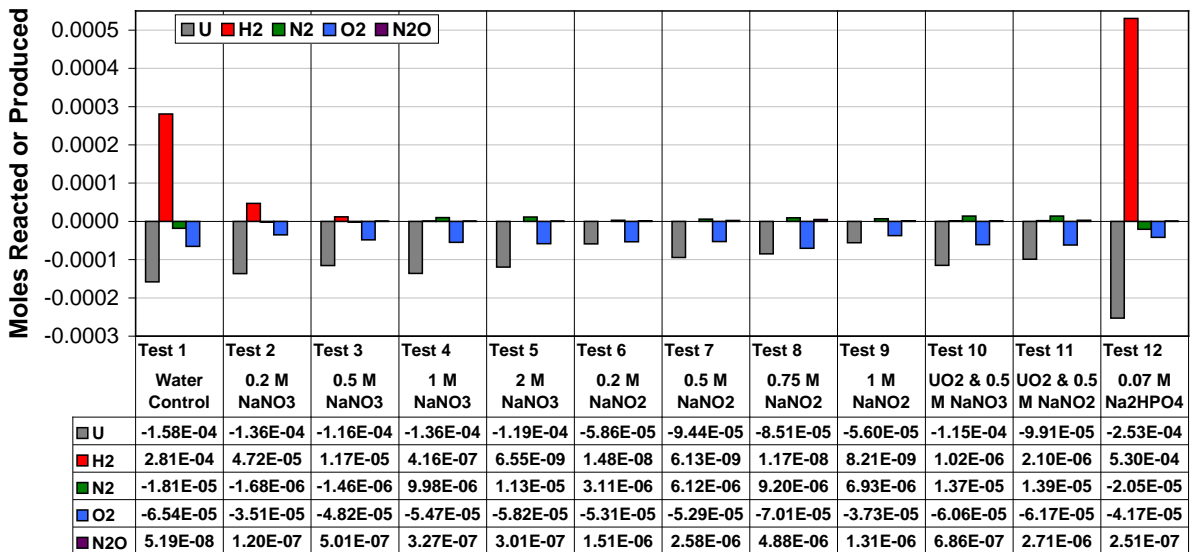


Figure 3.8. Moles of Gas Produced or Reacted and Moles of Uranium Metal Reacted in Series 4

Oxygen consumption from the air cover gas ranged from 3.73×10⁻⁵ to 7.01×10⁻⁵ moles. Small amounts of N₂ were produced in tests containing nitrite, for the tests with the highest nitrate concentrations (Tests 4 and 5), and for the two tests with UO₂. Small N₂ quantities were consumed, particularly in the control Test 1 and Test 12 with phosphate, 1.81×10⁻⁵ moles and 2.05×10⁻⁵ moles, respectively. The N₂:Ar mole ratio in air is 83.6 and was 78.5 and 77.2, respectively, in Tests 1 and 12. Because the losses of N₂ present in the starting air cover gas in Tests 1 and 12 are readily shown by their decreased ratio to the Ar concentration, the N₂ consumption appears to be genuine, requiring further study to determine the responsible reaction.

Nitrous oxide, N₂O, was produced at low concentrations in all tests, although only a trace in the control Test 1. Because N₂O is isobaric with CO₂ (i.e., has the same mass), its differentiation from CO₂ by mass spectrometry is difficult, especially at low concentrations, and fragmentation patterns must be used to distinguish the two species. Overall, about 4 to 10-times more N₂O was produced in the tests with nitrite than for the tests with nitrate. However, even the greatest N₂O production was 0.06 mole per mole of uranium corroded. Trace NO_x was found in the 0.5 M nitrate and nitrite tests with UO₂ (Tests 10 and 11) and in Test 9 with 1 M nitrite. Methane was found in each test and C₂H_x in many of the tests.

3.2.4 Gas Analysis Results for Series 5

Test Series 5 was performed to examine further the effects of varying nitrate and nitrite concentration on the reaction of uranium metal with water and the effects of added UO_2 . Two tests of the effects of added UO_2 , with 0.5 M nitrate and 0.5 M nitrite, were performed to supplement the results found for similar tests conducted under Series 4. In Series 3, it was found that Nochar in combination with 0.1 M NaNO_2 produced only about 1% of the H_2 that was found in the parallel test containing only 0.1 M NaNO_2 in the absence of Nochar. However, the Nochar/nitrite test also produced large quantities of N_2 as well as N_2O and NO_x . Therefore, Test 9 was included in Series 5 to determine if small amounts of added Nochar in the presence of 0.5 M NaNO_2 might improve the H_2 attenuation of nitrite but avoid the unwanted collateral production of N_2 , N_2O , and NO_x . The organic flocculating agent Optimer 7194 Plus was used in K Basin sludge processing to aid in coagulation and settling of fine sludge particles. Test 10 was included in Series 5 to determine if Optimer 7194 Plus would improve the H_2 attenuation of nitrite. Finally, tests of 0.5 M nitrate and 0.5 M nitrite in the presence of a full simulated K Basin sludge were included. The simulated sludge (composition given in Table 2.1) contained uraninite, metaschoepite, ferrihydrite, aluminum hydroxide, OIER, mordenite, Optimer 7194 Plus, water, and the requisite uranium metal beads.

The molar quantities of H_2 , O_2 , N_2 , N_2O , and NO produced or consumed are shown in Figure 3.9 with the molar quantities of U metal corroded in the Series 5 tests. No gas composition data are provided for Test 4 because the sample was lost during a power failure in the midst of analysis. Again, H_2 was produced in widely varying quantities. Control Test 1 produced the greatest amount of H_2 . Hydrogen and O_2 accounted for 1.71×10^{-4} moles (117%) of the 1.46×10^{-4} moles of U metal oxidized. Some of the O_2 consumption could have come from oxidation of UO_2 to $\text{UO}_3 \cdot 2\text{H}_2\text{O}$. Nitrate and nitrite both decreased H_2 production (Tests 2, 3, 5, and 6). The quantities of H_2 produced in Tests 7 and 8 for 0.5 M NaNO_3 and 0.5 M NaNO_2 in the presence of UO_2 were practically identical and about two orders of magnitude lower than the control test. Hydrogen production for 0.5 M NaNO_2 containing small amounts of added Nochar and Optimer 7194 Plus (Tests 9 and 10, respectively) was over four orders of magnitude lower than the control but roughly equivalent to the H_2 produced for 0.5 M NaNO_2 alone. Hydrogen evolved in Tests 11 and 12, 0.5 M NaNO_2 and 0.5 M NaNO_3 , respectively, with the simulated sludge, was two to three orders of magnitude lower than the control.

Oxygen was consumed from the air cover gas in all tests but with wide variation, ranging from 1.12×10^{-5} moles to 1.39×10^{-4} moles. The greatest amount of O_2 consumption was for Test 11, which contained simulated sludge and 0.5 M nitrite. Small amounts of N_2 were produced in most tests, most prominently in Tests 7, 8, 11, and 12 (UO_2 and simulated sludge with nitrite and nitrate). Again, N_2 was consumed in the control Test 1. The amount consumed, 7.84×10^{-6} moles, was roughly half that observed in the similar control tests in Series 3 and 4. The N_2 :Ar mole ratio in control Test 1 was 81.1 compared with the 83.6 value observed for air.

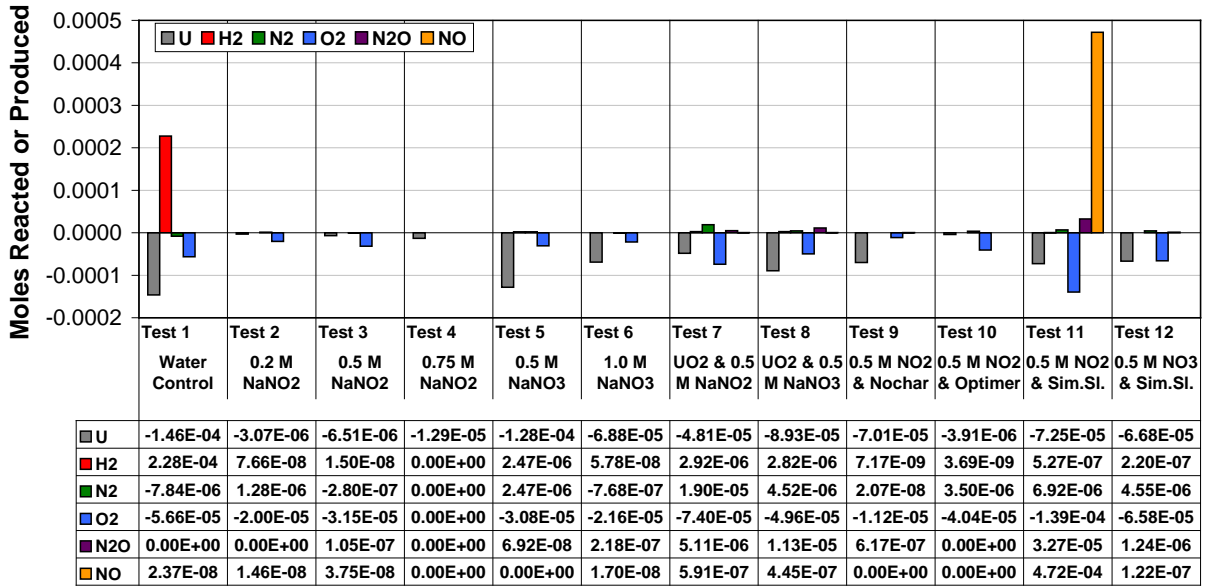


Figure 3.9. Moles of Gas Produced or Reacted and Moles of Uranium Metal Reacted in Series 5

Nitrous oxide, N₂O, was found in several tests, most prominently in the tests producing the larger N₂ quantities (i.e., Tests 7, 8, 11, and 12). The greatest amount of N₂O was found for Test 11, which contained 0.5 M nitrite and the simulated sludge. Methane was found in all but one test and C₂H_x in four of the tests.

The most conspicuous gas analysis observation in Series 5 was of the large amount of NO produced in Test 11 containing 0.5 M nitrite and the simulated sludge. Gas evolution began within minutes of adding the 0.5 M NaNO₂ to the simulated sludge and even before heating. Such behavior was not observed for Test 12 containing 0.5 M NaNO₃ and simulated sludge. The gas collected in Test 11 increased by about 10 mL within hours of mixing and heating and was about 13 mL when heating of Test 11 was terminated after ~3 days at 60°C. In contrast only about 0.5 mL of H₂ would have evolved under similar conditions with only water and U metal. Tests 11S and 12S, similar to Tests 11 and 12, were performed at room temperature but without the U metal beads or flocculent.

Tests 11S and 12S were run to determine the effects of the added salts on the mechanical properties of the simulated sludge. As was observed for Tests 11 and 12, significant gas evolution (bubbling within the sludge) was noted for Test 11S with nitrite but no gassing was noted for the Test 12S with nitrate. The appearances of Tests 11, 11S, and 12S are shown in Figure 3.10. Note the gas pockets in the settled solids in Tests 11 and 11S. As shown by the graduation marks on the test vessels, the gas bubbles held in Test 11S expanded the settled solids by about 1.5 mL (~30%) compared with Test 12S.

Gas samples were taken from Test 11 after three days of heating. The apparatus was removed from the heater block, cooled, disassembled, and new air cover gas added. The test was returned to the test temperature ~24 hours after cooling to continue the remaining four-week test duration.

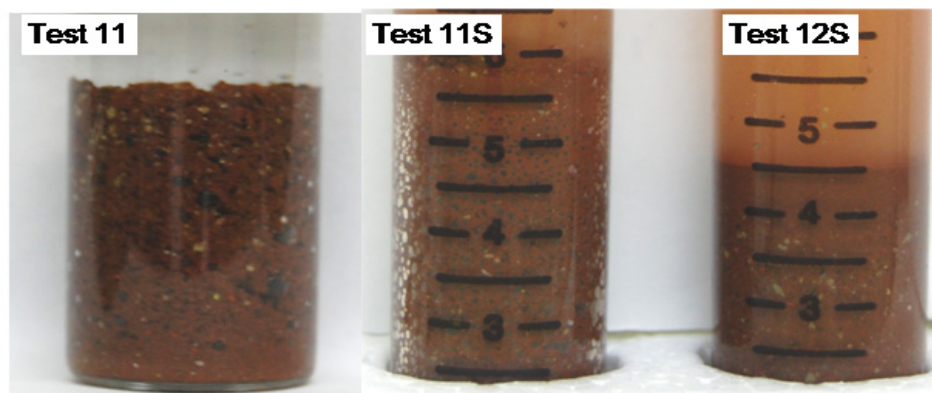
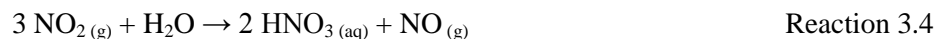


Figure 3.10. Appearances of Tests 11, 11S, and 12S Three Days after Mixing (~2× magnification)

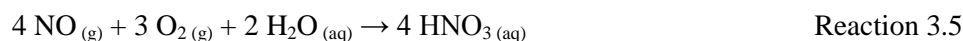
The gas analyses showed that the N_2 :Ar ratio was identical to that of air, meaning that little or no N_2 was consumed or generated. However, based on the O_2 :Ar ratio, about 98.5% of the original atmospheric O_2 was consumed. If no O_2 had been consumed, the O_2 :Ar mole ratio would have been 22.4; the observed O_2 :Ar ratio was 0.336. Nitric oxide, NO, was about 58.3% of the total sampled gas. The production of this relatively large fraction of NO explained the depletion of oxygen from the gas space. This depletion occurred by the Reaction 3.3:



The NO_2 product from Reaction 3.3 then reacts with water according to Reaction 3.4:



and the product NO can react with more O_2 according to Reaction 3.3. The net overall reaction of NO, O_2 , and H_2O produces HNO_3 as shown in Reaction 3.5.



The analysis and interpretation of the gas sampling data are described in further detail in Appendix B.

By comparing findings from Tests 11 and 12 and Tests 11S and 12S, it was shown that nitrite was required for the reaction; comparison of Tests 11 and 11S showed that neither U metal nor flocculent was required. The NO had to arise from the chemical reduction of nitrite based on the composition of the simulated sludge which contains no significant other source of nitrogen (the nitrogen in the quaternary ammonium groups in the OIER is too chemically stable to react). If nitrite was reduced, a sludge component had to be oxidized. The most likely component to be oxidized was UO_2 . Finally, it was observed that although the initial gas-forming reaction was rapid, the reaction soon subsided and only produced a modest quantity of gas compared with the molar quantities of the likely reactants (nitrite, UO_2). Analyses of the solution from Test 11S confirmed this, showing that only about 19% of the original nitrite had reacted. Therefore, the reaction stopped before complete consumption of the reactants.

A set of 1/10-scale scoping tests was performed to supplement the observations already gained from the existing Series 5 testing with the goal to identify which combination of reactants was needed for the gas-forming reaction. The matrix of the Series 5 and supplemental tests with the associated gas-formation observations are summarized in Table 3.3. It is seen that conspicuously large gas-forming reactions only were observed for the tests having nitrite, UO_2 , $\text{UO}_3 \cdot 2\text{H}_2\text{O}$, and ferrihydrite present together. The reaction did not require nitrate, U metal, Optimer flocculant, ALE sand, or the combination of $\text{Al}(\text{OH})_3$, mordenite, and OIER.

Table 3.3. Conditions and Results from Series 5 and Supplemental Testing

Test	Reaction Vigor	Reactant Presence									
		Nitrate	Nitrite	U metal	UO_2	$\text{UO}_3 \cdot 2\text{H}_2\text{O}$, MS	Ferrihydrite	ALE sand	Optimer 7194 Plus	Nochar	Others ^(a)
1	None			✓							
2	None		✓	✓							
3	None		✓	✓							
4	None		✓	✓							
5	None	✓		✓							
6	None	✓		✓							
7	None		✓	✓	✓						
8	None	✓		✓	✓						
9	None		✓	✓						✓	
10	None		✓	✓					✓		
11	Strong		✓	✓	✓	✓	✓	✓	✓		✓
12	None	✓		✓	✓	✓	✓	✓	✓		✓
11S-b ^(b)	Strong		✓		✓	✓	✓	✓			✓
11S-a ^(b)	Strong continued		✓		✓	✓	✓	✓	✓		✓
12S-b ^(b)	None	✓			✓	✓	✓	✓			✓
12S-a ^(b)	None	✓			✓	✓	✓	✓	✓		✓
1/10-scale tests	None		✓				✓		✓		
	None		✓					✓	✓		
	No immed. rxn.		✓		✓		✓				
	Add MS to above test – strong		✓		✓	✓	✓				
	No immed. rxn.		✓		✓		✓		✓		
	Add MS to above test – medium		✓		✓	✓	✓		✓		
	Little; after 20 h		✓		✓		✓				
	Little; after 4 h		✓			✓	✓				
	Mix above two tests – strong		✓		✓	✓	✓				

(a) Includes $\text{Al}(\text{OH})_3$, mordenite, and OIER.
(b) Before, b, and after, a, Optimer 7194 Plus flocculent addition.

The effects of addition of 0.5 M NaNO₂ to samples of genuine sludge were investigated under a new Test Instruction.¹² Four separate archive sludge materials; KC-2/3, KC-4, KE Floc Comp, and KE NLOP (Table 2.2); were retrieved from the sludge archive jars and placed into 15-mL polystyrene centrifuge tubes. The tubes were tapped to dislodge bubbles, settle the sludge, and obtain settled volumes. Then, 0.5 M NaNO₂ solution was added to each tube to within ~2 mL of the full capacity (i.e., ~13 mL total volume). The tubes and contents were shaken until all sludge was suspended and then the tubes were placed upright into racks to observe if any gassing occurred.

The gas observations, such as bubbles and foaming, for the four tests were made at contact times ranging from mixing up to 12 days of storage (see Table 3.4). Gassing was observed for all sludges except KE NLOP. The gassing intensity increased in the order KE Floc Comp < KC-4 Whole < KC-2/3 Comp. This order also corresponds to the order of increasing uranium concentration in the dry and settled sludges. Iron is present in all sludges as various oxides, hydrous oxides, or hydroxides at elemental concentrations ranging from about 2 to 24 wt% (dry basis; Table 2.2).

Table 3.4. Gas Formation Observations for Mixtures of K Basin Sludge with 0.5 M NaNO₂

Sludge	Wt% U, dry basis	Settled Volume, mL			Observations
		Initial	3 days	12 days	
KC-2/3 Comp	59.0	3.1	3.2	2.9	No immediate bubbles; bubbles after 1 hour and after 6 hours; bubbles released from settled solids after 3 days when tapped. No bubbles at 12 days. Supernate clear.
KC-4 Whole ^(a)	16.6	2.0	3.9	3.6	Stable foam (~0.2 mL) seen after mixing but no new bubbles; bubbles released from settled solids after 3 days when tapped. No bubbles at 12 days. Supernate turbid.
KE Floc Comp	10.3	4.3+ ^(b)	6.0	5.7	Bubbles initially after adding NaNO ₂ solution; no bubbles at any later time up to 12 days. Supernate clear.
KE NLOP	2.51	5.9	5.8	5.4	No bubbles at any time. Supernate clear.

(a) KC-4 initial pH was 3.47.
(b) Significant sludge was present, smeared on the wall of the centrifuge tube, making volume reading uncertain.

The settled sludge volumes also were observed to increase initially for all tests producing observable gas. The relative sludge swelling amounts increased in the order KC-2/3 Comp < KE Floc Comp < KC-4 Whole. The order of volume increase does not match the observed intensity of gas production. Thus, KC-2/3 Comp produced the most observable bubbling but had virtually negligible swelling. Because the initial sludge volume in the KE Floc Comp test was uncertain, the only test that showed significant swelling was KC-4 Whole. This sludge also did not settle well and, in contrast with the other three sludge tests, the supernatant solution still was turbid 12 days after mixing with the 0.5 M NaNO₂. However, sludge swelling in all cases could have been compromised by the tapping done to release bubbles and thus is not prototypic for stagnant sludge.

¹² *K Basin Sludge Aliquoting and Testing of Nitrate and Nitrite*. 53451-TI16, CH Delegard, PNNL, Richland, Washington (March 2009). The TI was executed under the current revision at the time of the procedure, *Routine Research Operations*, RPL-OP-001, Pacific Northwest National Laboratory, Richland, Washington.

The KC-4 Whole sample showed anomalous behavior in prior characterization as described in the following report excerpt:¹³

In contrast to the behaviors of other sludge samples, this composite has a slimy consistency, did not settle well, and the supernatant liquid remained turbid. Also, the sludge pH, as will be seen, was uncharacteristically low (3.47).

Uraninite oxidation by nitrite, mediated by ferrihydrite, has been described in the technical literature. The studies were of the long-term stability of nano-particulate biogenic uraninite formed *in-situ* to remediate U(VI) contamination frequently co-located with nitrate in soils underlying industrial process sites. Ferrihydrite and other iron-rich phases (lepidocrocite and goethite, both FeOOH phases) are ubiquitous in soil and it has been found that some of these iron oxyhydroxide phases can actively participate in oxidation of U(IV) to U(VI). Therefore, studies to investigate the stability of biogenic UO₂ have examined the combined roles of nitrate, nitrite, and the various iron oxyhydroxide phases. The following excerpt, from a recent review article on this topic (Bargar et al. 2008), implicates the joint involvement of nitrate/nitrite and iron oxide and U(IV) oxidation (as evidenced by solubilization):

The iron oxide ferrihydrite was found to be responsible for the oxidation of biogenic UO₂ in an abiotic, anaerobic system (Ginder-Vogel et al. 2006). Push-pull field experiments (Senko et al. 2002) unveiled a link between nitrate addition and uranium solubilization due to the abiotic oxidation of U(IV) by intermediates of microbial nitrate reduction, specifically nitrite.

As further described in that review, many of the biogenic uraninite materials are practically pure stoichiometric uraninite with compositions ranging from UO_{2.00} to UO_{2.05} and have primary particle sizes ranging from 2 to 10 nm. These values compare closely with the properties of uraninite prepared by corroding pure U metal in anoxic water at 60°C to model the uraninite present in the K Basin sludge. The 60°C synthetic uraninite was found to be effectively stoichiometric (UO_{2.008}) and to have primary particle sizes centered around 6 nm (Sinkov et al. 2008).

An abstract from a study of biogenic UO₂ stability (Senko et al. 2005), presented below, shows the interacting roles of nitrite and iron oxyhydroxide in the oxidation of UO₂ [described as insoluble U(IV)]. The study showed that Fe(III) oxyhydroxides can be more effective UO₂ oxidants than nitrite and that Fe(III) compound mineralization affects its participation in the redox reaction:

Microbiological reduction of soluble U(VI) to insoluble U(IV) is a means of preventing the migration of that element in groundwater, but the presence of nitrate in U(IV)-containing sediments leads to U(IV) oxidation and remobilization. Nitrite or iron(III) oxyhydroxides may oxidize U(IV) under nitrate-reducing conditions, and we determined the rate and extent of U(IV) oxidation by these compounds. Fe(III) oxidized U(IV) at a greater rate than nitrite (130 and 10 μM U(IV)/day, respectively). In aquifer sediments, Fe(III) may be produced during microbial nitrate reduction by oxidation of Fe(II) with nitrite, or by enzymatic Fe(II) oxidation coupled to nitrate reduction. To determine which of these mechanisms was dominant, we isolated a nitrate-dependent acetate- and Fe(II)-oxidizing bacterium from a U(VI)- and nitrate-contaminated aquifer. This organism oxidized U(IV) at a greater rate and to a greater extent under acetate-oxidizing (where nitrite accumulated to 50 mM) than under Fe(II)-oxidizing conditions. We show that the observed differences in rate and extent of U(IV) oxidation are due to mineralogical differences

¹³ Delegard CH, AJ Schmidt, and JW Chenault. 2007. "Characteristics of KE Basin Sludge Samples Archived in the RPL – 2007." Letter report 53451-RPT01. Pacific Northwest National Laboratory, Richland, Washington.

between Fe(III) produced by reaction of Fe(II) with nitrite (amorphous) and Fe(III) produced enzymatically (goethite or lepidocrocite). Our results suggest the mineralogy and surface area of Fe(III) minerals produced under nitrate-reducing conditions affect the rate and extent of U(IV) oxidation. These results may be useful for predicting the stability of U(IV) in aquifers.

Additional studies into the effectiveness of various iron oxyhydroxides show on both thermodynamic and experimental bases that ferrihydrite is more effective than either goethite or hematite in oxidizing UO_2 and that increased bicarbonate concentrations and decreased pH favor UO_2 oxidation (Ginter-Vogel et al. 2006). Continued studies by the same research group show that the decrease in ferrihydrite effectiveness with time can be attributed to its transformation into thermodynamically more stable goethite and lepidocrocite (Ginter-Vogel and Fendorf 2008). They also note observations made elsewhere (Thompson et al. 2006) that redox cycling promotes the conversion of less structured iron oxyhydroxide phases, such as ferrihydrite, to more crystalline forms such as goethite and hematite.

Overall, these published studies indicate that the efficacies of the iron oxyhydroxide phases to mediate the oxidation of U(IV) can differ strongly and, if initially effective, their effectiveness can decrease with time. The gas-forming reactions observed in Test 11 of Series 5, several of the supplemental 1/10-scale tests, and the tests with actual sludge thus appear to be analogous to those described by Senko and colleagues (2002, 2005) and others for the UO_2 oxidation by nitrite that is mediated by Fe(III) solid phases, particularly ferrihydrite.

The non-balanced Reactions 3.6 and 3.7 (below) illustrate a cycle consistent with the observations described in the technical literature and the observations made for simulated and actual sludge:



The iron oxyhydroxide oxidizes the UO_2 to form Fe^{2+} and dissolved U(VI). The Fe^{2+} , in turn, is oxidized by nitrite to form more iron oxyhydroxide and NO gas. However, with time, the iron oxyhydroxide becomes mineralized and ineffective as a UO_2 oxidant as shown by the cessation of NO gas formation.

3.2.5 Gas Analysis Results for Series 6

Test Series 6 was performed to examine the effects of 0.5 M nitrate and 0.5 M nitrite on uranium metal corrosion and H_2 generation in genuine K Basin sludge. Two archived K Basin sludges were used. The sludge KE Floc Comp was chosen to represent the containerized sludge from the pits, floors, and canisters of the KE Basin while KC-2/3 Comp was chosen to represent the uranium-rich settler tank sludge. Parallel tests in the absence of sludge also were performed. In an attempt to decrease artifacts thought to arise from the black rubber stoppers used in the earlier test series, chemically benign silicone stoppers were used in this test series. This test series also was conducted with a starting inert cover gas of neon instead of the air cover gas used in all prior tests.

Unexpectedly, the gases in all Series 6 experiments at the conclusion of testing had low neon concentrations and high concentrations of atmospheric air components, including argon. These

observations showed that gas confinement was imperfect and that gases both entered and were lost from the test apparatus. As described in Section 2.2, the gas loss and in-leakage most likely occurred through the silicone rubber stoppers. Silicone has individual gas permeabilities tens to hundreds of times greater than those of the natural black rubber used in the prior test series (see Table 2.3). As a result, the gas compositions do not quantitatively reflect what would have been observed had gas confinement been tight. However, judgments of trends and proportions still may be made based on comparative data.

The quantities of H₂, O₂, N₂, N₂O, and Ne produced (and diffused in) or consumed (and diffused out) are shown in Figure 3.11 and compared with the quantities of U metal corroded in the Series 6 tests. The gas analysis problems described in the previous paragraph, based on the analyses detailed in Appendix B, are immediately apparent in Figure 3.11. On average, about 71% of the original $5.3 \pm 0.7 \times 10^{-4}$ moles of inert Ne cover gas originally present in each test apparatus was lost over the four-week test duration. Because N₂ and O₂ also diffused into the test apparatus, and at different rates than the inert atmospheric Ar, quantitative evaluations of their participation in the reactions in the sludge/solution mixtures are not possible.

However, the O₂:Ar and N₂:Ar ratios may be compared across the test series. The O₂:Ar ratios are roughly equal for most tests while Test 9, containing KC-2/3 Comp sludge and 0.5 M NaNO₂ had an O₂:Ar ratio about 1/3 that of the other tests. This finding presents strong evidence that O₂ was consumed in Test 9. The N₂:Ar ratios are about 10% and 6% higher for Tests 8 and 9, containing KC-2/3 Comp sludge and 0.5 M NaNO₃ and 0.5 M NaNO₂, respectively, than for the other tests indicating that some N₂ likely was produced in these tests.

Because of the gas leakage into and out of the apparatus, the material balance for U metal corrosion in the Test 1 control is poor. The H₂ evolved in Test 1 only accounts for 17% of the U metal corrosion. The extent of O₂ participation in U metal corrosion and UO₂ oxidation is impossible to determine because of the unquantified diffusion of O₂ into the test vessels.

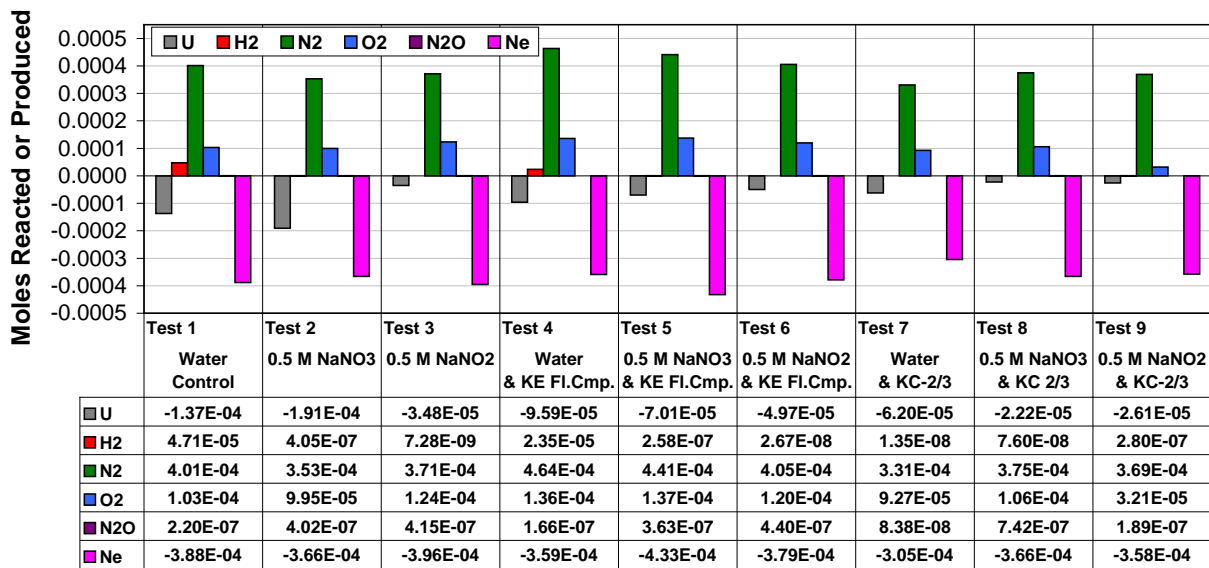


Figure 3.11. Moles of Gas Produced or Reacted and Moles of Uranium Metal Reacted in Series 6

Additional useful information is provided in the gas analyses of the Series 6 tests. First, measurable amounts of H₂ were detected in each experiment. The H₂ quantities relative to the control Test 1 give estimates of the extent of H₂ attenuation. Because the rate of gas permeation through the silicone stoppers is proportional to the gas concentration difference across the stoppers, the H₂ attenuation coefficients calculated for the tests in Series 6 (i.e., [H₂ quantity in the control test]/[H₂ quantity in the test of interest]) are lower bounds of the actual values. This is because the relative amount of H₂ lost from the control test, due to its higher H₂ concentration, will be greater than the relative amounts of H₂ lost from any of the other tests which had much lower H₂ concentrations. The H₂ attenuation factors provided for the Series 6 tests, therefore, are lower limits or “greater than” values.

The H₂ attenuation factors observed for the genuine sludges in the absence of added nitrate or nitrite were determined by comparing the behaviors of Test 4 (containing KE Floc Comp sludge) and Test 7 (containing KC-2/3 Comp sludge) with the behavior of the control Test 1 (in water alone). The H₂ attenuation factor was 2.0 for Test 4, in agreement with the U metal corrosion rate attenuation factor of 1.5. This corrosion rate attenuation factor, obtained with U metal beads of nominal 700- μm diameter, is identical to the corrosion rate inhibition factor of 1.5 observed in prior 60°C testing of crushed irradiated N Reactor fuel having 500 to 2,000 μm particle size blanketed by K Basin sludge (Tests 2 and 3, with and without sludge overburden, respectively, as described in Schmidt et al. 2003). The corrosion rate attenuation factor for Test 7 (with KC-2/3 Comp sludge) was 2.4, similar to the 1.5 factor observed in prior tests with crushed N Reactor fuel and sludge overburden.

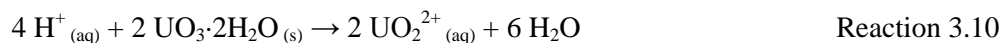
Although the corrosion rate in Test 7 with KC-2/3 Comp sludge overburden decreased by a factor of 2.4, the H₂ rate decreased by a factor of 3500. This surprising H₂ generation rate attenuation in Test 7 occurred in the absence of any salt additive and is at odds with the H₂ attenuation factor of 2.0 observed for the parallel Test 4 with KE Floc Comp sludge.

Both sludge materials were prepared from archived sludge samples obtained in 1999. The sludge samples have been maintained in wetted conditions but had undergone extensive oxidation such that the U(IV) phase uraninite had been largely supplanted by U(VI) phases. The fraction of uranium present as U(VI) in the KE Floc Comp sludge was assayed in 2008 to be ~98% (Table 2.2). The dry-basis (i.e., water-free) uranium concentrations in KE Floc Comp and KC-2/3 Comp were 10.3 and 59.0 wt%, respectively.

The elevated H₂ attenuation factor observed for the uranium-rich KC-2/3 Comp sludge may have been caused by hydrogen radical scavenging by the abundant U(VI) solid phases or by dissolved hexavalent uranium, UO₂²⁺_(aq). That is, the H \cdot produced by U metal corrosion could have interacted with U(VI) solid phases such as metaschoepite, UO₃·2H₂O, or reacted with dissolved UO₂²⁺_(aq) to form U(IV) phases such as uraninite, UO₂, as shown in Reactions 3.8 and Reaction 3.9, respectively:



It is seen that Reaction 3.9 produces acid and thus provides the conditions needed to maintain U(VI) in solution by dissolving metaschoepite by Reaction 3.10:



However, the overall reaction (Reaction 3.11) is pH indifferent, neither producing nor consuming H^+ .



The action of U(VI) to act as a hydrogen radical scavenger is reasonable based on knowledge that zinc, aluminum, copper, and magnesium metal are active metals in water, form hydrogen radicals by aqueous corrosion, and are used to chemically reduce dissolved U(VI) to U(IV) (Booman et al. 1962). Uranium metal, a more powerful reductant than many of the named metals, likely acts in the same manner, forming hydrogen radicals that then can convert dissolved U(VI) to U(IV). The U(IV), in turn, then forms the low solubility solid UO_2 as shown in Reaction 3.9.

The U(VI) solution concentrations in pH neutral water in equilibrium with metaschoepite decrease in the presence of Na^+ , K^+ , or Ca^{2+} by the formation of the corresponding alkali or alkaline U(VI) materials, clarkeite and sodium compregnacite, compregnacite (with potassium), and becquerelite, respectively. The solubilities of these U(VI) phases as functions of pH are at minima between about 6 and 8 (Meinrath 1998; Gorman-Lewis et al. 2008a and 2008b). As pH decreases below neutrality, the phases dissolve to release hydrolyzed dissolved U(VI) species to solution; non-hydrolyzed $\text{UO}_2^{2+}_{(\text{aq})}$ forms with further pH decrease. As the pH increases above neutrality, carbonate complexation of UO_2^{2+} occurs because of the dissolution of CO_2 gas into the increasingly alkaline solution and $\text{UO}_2(\text{CO}_3)_3^{4-}_{(\text{aq})}$ and related carbonate complexes are found.

Spectrophotometric analyses implicated dissolved U(VI) in the scavenging reaction by its relatively high concentration in the Test 7 supernatant solution. The prominent peak multiplet centered at 420 nm characteristic of U(VI) was found in the Test 7 solution while no such spectrum was shown in Test 4. The solutions' pH values also were measured in all tests. The supernatant pH in Test 7 was 5.47 at the beginning of the test and 5.68 at the end. Test 4 began at pH 7.26 and ended at pH 7.65. The much lower pH found in Test 7 (compared with the near neutral pH for Test 4 and all other tests) favors the dissolution of U(VI) phases, such as metaschoepite, becquerelite, and others, found in K Basin sludge.

The solution from Test 7 was acidified to convert the dissolved U(VI) to its non-hydrolyzed form so that the U(VI) concentration, about 6×10^{-4} M, could be accurately determined by spectrophotometry. The uranium concentration in Test 4 was at least a factor of ninety lower. Because metaschoepite solubility increases with pH decrease below about pH 7, the low pH in Test 7 explains its correspondingly high U(VI) solution concentration.

Although atmospheric O_2 diffused into the initially pure Ne gas spaces of all tests, the amounts of O_2 differed. This disparity was greatest in Tests 7, 8, and 9 with the KC-2/3 Comp sludge. While about 1.0×10^{-4} moles of O_2 were present at the end of Tests 7 and 8, only about 3.2×10^{-5} moles of O_2 were present at the end of Test 9 indicating that O_2 was consumed in Test 9. Test 9, which contained 0.5 M NaNO_2 , also showed a rapid initial gain in gas volume over the first few days of testing, a behavior similar to that observed in Test 12 of Series 5 which contained 0.5 M NaNO_2 and simulated sludge. Because the gas responsible for the surge in Test 12 of Series 5 was NO, the gas evolved in this initial

surge of Test 9 in Series 6 likely also was NO. With time, however, the gas volume in Test 9 decreased. In analogy with the behavior shown by Test 12 of Series 5, the gas volume decrease in Test 9 of Series 6 likely was by the reaction of NO with water and the influent O₂ to form HNO₃ according to Reaction 3.5. As a result of the replenishment of O₂ provided by the silicone permeability, the NO was completely consumed with none being detected at the end of Test 9. The depleted O₂ concentration compared with the concentrations observed in the parallel Tests 7 and 8 is consistent with this hypothesis.

Nitrous oxide was found in all tests. Test 8, the KC-2/3 Comp sludge with 0.5 M NaNO₃, produced the greatest amount. Methane was observed in all tests but C₂H_x compounds were not detected.

3.2.6 Gas Analysis Results for Series 7

Test Series 7 was performed to examine the effects of dissolved hexavalent uranium on uranium metal corrosion and H₂ generation in aqueous solution. The tests were run at 90°C for about 5 days. As in all prior test series, Test 1 was a control with uranium metal beads in water only. Test 2 was performed to determine the effect, if any, of the presence of chloride (added as 0.05 M NaCl) on the corrosion of uranium metal. In Tests 3, 4, and 5, U(VI) was introduced by dissolving from metaschoepite, UO₃·2H₂O, with the concentration controlled by variations in pH made by addition of hydrochloric acid, HCl. In Test 6, the 6×10⁻⁴ M U(VI) concentration was set by addition of uranyl chloride, UO₂Cl₂, prepared by the dissolution of metaschoepite with stoichiometrically controlled amounts of HCl. The pH levels selected for the tests with metaschoepite were about 6.9 (no added HCl), 5.1, and 4.3.

The U(VI) concentrations in Tests 3, 4, and 5 increased with decreasing pH as shown in Table 3.5. The U(VI) concentrations were determined by preparation of the U(VI) Arsenazo III complex at pH ~2 and measurement of the absorbance of the complex at 680 nm by spectrophotometry. Calibration testing showed the complex obeys the Beer-Lambert Law (R² = 0.9996) from ~10⁻⁶ to ~10⁻⁵ M; solutions were adjusted to this concentration range for measurement.

Table 3.5. U (VI) Concentration and pH in Tests 3, 4, and 5 in Series 7 Experiments

Test	Condition	Initial pH	Initial [U], M	Final pH	Final [U], M
1	None	6.44	Not applicable	8.34	Not applicable
2	0.05 M NaCl	Not measured	Not applicable	6.73	Not applicable
3	2 mL MS ^(a) slurry; pH 6.9	6.86	7.07×10 ⁻⁵	6.69	7.78×10 ⁻⁵
4	2 mL MS slurry; pH 5.1	5.13	2.08×10 ⁻³	5.68	6.63×10 ⁻⁴
5	2 mL MS slurry; pH 4.3	4.32	1.94×10 ⁻²	4.30	1.47×10 ⁻²
6	0.6 mM UO ₂ ²⁺ as UO ₂ Cl ₂	4.53	4.45×10 ⁻⁴	8.05	5.27×10 ⁻⁵

(a) MS is metaschoepite.

As expected, the metaschoepite solubility decreases with increasing pH (Figure 3.12). The measured metaschoepite solubility corresponds to the U(VI) concentrations observed in Tests 4 (KE Floc Comp sludge) and 7 (KC-2/3 Comp sludge) in Series 6 and offers confirmation that the U(VI) concentration in at least Test 7 was controlled by metaschoepite.

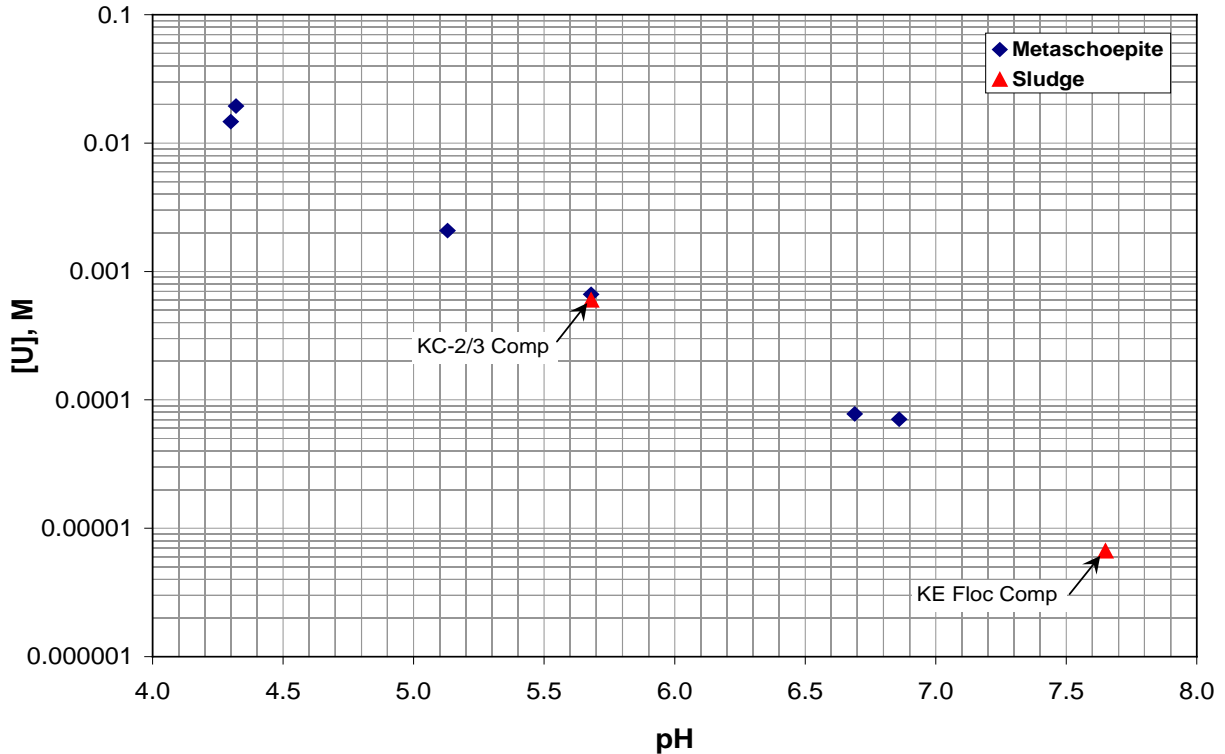


Figure 3.12. Metaschoepite Solubility as a Function of pH

The H_2 , O_2 , N_2 , and N_2O quantities produced or consumed and the quantities of U metal corroded in the Series 7 tests are shown in Figure 3.13. The control Test 1 produced H_2 near the nominal expected rate. Hydrogen production in Test 2, in the presence of 0.5 M NaCl, was about 25% higher than the control. The H_2 production decreased as U(VI) concentration increased in Tests 3, 4, and 5. However, the H_2 attenuation factor only reached 4.2 for Test 5 at ~ 0.015 M U(VI) and was 2.6 for Test 4 which contained 6.6×10^{-4} M U(VI). At a similar U(VI) concentration (6×10^{-4} M), Test 7 with KC-2/3 Comp sludge (Series 6) had a H_2 attenuation factor of 3500. The reason for the much greater H_2 attenuation factor for the genuine sludge is not known but may be due to the presence of dissolved iron, which could be active mediating the hydrogen scavenging reaction.

Oxygen was consumed from the air cover gas in all tests. The amounts consumed ranged from 1.88×10^{-5} to 3.14×10^{-5} moles. Small amounts of N_2 were consumed in all tests, ranging from 4.79×10^{-7} moles to 1.91×10^{-5} moles. The quantities of N_2 consumed, similar to the amounts observed in other test series, appear to be genuine as they are determined by the decreased N_2 :Ar concentration ratios.

Nitrous oxide was produced at low concentrations in all tests. Methane was found in each test and C_2H_x in many of the tests.

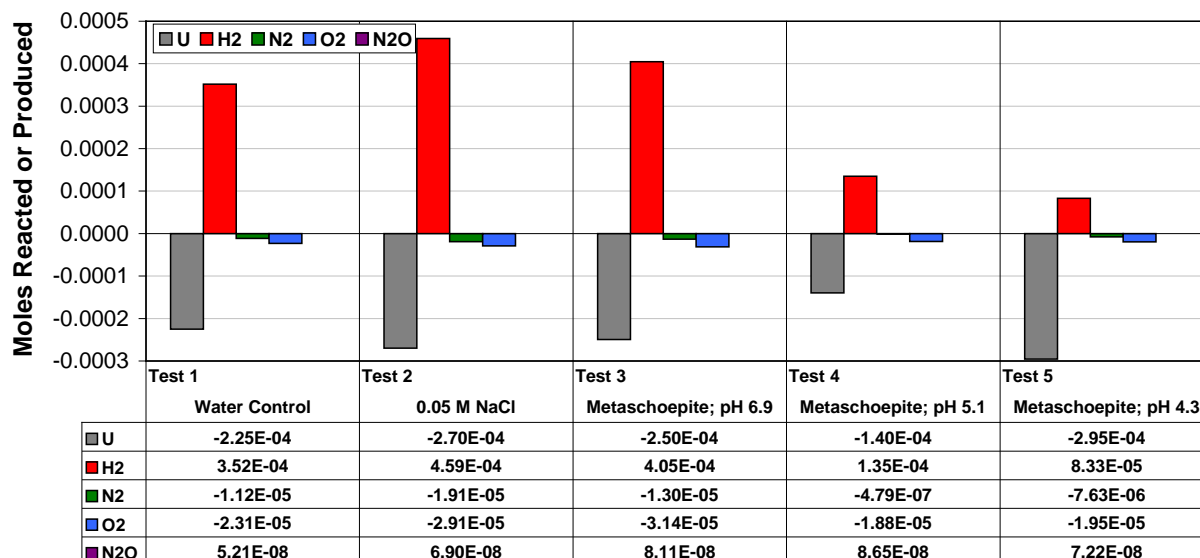


Figure 3.13. Moles of Gas Produced or Reacted and Moles of Uranium Metal Reacted in Series 7

3.3 Nitrate and Nitrite Reduction Products and Material Balance

As shown in Section 3.2, nitrate and especially nitrite are effective in attenuating H₂ gas from the reaction of uranium metal with water. Some of the effect is due to inhibition of the corrosion reaction but most is due to scavenging of the nascent hydrogen by nitrate and nitrite.

Based on the related published studies described in Section 1.4.1, plausible products from the reduction of nitrate include nitrite and ammonia while nitrite reduction can form ammonia. In the present testing, nitrite and ammonia have been detected and quantified. The gas analyses for products from the Series 3, 4, 5, and 6 tests also show the formation of N₂, N₂O, and NO_x (including significant NO for some tests). The observations of gaseous nitrogen products occur more often and to much greater extent for the tests with nitrite.

However, nitrogen chemistry is complex and other chemical reduction products might appear, including solution phase hydroxylamine, NH₂OH, and hydrazine, N₂H₄. Dissolved hyponitrous acid, HONNOH, and its base, hyponitrite (HONNO⁻), also might form.¹⁴ However, hydroxylamine, NH₂OH, reportedly disproportionates to N₂ and NH₃ in alkaline solution (page 501 of Greenwood and Earnshaw 1984) and reacts quickly with O₂ dissolved in alkaline solution to form nitrite (Stedman 1979). Therefore, NH₂OH is not expected to be present as a reaction product. Between pH 4 and 14, hyponitrite reportedly decomposes to N₂O and OH⁻ (page 529 of Greenwood and Earnshaw 1984) but hyponitrite decomposition is rapid only for the *cis* isomer; the *trans* isomer is more stable (Poskrebyshev et al. 2004). The hyponitrite isomers are depicted in Figure 3.14.

¹⁴ Hyponitrous acid, H₂N₂O₂, is weakly acidic (pK₁ = 7.21, pK₂ = 11.54) and decomposes to form N₂O + H₂O. However, hyponitrous acid is not the hydrate of N₂O because the reverse reaction, the uptake of N₂O in water to form hyponitrous acid, N₂O + H₂O → H₂N₂O₂, does not occur, (page 660 of Wiberg 2001).



Figure 3.14. *cis*- and *trans*-hyponitrite

Thus, N_2H_4 , *trans*- HONNO^- , and, perhaps, NH_2OH are potential additional NO_2^- and NO_3^- reduction products. Other nitrogenous reduction products may be posited but are much less likely. However, comparisons of spectra for the current tests with published spectra failed to show evidence for hydroxylamine and hydrazine (Figure 10 of Price et al. 1948) or for hyponitrite (Addison et al. 1952). These species, if they exist at all in the studied systems, must be only transitory.

It has been noted that nitrate produces only NO_2^- and NH_3 with trace H_2 from hydrogen scavenging in the dissolution of aluminum and zinc in alkaline solution and only H_2 and NH_3 in the dissolution of zirconium in ammonium fluoride with ammonium nitrate through the Zirflex process (Sections 1.4.1.1 and 1.4.1.2, respectively). However, as shown in the present testing, nitrite forms a wider array of reduction products, particularly in the presence of organics such as Nochar or Optimer 7194 Plus and in the presence of UO_2 , simulated sludge, and actual sludge. This behavior is similar to that found by Burroughs (1959) in which nitrite formed a greater variety of reduction products than did nitrate in their actions as atomic hydrogen scavengers from corrosion of metal in aqueous polishing processes. As postulated by Burroughs (1959), nitrite, being much more reactive than nitrate, interacts rapidly with intermediate nitrite reduction products to form N_2 and hyponitrite, which then decomposes to N_2O and water. Because of their low aqueous solubilities, the N_2O and N_2 escape to the gas phase and are lost as potential atomic hydrogen scavengers and further reduction to ammonia. In contrast, nitrate, being relatively unreactive towards its intermediate products, allows the intermediates to continue to scavenge atomic hydrogen until full reduction to ammonia occurs.

The nitrogen species potentially present in alkaline media and their oxidation states are shown in the following diagram. Based on the prior discussions, the species marked by shading are unstable or were not observed in any test. The species that are not shaded were observed (N_2O_4 as NO_x) and their concentrations were measured for most tests from Series 3, 4, 5, 6, and 7.

NO_3^- (aq)	N_2O_4 (g)	NO_2^- (aq)	NO (g)	N_2O (g) HONNO ⁻ (aq)	N_2 (g)	NH_2OH (aq)	N_2H_4 (aq)	NH_3 (aq)
5	4	3	2	1	0	-1	-2	-3

Nitrate and nitrite were measured by spectrophotometry in all test series and ammonia was measured by ion selective electrode in Series 4, 5, and 6. Gas concentrations were analyzed from Series 3 onward by mass spectrometry and gas volumes were measured at the beginnings and ends of each test. The gases detected and measured by mass spectrometry were NO_x (NO and NO_2), N_2O , and N_2 . Because the NO_x species are difficult to distinguish by mass spectrometry, identification was performed only for tests in Series 5 for which only NO was found. As noted previously, the gas analyses for tests in Series 6 were compromised by leakage of the silicone stoppers, allowing produced gas to escape and air to enter. Ammonia was measured indirectly for the first three test series based on the NaOH produced collaterally in the reduction of NaNO_3 or NaNO_2 to NH_3 . As shown in Table 1.1, each mole of nitrate or nitrite that reduced to one mole of ammonia produced one mole of NaOH while reduction of NaNO_3 to NaNO_2 produced no NaOH .

Chemical material balances were calculated for each test for which sufficient data exists. The material balance must account the reaction stoichiometries, which in turn depend on changes in the reacting compounds' oxidation states. For example, in the corrosion of uranium metal in water, the uranium metal oxidation state increases from 0 in the metal to +4 in the product UO_2 . Therefore, the oxidation of 1 mole of uranium metal is a $1 \times 4 = 4$ equivalent change. The UO_2 can be further oxidized (e.g., by O_2) to yield metaschoepite, $\text{UO}_3 \cdot 2\text{H}_2\text{O}$, with U in the +6 oxidation state, to produce a further 2 equivalent change for the oxidation of UO_2 to $\text{UO}_3 \cdot 2\text{H}_2\text{O}$. The change involved in the reduction of O_2 to hydroxide, OH^- , is 2 equivalents per oxygen atom or 4 equivalents per O_2 molecule. Similarly, the change in the reduction of hydrogen in water (+1 oxidation state) to form H_2 (0 oxidation state) is 1 equivalent per hydrogen atom or 2 equivalents per H_2 molecule. The oxidation state change for nitrogen in nitrate to form ammonia is 8 (1 mole of nitrate, +5 oxidation state, reduced to ammonia, -3 oxidation state, is 8 equivalents) while nitrogen reduction in nitrite to ammonia is a 6 equivalent change.

Oxidations involving organic species also occurred in some of the testing. For example, oxidation of Nochar by nitrite clearly occurred in Test 12 of the Series 3. However, the Nochar oxidation products, aside from the observed elevated CO_2 , were neither identified nor measured. Except for the eight Series 3 tests in which Nochar was added in gram quantities as a sorbent for water, organic components were not present in the current testing or were only present in small concentrations (e.g., as Optimer 7194 Plus in several tests and the small amount of Nochar in Test 9 of Series 5). Because the organic oxidation products were not identified and most tests involved little or no added organic material, no analysis of the material balance of organic carbon was performed.

Based on the foregoing discussions and the gas analysis data presented in Section 3.2, the primary uranium metal and UO_2 oxidation and water, nitrate, and nitrite reduction half-reactions observed in the present testing are summarized in Table 3.6.

Because both nitrate and nitrite are reduced to form various products (i.e., NO , N_2O , N_2 , and NH_3 , and, for nitrate, nitrite), the reactions of nitrate and nitrite cannot be determined solely by decreases in their concentrations but must be determined by the quantities of their reduction products. Therefore, the chemical equivalent material balance for U metal corrosion to form UO_2 and U(VI) in the presence of nitrate or nitrite and oxygen is expressed by Equation 3.1:

$$\begin{aligned} \text{Equivalents of U corroded} + \text{equivalents of } \text{UO}_2 \text{ oxidized to U(VI)} = & \text{Equation 3.1} \\ & \text{equivalents of } \text{O}_2 \text{ consumed} + \\ & \text{equivalents of } \text{H}_2 \text{ produced} + \\ & \text{equivalents of } \text{NO}_2^- \text{ produced from } \text{NO}_3^- \text{ reduction} + \\ & \text{equivalents of } \text{NO} \text{ produced from } \text{NO}_2^- \text{ reduction} + \\ & \text{equivalents of } \text{N}_2\text{O} \text{ produced from } \text{NO}_3^- \text{ and } \text{NO}_2^- \text{ reduction} + \\ & \text{equivalents of } \text{N}_2 \text{ produced from } \text{NO}_3^- \text{ and } \text{NO}_2^- \text{ reduction} + \\ & \text{equivalents of } \text{NH}_3 \text{ produced from } \text{NO}_3^- \text{ and } \text{NO}_2^- \text{ reduction.} \end{aligned}$$

The analytical findings and chemical material balances for most tests in all seven test series are shown in Table 3.7. Because gases were not sampled and analyzed in Series 1 and 2 experiments, chemical material balances for the nitrate, nitrite, and water reduction products could not be obtained for these tests. The Nochar present in many of the Series 3 tests prevented analyses for nitrate, nitrite, or hydroxide because the solution could not be separated from the Nochar. Complete material balances

could be calculated only for the four Nochar-free tests done in Series 3 that had solution analytical data. The gas sample in Test 4 of Series 5 was lost and all gas samples were compromised in the Series 6 tests.

Table 3.6. Uranium Metal and UO₂ Oxidation and Water, Oxygen, Nitrate, and Nitrite Reduction Half Reactions

Oxidations
<i>Uranium Metal</i>
$\text{U} + 4 \text{OH}^- \rightarrow \text{UO}_2 + 2\text{H}_2\text{O} + 4 \text{e}^-$
<i>Uranium Dioxide</i>
$\text{UO}_2 + 2 \text{OH}^- + \text{H}_2\text{O} \rightarrow \text{UO}_3 \cdot 2\text{H}_2\text{O} + 2 \text{e}^-$
Reductions
<i>Water</i>
$2 \text{H}_2\text{O} + 2 \text{e}^- \rightarrow \text{H}_2 + 2 \text{OH}^-$
<i>Oxygen</i>
$\text{O}_2 + 2 \text{H}_2\text{O} + 4 \text{e}^- \rightarrow 4 \text{OH}^-$
<i>Nitrate</i>
$\text{NO}_3^- + \text{H}_2\text{O} + 2 \text{e}^- \rightarrow \text{NO}_2^- + 2 \text{OH}^-$
$2 \text{NO}_3^- + 5 \text{H}_2\text{O} + 8 \text{e}^- \rightarrow \text{N}_2\text{O} + 10 \text{OH}^-$
$\text{NO}_3^- + 3 \text{H}_2\text{O} + 5 \text{e}^- \rightarrow \text{N}_2 + 6 \text{OH}^-$
$\text{NO}_3^- + 6 \text{H}_2\text{O} + 8 \text{e}^- \rightarrow \text{NH}_3 + 9 \text{OH}^-$
<i>Nitrite</i>
$\text{NO}_2^- + \text{H}_2\text{O} + \text{e}^- \rightarrow \text{NO} + 2 \text{OH}^-$
$2 \text{NO}_2^- + 3 \text{H}_2\text{O} + 4 \text{e}^- \rightarrow \text{N}_2\text{O} + 6 \text{OH}^-$
$2 \text{NO}_2^- + 4 \text{H}_2\text{O} + 6 \text{e}^- \rightarrow \text{N}_2 + 8 \text{OH}^-$
$\text{NO}_2^- + 5 \text{H}_2\text{O} + 6 \text{e}^- \rightarrow \text{NH}_3 + 7 \text{OH}^-$

As explained in Section 3.2, oxidation by atmospheric O₂ accounted for a large and relatively constant amount of the uranium metal corrosion in Series 3 [(4.92 ± 0.61) × 10⁻⁵ moles or 0.197 ± 0.024 meq at one σ for Tests 1 through 9]. Thus, about 16% of the uranium metal oxidation is by O₂ in control Test 1 in Series 3 but is about 24% of the oxidation in Test 7 containing 0.1 M NaNO₃. Uranium metal oxidation is dominated by O₂ in Tests 8 and 9, which contained 1.0 and 0.1 M NaNO₂, respectively.

The test data in Figure 3.6 show that nitrate or nitrite addition had no discernible effect on the amount of uranium metal oxidation by O₂ in Series 3. The data do show, however, that nitrate and particularly nitrite significantly decreased the amount of uranium metal oxidation by anoxic water pathways. The effect can be quantified by comparing the amount of anoxic water uranium metal oxidation in Tests 7, 8, and 9 with the amount of anoxic water uranium metal oxidation in control Test 1, all in Series 3. The anoxic water oxidation is manifest by H₂ production and the NO₂⁻ and NH₃ hydrogen radical scavenging products from nitrate or nitrite for Tests 7, 8, and 9. The amount of uranium metal oxidation that occurred by anoxic water is manifest only as H₂ production for control Test 1.

Table 3.7. Chemical Equivalents and Material Balances

Test	Test Composition			Chemical Quantities, milliequivalents							Chemical Balance ^(b)
	Conc., M		Other	Reactants			Products				
	NaNO ₃	NaNO ₂		U	UO ₂	O ₂	H ₂	N ₂ O	NO ₂ ⁻	NH ₃ ^(a)	
<i>Test Series 1, 53451-TI10</i>											
1	0	0	none	0.742	NM ^(c)	NM	NM	NM			
2	1	0	none	0.525	NM	NM	NM	NM	0.126	0.125	
3	3	0	none	0.343	NM	NM	NM	NM	0.11	0.055	
4	6	0	none	0.315	NM	NM	NM	NM	0.125	0.0565	
5	0	6	none	0.146	NM	NM	NM	NM		0.317	
<i>Test Series 2, 53451-TI11</i>											
1	0	0	none	0.770	NM	NM	NM	NM			
2	0	0.1	none	0.403	NM	NM	NM	NM		0.176	
3	0	1	none	0.251	NM	NM	NM	NM		0.205	
4	0	3	none	0.231	NM	NM	NM	NM		0.265	
5	6	0	none	0.353	NM	NM	NM	NM	0.184	0.0357	
<i>Test Series 3, 53451-TI12</i>											
1	0	0	none	1.12	NM	0.183	0.552	ND ^(d)	NM	NM	1.52
2	0	0	0.2 g Nochar/g	0.997	NM	0.207	0.393	ND	NM	NM	
3	0	0	0.2 g Nochar/g	0.966	NM	0.239	0.435	ND	NM	NM	
4	0	0	0.5 g Nochar/g	0.862	NM	0.178	0.252	ND	NM	NM	
5	0	0	0.5 g Nochar/g	0.815	NM	0.174	0.208	ND	NM	NM	
6	0	0	1.0 g Nochar/g	0.820	NM	0.222	0.301	ND	NM	NM	
7	0.1	0	none	0.844	NM	0.203	0.172	ND	ND	0.0172	2.16
8	0	1	none	0.185	NM	0.210	0.000096	ND	ND	0.0251	0.79
9	0	0.1	none	0.269	NM	0.164	0.0133	ND	ND	0.0299	1.30
10	0.1	0	0.2 g Nochar/g	NM	NM	0.286	0.0843	ND	NM	NM	
12	0	0.1	0.2 g Nochar/g	NM	NM	0.313	0.000134	0.0979	NM	NM	
<i>Test Series 4, 53451-TI13</i>											
1	0	0	none	0.633	0.0536	0.262	0.561	0.000000	ND	0.000	0.83
2	0.2	0	none	0.546	0.0658	0.141	0.0943	0.000958	0.0828	0.187	1.21
3	0.5	0	none	0.463	0.0917	0.193	0.0234	0.00401	0.0958	0.223	1.03
4	1	0	none	0.544	0.1130	0.219	0.000832	0.00262	0.108	0.237	1.16
5	2	0	none	0.477	0.0790	0.233	0.0000131	0.00241	0.176	0.178	0.94
6	0	0.2	none	0.235	0.0147	0.212	0.0000296	0.00605		0.0491	0.93
7	0	0.5	none	0.378	0.0328	0.212	0.0000123	0.0103		0.127	1.18
8	0	0.75	none	0.340	0.0162	0.280	0.0000234	0.0195		0.108	0.87
9	0	1	none	0.224	0.0234	0.149	0.0000164	0.00525		0.0372	1.29
10	0.5	0	UO ₂	0.460	NM	0.242	0.00204	0.00548	0.0364	0.427	0.65
11	0	0.5	UO ₂	0.396	NM	0.247	0.00419	0.0109		0.204	0.85
12	0	0	Na ₂ HPO ₄	1.011	0.0000	0.167	1.061	0.000000		0.00213	0.82
<i>Test Series 5, 53451-TI15</i>											
1	0	0	none	0.585	0.0603	0.228	0.456	ND		0.00211	0.94
2	0	0.2	none	0.0123	0.000	0.0825	0.000153	ND		0.00046	0.15
3	0	0.5	none	0.0260	0.00493	0.128	0.000030	0.00042		0.00129	0.24
4	0	0.75	none	0.0514	0.00496		Gas sample lost			0.00244	
5	0.5	0	none	0.512	0.0725	0.125	0.00494	0.00055	0.0387	0.179	1.68
6	1	0	none	0.275	0.0374	0.0885	0.000116	0.00174	0.0309	0.114	1.33
7	0	0.5	UO ₂	0.192	NM	0.297	0.00585	0.0204		0.130	0.42
8	0.5	0	UO ₂	0.357	NM	0.200	0.00564	0.0903	0.0206	0.370	0.52
9	0	0.5	Nochar	0.280	NM	0.0473	0.000014	0.00247		0.146	1.43
10	0	0.5	Optimer	0.0156	0.00306	0.164	0.000007	0.00003		0.00202	0.11
11	0	0.5	Sim. sludge	0.290	NM	0.559	0.00105	0.131		0.00334	0.42
12	0.5	0	Sim. sludge	0.267	NM	0.265	0.000439	0.00993	0.0000	0.0788	0.76

Table 3.7. (contd)

Test	Test Composition			Chemical Quantities, milliequivalents							Chemical Balance ^(b)
	Conc., M		Other	Reactants			Products				
	NaNO ₃	NaNO ₂		U	UO ₂	O ₂	H ₂	N ₂ O	NO ₂ ⁻	NH ₃ ^(a)	
<i>Test Series 6, 53451-TI18</i>											
1	0	0	none	0.549	0.0840	Gas sample invalid			0.00018		
2	0.5	0	none	0.764	0.179	Gas sample invalid			0.144	0.396	
3	0	0.5	none	0.139	0.0447	Gas sample invalid				0.0413	
4	0	0	KE Floc Comp	0.384	NM	Gas sample invalid				0.0203	
5	0.5	0	KE Floc Comp	0.280	NM	Gas sample invalid				0.203	
6	0	0.5	KE Floc Comp	0.199	NM	Gas sample invalid				0.0313	
7	0	0	KC-2/3 Comp	0.248	NM	Gas sample invalid				0.00078	
8	0.5	0	KC-2/3 Comp	0.0887	NM	Gas sample invalid				0.0429	
9	0	0.5	KC-2/3 Comp	0.105	NM	Gas sample invalid				0.00055	
<i>Test Series 7, 53451-TI19</i>											
1	0	0	none	0.900	NM	0.0925	0.704	0.000104			1.13
2	0	0	0.05 M NaCl	1.078	NM	0.117	0.919	0.000138			1.04
3	0	0	2 mL pH 6.9 MS	0.998	NM	0.126	0.810	0.000162			1.07
4	0	0	2 mL pH 5.1 MS	0.559	NM	0.0750	0.270	0.000173			1.62
5	0	0	2 mL pH 4.3 MS	1.182	NM	0.0781	0.167	0.000144			4.83
6	0	0	0.6 mM UO ₂ Cl ₂								
(a) Ammonia measured indirectly as NaOH co-product by pH in Test Series 1, 2, and 3 and with ammonia ion selective electrode in Test Series 4, 5, and 6.											
(b) Chemical balance is the ratio of the number of chemical equivalents oxidized to the number of chemical equivalents reduced. The number of chemical equivalents oxidized includes uranium metal oxidized to UO ₂ and UO ₂ oxidized to UO ₃ ·2H ₂ O. The chemical equivalents reduced includes equivalents for O ₂ gas reduction, H ₂ from water reduction, NO ₂ ⁻ from NO ₃ ⁻ reduction, N ₂ O from NO ₂ ⁻ and NO ₃ ⁻ reduction, and NH ₃ from NO ₂ ⁻ and NO ₃ ⁻ reduction. For tests containing UO ₂ (including those with simulated and actual sludge), the contribution from oxidation of UO ₂ to U(VI) in the solid phase was not accounted because of the large and imprecisely known quantity of UO ₂ from the starting solids compared with the small amount of UO ₂ obtained by U metal corrosion. For tests containing Nochar, the amount of Nochar oxidized could not be accounted because the oxidation products, aside from CO ₂ , were unknown and were not measured.											
(c) NM – Not measured. Gas compositions were not measured in Series 1 and 2.											
(d) ND – Not determined or below detection limit. The UV spectrum indicated that little, if any, NO ₂ ⁻ was present. The solution spectrum is not consistent with either NO ₂ ⁻ or NO ₃ ⁻ (see text).											

As shown in Table 3.7, the presence of 0.1 M NaNO₃ in Test 7 of Series 3 decreased the amount of uranium metal corroded by anoxic pathways (to form H₂ or reduce nitrate to nitrite and ammonia) to about 33% of what was observed in the absence of nitrate in control Test 1. The presence of 0.1 M NaNO₂ (Test 9) had a greater effect than did 0.1 M NaNO₃, decreasing the amount of uranium metal corroded by anoxic water mechanisms to 5.6% of what was observed in the absence of nitrite (control Test 1). In 1 M NaNO₂ (Test 8), the amount of uranium metal corroded by anoxic pathways was 2.7% of the amount observed in Test 1 without nitrite. The effectiveness of nitrate and especially nitrite in decreasing H₂ generation thus is partially due to inhibition of the anoxic uranium metal corrosion reaction and partially due to scavenging of the nascent hydrogen that arises in whatever anoxic uranium metal corrosion that does occur. Because uranium metal corrosion in anoxic water is mediated by reaction of hydrogen radicals with uranium metal to form UH₃, it is very likely that the hydrogen radical scavenging afforded by nitrate or nitrite is responsible for the collateral inhibition of the uranium metal corrosion reaction.

The conversion of nitrate to nitrite in the testing was registered by measuring their respective UV absorbances at ~355 nm and ~302 nm (Figure 2.3). The UV spectra of the starting 0.1 M NaNO₃ solution and the solution after running Test 7 in Series 3 are shown in Figure 3.15. Although residual nitrate likely contributes to the spectrum obtained at the end of Test 7, little or no nitrite was found in the product

spectrum. Comparisons with published spectra for hydroxylamine and hydrazine (Figure 10 of Price et al. 1948) and for hyponitrite (Addison et al. 1952) show that none of these species contributed to the product solution spectrum. However, the product solution spectrum differs significantly from the initial broad nitrate peak at ~ 302 nm (see Figure 2.3). A 53-hour exposure of a new rubber stopper in the test apparatus (Figure 2.1; part B) to water at 92°C was done using to determine if the black rubber stoppers used in test Series 1 through 5 contribute to the product solution spectrum. The resulting stopper spectrum, also shown in Figure 3.15, shows significant absorption in the region observed for nitrate but provides only featureless low absorbance in the ~ 355 -nm region where nitrite absorbs.

Because of the black rubber stopper artifact in the solution absorbance spectra, substitution of other stopper material that would not contribute to the solution UV absorbance was investigated. It was found that silicone rubber provided no significant UV absorbance contribution to water after 72 hours of exposure at 90°C (see Figure 3.15). Accordingly, silicone stoppers were adopted for use in test Series 6. However, in Series 6, silicone rubber was discovered to have unacceptably high gas permeability. Therefore, another stopper material was sought that would impart little or no artifact to the UV spectrum and have low gas permeability. Based on its availability and relatively low gas permeability, neoprene was tested for its potential contributions to the UV spectrum by 24-hours of immersion in 60°C water. Because the UV spectrum from this test is relatively featureless and shows low absorbance (Figure 3.15), neoprene stoppers were used in Series 7.

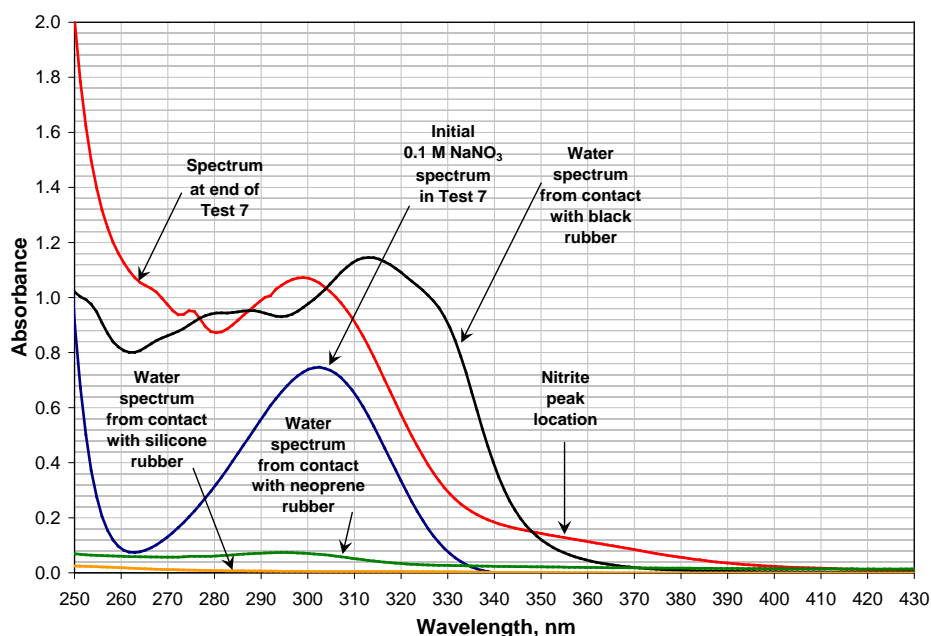


Figure 3.15. Spectra of 0.1 M NaNO₃ and Product Solution in Test 7 of Series 3, from Water Condensate on a New Black Rubber Stopper, Water Condensate on a New Silicone Rubber Stopper, and Water Contact with a New Neoprene Rubber Stopper

3.4 Nitrate and Nitrite Reaction with UO_2

UO_2 is the principal uranium metal oxidation product observed in K Basin sludge. Because both nitrate and nitrite are oxidants, each potentially can react with UO_2 and the UO_2 parasitically consume the nitrate or nitrite reagents added to diminish H_2 release. To test this potential, survey experiments were conducted in Series 2 to determine the extent of reaction of 0.2 M solutions of NaNO_3 and NaNO_2 with UO_2 at 84.8°C over the ~140-hour test interval.

Oxidation of the UO_2 to yellow U(VI) solids was visible in the tests with nitrite but not with nitrate (Figure 3.16). The yellow solids likely are sodium diuranate, $\text{Na}_2\text{U}_2\text{O}_7$, based on known hexavalent uranium chemistry and compound solubilities. The UV absorption spectra of the solutions before and after contact with UO_2 were measured to determine if nitrate or nitrite concentrations changed.



Figure 3.16. UO_2 in 0.2 M NaNO_2 (left two vials; note yellow solids) and in 0.2 M NaNO_3 (vial on right) after 140 Hours at 84.8°C

No net decrease in the absorbance or change in the shape of the spectrum, except for an increase in the low wavelength baseline, was observed for the test with 0.2 M NaNO_3 and UO_2 . However, the absorption spectra intensities decreased to 81% and 83% of their starting values in the duplicate tests with 0.2 M NaNO_2 and UO_2 . The nitrite concentrations thus decreased from 0.188 M in the starting solutions (which were diluted from the original 0.2 M by the interstitial water present with the UO_2) to 0.154 M. No other features or changes in the nitrite absorption spectral shapes were observed in the duplicate tests. These findings indicate that UO_2 is a parasitic consumer of nitrite but does not react with nitrate. The nitrite reduction product was not determined but likely is ammonia.

3.5 Nochar Properties

The behavior of Nochar Acid Bond N960 as a potential uranium metal corrosion inhibitor and suppressor of hydrogen generation in anoxic water was discussed in sections 3.1.1 and 3.2.2. Because the postulated mechanism of corrosion inhibition would be through its action as a desiccant, the uptake of water from saturated 60°C vapor was measured by exposing weighed amounts of Nochar to water vapor in a closed temperature-controlled humidor. As part of these investigations, swelling of Nochar also was tested at 0.2:1, 0.5:1, and 1:1 Nochar:water weight ratio loadings. Nochar's stickiness and affinity for finely divided uranium oxide particles may commend it as an agglomerating agent to reduce the respirable particulate fraction in sludge.

The moisture uptake of Nochar N960 was measured under saturated water vapor conditions at 60°C . Moisture uptake was at steady state after ~3 days, reaching about 84% of the weight of the Nochar N960.

The Nochar:water weight ratio at 60°C water saturation therefore was about 1.19:1, meaning that the amount of Nochar application must exceed 1.19:1 to provide any decrease in water vapor pressure (desiccation) in a 60°C package. The highest Nochar:water weight ratio recommended and tested was 1:1 and thus is below the level at which Nochar begins to act as a desiccant.

Mixtures of Nochar N960 and water were prepared at the vendor-recommended test weight ratios ranging from 0.2:1 to 1:1 Nochar:water. The mixtures were made in 4-dram (~16-mL) vials and allowed several hours contact for water absorption into the Nochar. The mixtures then were centrifuged at the highest setting to minimize air entrainment and the volumes of the centrifuged mixtures determined by comparison to a volume-calibrated vial. The percentage expansion from the original water volume and the mixture densities at various Nochar:water weight ratios are shown in Figure 3.17. The Nochar-water mixture swelling increase was over 120% (i.e., >220% of the original water volume) at the highest recommended Nochar loading. The centrifuge-packed densities of the Nochar-water mixtures were about 0.75 g/cm³ at the lowest tested Nochar:water weight ratio of 0.2:1 and increased to about 0.89 g/cm³ at the highest tested 1:1 Nochar:water weight ratio. According to the Material Safety Data Sheet, Nochar N960 has a particle density of 0.80 g/cm³.

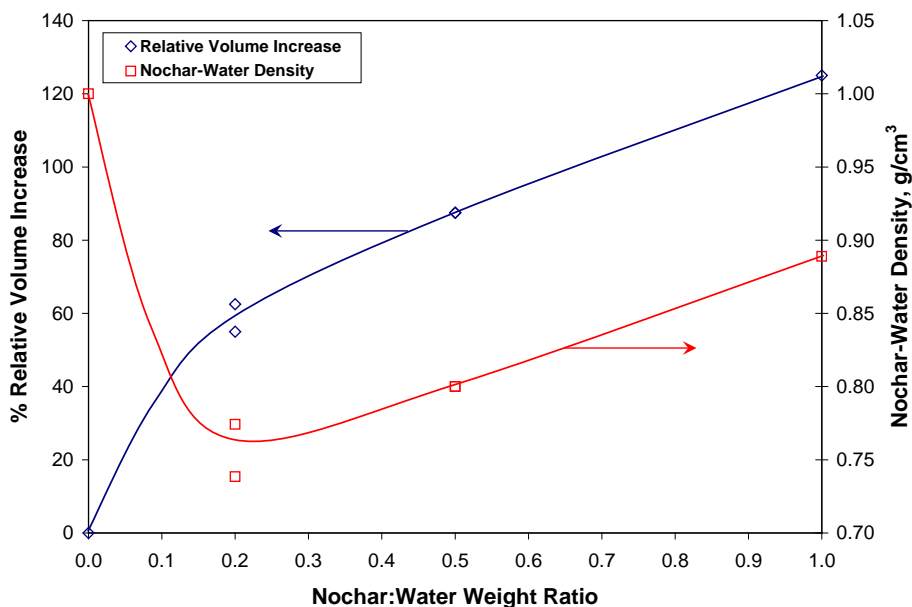
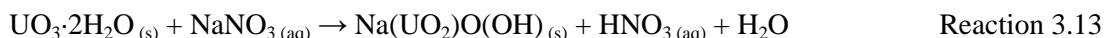


Figure 3.17. Immobilized Water Product Expansion at Various Nochar:Water Weight Ratios

3.6 Additional Testing

Based on the favorable results obtained for nitrate, its lack of extraneous gas formation (i.e., unlike nitrite which formed NO), and its lack of parasitic loss by oxidation of UO₂ (which was observed with nitrite), further tests with genuine sludge into the effects of nitrate on H₂ attenuation should be performed. In addition to determining H₂ attenuation, the expected reactions of the sodium salt with metaschoepite to form sodium compregnacite [Na₂(UO₂)₆O₄(OH)₆·7H₂O; Reaction 3.12] and clarkeite [Na(UO₂)O(OH); Reaction 3.13] should be examined.



These reactions decrease pH and potentially could alter the mechanical strength of the sludge (shear strength, agglomeration) by causing bridging or cementation of the sludge particles through precipitation of the newly formed sodium – U(VI) phases. Increases in sludge strength with storage could complicate sludge retrieval for further processing. Long-term tests should be undertaken to examine these potential reactions at expected sludge storage temperatures. Parameters to be measured include temperature, phase changes, gas volume and composition, uranium metal weight losses, nitrite and ammonia formation from nitrate, and sludge volume and strength as a function of storage time. The impact of sorption of nitrate onto the organic ion exchange resin known to be present in K Basin sludge also must be determined if nitrate addition to control H₂ generation technique is to be successfully applied.

As shown in Series 7, dissolved U(VI) also can act as a hydrogen radical scavenger. The effects of other sludge components, particularly iron hydroxide phases, on the effectiveness of U(VI) should be determined. Because of its potential for process application, long-term tests also should be undertaken to examine the effects of storage on sludge mechanical and chemical properties. In this case, however, the reactions are limited to oxidation of sludge phases by interaction with atmospheric oxygen diffusing into the sludge. The decreased pH imposed to increase the U(VI) solution concentration is not expected to affect the oxygen diffusion rate but the pH change could alter the UO₂ oxidation rate.

Means to introduce dissolved U(VI) to sludge streams containing little U(VI) solid phase but, as is the case, containing tetravalent uranium as UO₂ also should be investigated. One way to introduce U(VI) to sludge containing uranium oxide present only as UO₂ is to add nitric acid (HNO₃). The HNO₃ acts both to dissolve the UO₂ and oxidize it to U(VI) as aqueous UO₂(NO₃)₂ (Reaction 3.14).



Experiments to test the effectiveness and process control aspects of this approach, such as attaining target pH and U(VI) concentrations, must be performed with simulated and genuine sludge. The objective of this testing would be to determine HNO₃ reagent demand and the extent of dissolution of other sludge components (e.g., transuranics) in reaching the target pH (~4-5).

Testing to-date has occurred at ~60°C and 90°C for nitrate and nitrite and only at ~90°C for U(VI). Candidate reagents for process use should be tested for their efficacies at lower temperatures representative of their potential application (e.g., trans-site shipment, long-term on-site storage, and processing for WIPP disposal). The testing could be incorporated as part of the long-term testing envisioned to determine sludge mechanical properties.

The reagents also should be tested for their impact on diminishing the H₂ arising from radiolysis. The attractiveness of pursuing this avenue of investigation would be increased if credit for decreasing radiolytic H₂ could be obtained from WIPP authorities. Such credit would allow greater waste loading for containers destined for WIPP.

The efficacies of the candidate reagents should be tested in the waste form(s) to be disposed to WIPP (e.g., in grout or other solidifying matrix). If the H₂ attenuation is sufficient, and the sludge can be dewatered so that no drainable liquid exists, grout or another solidifying material may not even be necessary for a WIPP-bound waste. If grout is used, however, U(VI) could not attenuate H₂ effectively because its solution concentration would decrease below effective levels (10⁻⁵ M or lower, depending on pH; Ewart et al. 1992) by precipitation in the cement waste form.

The acceptability of any product waste for WIPP disposal must be determined. The introduction of nitrate, nitrite, or U(VI) to the sludge may be of concern to WIPP. However, objection to the use of nitrate, nitrite, or U(VI) is unlikely given the existence of these constituents in prior wastes disposed to WIPP from Rocky Flats and Hanford. Depending on the desired implementation strategy, the management of the excess nitrate or nitrite solution and the impact of lower pH caused by reaction of sodium ion with metaschoepite or intentional mild acidification (pH ~4-5) if U(VI) is used as the hydrogen radical scavenger also must be evaluated.

Finally, future testing should be tailored to target waste streams (e.g., Knock Out Pot, settler tank, and container sludge; orphan materials in sludge processing; and decommissioning and decontamination rubble) to meet specific functional design criteria within the particular points of operational insertion (e.g., storage, treatment, or shipping).

4.0 Conclusions

Survey of the technical literature and laboratory testing were performed to identify methods to decrease the rate of hydrogen gas generation from corrosion of uranium metal in anoxic water for K Basin sludge applications. The literature survey identified four means to decrease the H₂ evolution rate: decreased temperature, reactant isolation (separation of the uranium metal from the water), corrosion inhibitors, and hydrogen scavengers.

Decreased temperature is applicable to controlled systems but is not applicable to shipments destined for WIPP where transported packages must demonstrate suitably low H₂ generation rates at 60°C. Information on the effects of temperature on uranium metal corrosion rate is provided in STP publications.

Grouting as a means to improve reactant isolation has been shown to decrease H₂ generation rate by up to a factor of 3 for simulated sludge. Higher impacts likely were not obtained because appreciable water vapor pressures, which allow reaction of uranium metal with the condensing water films, still exist in the grouted products. More effective desiccants such as magnesium and calcium oxide, which can decrease water vapor pressures by factors of ~6000 below water saturation, may perform better than grouts in suppressing the rate of the uranium metal – water reaction. Nochar N960, a superabsorbent organic polymer, also has been proposed as a potential desiccant based on its high capacity to sorb aqueous solutions.

Uranium metal corrosion inhibitors in water have been investigated for over 60 years. The most effective inhibitors include some organic compounds that also are useful to control steel corrosion. However, the best organic inhibitors must be replenished to maintain efficacy. The most promising of the inorganic inhibitors are nitrite and neutral to alkaline phosphate salts. Although dissolved oxygen is known to inhibit the uranium metal corrosion rate, the practical difficulty of maintaining active aeration in dense heterogeneous sludge likely precludes its use under storage and transportation conditions.

Scavengers of the “nascent” hydrogen that appears in the corrosion of uranium and other active metals in water include nitrate, nitrite, permanganate, and chromate. Of these agents, nitrate and nitrite offer the most promise in terms of compatibility with the K Basin system, Hanford experience, and applicability.

Based on the survey, laboratory experimentation was conducted to determine the effects of nitrate, nitrite, phosphate, and Nochar to lower the rate of H₂ generation from the reaction of uranium metal with water. The tests used nearly spherical high-purity uranium metal beads in water, in aqueous salt solutions, in UO₂ aqueous slurries, in simulated sludge, and in genuine sludge aqueous slurries under controlled temperature conditions. The gas space above the reacting mixtures was air in most tests. The reaction progress was monitored by measuring the gas volume, the extent of uranium metal corrosion (as determined by weight loss), the nitrate and nitrite reduction product concentrations, and the product gas compositions and quantities.

The testing showed that Nochar, applied at vendor-recommended Nochar:water weight dosages ranging from 0.2:1 to 1:1, decreased H₂ generation rates by factors ranging from 1.3 to 2.6 compared with control tests with uranium metal and water only. Associated characterization of Nochar-water mixtures at

60°C showed that while Nochar is a good liquid water sorbent, it is not an effective desiccant. Thus, in terms of decreasing the H₂ generation rate from reaction of uranium metal with water, Nochar's performance proved to be roughly equivalent to that of grouting. Nochar's stickiness and affinity for finely divided uranium oxide particles, however, may make it attractive as an agglomerating agent to reduce the respirable particulate fraction in sludge handling.

Nitrate and nitrite, added as their sodium salts, were more effective than Nochar N960 in decreasing uranium corrosion in water and much more effective in diminishing H₂ generation. Of the two salts, sodium nitrite was more effective in decreasing H₂ generation. For example, H₂ generation was attenuated by a factor of 3.2 in 60°C 0.1 M NaNO₃ while 0.1 M NaNO₂ decreased H₂ generation by a factor of about 42 compared with parallel tests without added salt. With 1 M NaNO₂, the H₂ generation attenuation factor was at least 5800. Overall, the H₂ attenuation factors for nitrite in aqueous solution were at least a factor of ten greater than for nitrate at a similar concentration. The differences in H₂ attenuation between nitrite and nitrate decreased for UO₂ and simulated and genuine sludge slurries. Tests of Nochar with 0.1 M NaNO₃ and 0.1 M NaNO₂ gave better attenuation factors than the parallel tests of Nochar or salt solution alone. In the tests of mixed Nochar-salt, reaction of the salt with Nochar occurred and produced oxides of nitrogen (NO_x). The effects were more severe for the Nochar test with 0.1 M NaNO₂, which also produced significant nitrogen and nitrous oxide (N₂ and N₂O, respectively). The gas formation may prohibit the joint use of Nochar with nitrate or nitrite for WIPP purposes as the Nochar/salt mixtures appear to be chemically reactive.

A single test was performed with 0.07 M phosphate as a uranium corrosion inhibitor. It was found that phosphate did not decrease H₂ generation and actually increased the U metal corrosion and H₂ generation rates compared with control tests in water only and the absence of added salt.

The attenuation of H₂ production by nitrate or nitrite was due to both scavenging of hydrogen and a much smaller underlying decrease in uranium metal corrosion rate. The effects likely are related as uranium metal corrosion in anoxic water is known to be mediated by hydrogen radicals through the formation of uranium hydride. The effects of nitrate and nitrite to act as chemical scavengers of hydrogen arising by radiolysis are known and also may be worth accounting in achieving transportation safety goals for the WIPP and in achieving storage and process safety in plant operations.

Scoping tests showed that nitrite reacts with uranium dioxide, UO₂, while no reaction was observed between nitrate and UO₂. The nitrite reduction product was not determined but likely is ammonia; the UO₂ oxidation product is a U(VI) compound such as sodium diuranate. The reaction of nitrite with UO₂ means that additional nitrite may be required if nitrite salts are used to decrease H₂ generation rates from K Basin sludge.

NO gas was observed to form initially upon mixing simulated or actual sludge with nitrite. The gas volume was relatively small and the gassing complete in several hours. The reaction also did not deplete any key reagent (e.g., nitrite, UO₂) nor require U metal to occur. Further testing showed that ferrihydrite, UO₂, metaschoepite, and nitrite all were required for the NO gas-forming reaction to occur. These observations paralleled similar observations reported in the technical literature made in oxidation, to U(VI), of UO₂ formed in soil through biological reduction pathways. Because no similar gassing was observed when nitrate was used in place of nitrite, nitrate may be preferred to nitrite to attenuate hydrogen from the anoxic corrosion of uranium metal in water-saturated K Basin sludge.

The primary nitrate and nitrite reduction products are nitrite (from nitrate) and ammonia. Nitrite was observed by UV spectroscopy and the ammonia by ion selective electrode measurements. The ammonia is accompanied by production of hydroxide as observed by increase in the solution pH. Small quantities of N₂O also were observed in many tests with the N₂O production generally higher with nitrite than with nitrate. Chemical material balance calculations were obtained where possible (i.e., where reactant and product quantities could be measured). The ratios of chemical equivalents oxidized to the chemical equivalents reduced generally were near unity. Material balances were not obtained for compositions containing gross quantities of Nochar as the Nochar oxidation products, aside from CO₂, were not known and were not measured. Based on UV spectra gathered from the solution tests, no hydroxylamine, hydrazine, or hyponitrite (potential nitrate or nitrite reduction products) was observed.

The relative benefits of application of nitrate and nitrite to attenuate hydrogen from uranium metal corrosion in anoxic water are shown in Table 4.1. Table 4.1 compares, at a high level, the key features of nitrate and nitrite addition and may be useful to assist in selecting and developing approaches to mitigate H₂ generation in any stage of sludge handling, treatment, or shipping. It is seen that although nitrite provides a greater H₂ attenuation factor than nitrate for a given salt concentration in aqueous solution, the advantage diminishes in genuine sludge. Nitrate generally has less effect on decreasing the uranium metal corrosion rate but the difference in effect between nitrate and nitrite is small in genuine sludge. Disposal pathways for nitrate or nitrite are equivalent. Nitrate offers advantages over nitrite in process behavior (predictability, side reactions), stoichiometric capacity, and safety in handling. Overall, nitrate seems to be a better choice for process application.

Table 4.1. Comparison of Nitrate and Nitrite Qualities in Application to Attenuate Hydrogen from Uranium Metal Corrosion

Property	Advantage		Discussion
	Nitrate	Nitrite	
Attenuate H₂			
In water only		✓	~10× higher attenuation coefficient for nitrite than nitrate at equal salt concentrations
With UO ₂	✓		Slightly higher attenuation coefficient for nitrate
In simulated sludge	✓		~2× higher attenuation coefficient for nitrate
In genuine sludge	✓		~4× higher for nitrate in KE canister composite sludge
		✓	~10× higher for nitrite in KE floor/pit composite sludge
Inhibit U corrosion rate			
In water only	✓		Highest corrosion rate inhibition factor ~2.4 for nitrate; corrosion rate inhibition factors range from 2 to 60 for nitrite
With UO ₂	✓		Slightly better (lower corrosion rate) for nitrate
In simulated sludge	✓		Slightly better (lower corrosion rate) for nitrate
In genuine sludge	✓		Slightly better for nitrate in KE floor/pit composite sludge
		✓	Slightly better for nitrite in KE canister composite sludge
Stoichiometry/capacity	✓		Nitrate provides 8 equivalents/mole; nitrite provides 6 eq./mole
Predictability of efficacy	✓		Nitrite efficacy in H ₂ attenuation is generally improved by organics but can give significant unwanted corrosion rate inhibition
Side reactions	✓		Nitrite participates in unwanted side reactions (e.g., producing NO in sludge; UO ₂ oxidation) which also increases its consumption
Solubility	≅	≅	Both salts dissolve to >7 M saturated solution at room temperature
Hazard	✓		Both salts are oxidants; nitrite has higher toxicity
Disposal	≅	≅	Both salts are major Hanford underground tank waste components and both may be disposed as low-level waste (LLW)

Results of tests with genuine sludge in the absence of nitrate or nitrite and consideration of the associated oxidation-reduction chemistry suggest that dissolved hexavalent uranium might also be an effective scavenger of hydrogen radicals from anoxic aqueous corrosion of uranium metal. Accordingly, several scoping tests were performed to determine if dissolved U(VI), maintained by partial dissolution of metaschoepite using slightly acidic pH (pH ~4 to 5), would provide H₂ attenuation. The testing was performed in aqueous metaschoepite slurries at ~90°C using apparatus similar to that used in other testing with nitrate and nitrite. Because of the higher temperature, 50-mL rather than 15-mL gas collection centrifuge tubes were used to accommodate the gas expansion. A parallel test of the reaction of dissolved U(VI) and a uranium metal bead also was performed to determine if the U(VI) reacted with the nascent hydrogen from the uranium metal corrosion. This reaction would be indicated by disappearance of the U(VI) from solution to form UO₂. This latter test showed that dissolved U(VI) was chemically reduced by the corroding uranium metal and its nascent hydrogen. The former tests showed that dissolved U(VI) in equilibrium with the slightly acidified metaschoepite slurry attenuates H₂ generation from corroding uranium metal and that the effectiveness increases with the increasing U(VI) concentration brought about by decreasing pH. However, the degree of H₂ attenuation was not as great as was observed for tests with genuine sludge KC-2/3 Comp. Other factors, such as the presence of iron hydroxide or other sludge components, may have been responsible for the greater H₂ attenuation factor shown by KC-2/3 Comp sludge.

Overall, the testing showed that significant attenuation of H₂ production from anoxic corrosion of uranium metal in water, sludge, or sludge-like matrices could be obtained by the addition of nitrate or nitrite salt or by increasing the U(VI) solution concentration. For genuine sludge, in particular, H₂ attenuation factors of approximately 100 to 1000 are observed for 0.5 M nitrate or nitrite salt and, in one case, a factor of 3500 for U(VI) in sludge at pH ~5.5. All of these agents likely act as hydrogen scavengers and are effective because they react with the hydrogen radicals and are, themselves, chemically reduced.

Based on these promising findings, further testing is suggested. Due to nitrate's predictable and adequate H₂ attenuation performance, its lack of extraneous gas formation compared with nitrite (to form NO), and its lack of parasitic loss by oxidation of UO₂ (also shown by nitrite), further tests with genuine and simulated sludge into the effects of nitrate concentration on H₂ attenuation should be performed. Besides investigating the effects on H₂ generation, long-term tests should investigate potential changes in sludge mechanical strength (shear strength, agglomeration) caused by bridging of the sludge particles through precipitation of the newly formed sodium uranate phases (e.g., clarkeite, Na-compreignacite). Increased sludge strength during storage could complicate sludge retrieval for further processing. Measured parameters should include temperature, phase changes, gas volume and composition, uranium metal weight losses, nitrite and ammonia formation from nitrate, and sludge strength as a function of storage time. The impact of sorption of nitrate onto organic ion exchange resin also must be tested if nitrate is to be added to control H₂ generation.

Tests to study further the performance of dissolved U(VI) as a hydrogen radical scavenger also are recommended. As in the proposed tests for nitrate, similar long-term storage tests with dissolved U(VI) should be undertaken to examine the mechanical and chemical property effects. The effects of sludge components, particularly iron hydroxide, should be determined. Means to add dissolved U(VI) to sludge streams containing little U(VI) solid phase (e.g., acidification by nitric acid) also should be investigated.

Testing summarized in this report has occurred at ~60°C and 90°C for nitrate and nitrite and only at ~90°C for U(VI). The efficacies of candidate reagents for process use should be confirmed at lower temperatures representing their potential applications in trans-site shipment, long-term on-site storage, and processing for WIPP. The reagents also should be tested for their potential to diminish radiolytic H₂, particularly if credit for radiolytic H₂ generation could be obtained from WIPP authorities, and thus allow greater loading for WIPP-bound containers.

The efficacy of the candidate reagents should be tested in WIPP waste form(s) such as grout or other solidifying matrices. If the H₂ attenuation is sufficient, and the sludge can be treated to preclude or absorb drainable liquid, solidifying material and a mixing step may be unnecessary to craft an acceptable WIPP waste form. If grout is used, U(VI) would not be an effective H₂ scavenger because of the low solubility of U(VI) in cement.

The acceptability of any waste form to be disposed to WIPP must be determined, including the potential introduction of nitrate, nitrite, or U(VI) to the sludge. Management of excess nitrate solution may be an issue in certain applications. The impact of lower pH caused by sodium ion's reaction with metaschoepite or by intentional pH ~4 to 5 sludge acidification if U(VI) is used also must be evaluated.

All future testing should be tailored to the target waste stream (e.g., Knock Out Pot, settler tank, and container sludge; orphan materials in sludge processing; and decommissioning and decontamination rubble) and the particular point of operational insertion (e.g., treatment, storage, or shipping).

5.0 References

- Abrefah J, WJ Gray, and CV Shelton-Davis. 2000. *Dissolution Rate of Unirradiated N-Reactor Fuel*. PNNL-SA-33740, Pacific Northwest National Laboratory, Richland, Washington.
- Addison CC, GA Gamlen, and R Thompson. 1952. "The Ultraviolet Absorption Spectra of Sodium Hyponitrite and Sodium α -Oxyhyponitrite: The Analysis of Mixtures with Sodium Nitrite and Nitrate." *Journal of the Chemical Society* 338-345.
- Baker JT. 2008. *Desiccant Selection Guide*. JT Baker, Phillipsburg, New Jersey. Available at: <http://www.mallbaker.com/techlib/documents/americas/3045.html>.
- Bargar JR, R Bernier-Latmani, DE Giammar, and BM Tebo. 2008. "Biogenic Uraninite Nanoparticles and Their Importance for Uranium Remediation." *Elements* 4:407-412.
- Booman GL, CF Metz, JE Rein, and GR Waterbury. 1962. Page 86 of *Treatise on Analytical Chemistry*, "Part II, Analytical Chemistry of the Elements, Volume 9 Uranium • The Transuranium Actinide Elements." IM Kolthoff and PJ Elving, editors, Interscience Publishers, New York, New York.
- Bradley MJ and LM Ferris. 1962. "Hydrolysis of Uranium Carbides between 25 and 100°. I. Uranium Monocarbide." *Inorganic Chemistry* 1(3):683-687.
- Bradley MJ and LM Ferris. 1964. "Hydrolysis of Uranium Carbides between 25 and 100°. II. Uranium Dicarbide, Uranium Metal-Monocarbide Mixtures, and Uranium Monocarbide-Dicarbide Mixtures." *Inorganic Chemistry* 3(2):189-195.
- Bryan SA, CH Delegard, AJ Schmidt, RL Sell, KL Silvers, SR Gano, and BM Thornton. 2004. *Gas Generation from K East Basin Sludges – Series II Testing*. PNNL-13446, Rev. 1, Pacific Northwest National Laboratory, Richland, Washington. Available at: http://www.pnl.gov/main/publications/external/technical_reports/PNNL-13446Rev1.pdf.
- Burroughs WP. 1959. "Hydrogen Elimination in Treatment of Metals." U.S. Patent 2893181, U.S. Patent Office, Washington, D.C. Available at: <http://www.freepatentsonline.com/2893181.pdf>.
- Butcher EJ, IH Godfrey, and M Brogden. 2004. *Final Report on the Minimisation of Uranium Corrosion when Treating Hanford KE and KW Basin Wastes Using Cementation*. NSTS (04) 5438, Issue 01, British Nuclear Fuels Limited, Inc., Richland, Washington.
- Choe S, HM Liljestrand, and J Khim. 2004. "Nitrate Reduction by Zero-Valent Iron under Different pH Regimes." *Applied Geochemistry* 19:335-342.
- Cristy SS, RK Bennett Jr, JJ Dillon, HL Richards, RD Seals, and VR Byrd. 1986. *Characterization of Uranium Surfaces Machined with Aqueous Propylene Glycol-Borax or Perchloroethylene-Mineral Oil Coolants*. Y-2359, Y-12 Plant, Oak Ridge, Tennessee. Available at: <http://www.osti.gov/bridge/servlets/purl/6973560-wb5DG5/6973560.PDF>.

Delegard CH, SA Bryan, AJ Schmidt, PR Bredt, CM King, RL Sell, LL Burger, and KL Silvers. 2000. *Gas Generation from K East Basin Sludges – Series I Testing*. PNNL-13320, Pacific Northwest National Laboratory, Richland, Washington. Available at: http://www.pnl.gov/main/publications/external/technical_reports/PNNL-13320.pdf.

Delegard CH, AJ Schmidt, RL Sell, SI Sinkov, SA Bryan, SR Gano, and BM Thornton. 2004. *Final Report – Gas Generation Testing of Uranium Metal in Simulated K Basin Sludge and in Grouted Sludge Waste Forms*. PNNL-14811, Pacific Northwest National Laboratory, Richland, Washington. Available at: http://www.pnl.gov/main/publications/external/technical_reports/PNNL-14811.pdf.

Delegard CH and AJ Schmidt. 2008. *Uranium Metal Reaction Behavior in Water, Sludge, and Grout Matrices*. PNNL-17815, Pacific Northwest National Laboratory, Richland, Washington. Available at: http://www.pnl.gov/main/publications/external/technical_reports/PNNL-17815.pdf.

Delegard CH, SI Sinkov, AJ Schmidt, and JW Chenault. 2008. *Uranium Metal Analysis via Selective Dissolution*. PNNL-17800, Pacific Northwest National Laboratory, Richland, Washington.

Draley JE and GC English. 1944. *Corrosion Research-Uranium and Alloys*. CT-1943, University of Chicago. Available at: <http://www.osti.gov/energycitations/servlets/purl/4357484-c3tJ7U/4357484.PDF>.

Ewart FT, JL Smith-Briggs, HP Thomason, and SJ Williams. 1992. “The Solubility of Actinides in a Cementitious Near-Field Environment.” *Waste Management* 12(2-3):241-252.

Fanning JC. 2000. “The Chemical Reduction of Nitrate in Aqueous Solution.” *Coordination Chemistry Reviews* 199:159-179.

Fonnesbeck JE, JR Krsul, and SG Johnson. 1998. “EBR-II Blanket Fuel Leaching Test Using Simulated J-13 Well Water.” *Proceedings of Third Topical Meeting on DOE Spent Nuclear Fuel and Fissile Materials, Vol. 2, September 1998*, American Nuclear Society, Charleston, South Carolina.

Ginder-Vogel M, CS Criddle, and S Fendorf. 2006. “Thermodynamic Constraints on the Oxidation of Biogenic UO₂ by Fe(III) (hydr)oxides.” *Environmental Science and Technology* 40:3544-3550.

Ginder-Vogel M and S Fendorf. 2008. “Biogeochemical Uranium Redox Transformations: Potential Oxidants of Uraninite.” Chapter 11 of *Developments in Earth & Environmental Sciences, Volume 7, Adsorption of Metals by Geomedia II: Variables, Mechanisms, and Model Applications*, MO Barnett and DB Kent, editors, Elsevier, Amsterdam, Netherlands. Available at: <http://elsevier.insidethecover.com/searchbook.jsp?isbn=9780444532121> – go to Chapter 11.

Godfrey IH, M Brogden, and S Curwen. 2004. *BNFL Historical Data on the Corrosion of Uranium in BFS/OPC Cement in Support of Treating Hanford KE and KW Basin Wastes Using Cementation*. NSTS (04) 4992, Issue 2, British Nuclear Fuels Limited, Inc., Richland, Washington.

Godfrey IH, EJ Butcher, and JL Parr. 2005. *Encapsulation of Hazardous Waste Materials*. European Patent EP1741109, U.S. Patent Application 10/599,897 (2007). Available at: <http://www.wipo.int/pctdb/en/wo.jsp?wo=2005101426> and <http://appft1.uspto.gov/netacgi/nph-Parser?Sect1=PTO2&Sect2=HITOFF&p=1&u=%2Fnetacgi%2FPTO%2Fsearchbool.html&r=1&f=G&l=50&co1=AND&d=PG01&s1=10%2F599897&OS=10/599897&RS=10/599897>.

Gorman-Lewis D, JB Fein, PC Burns, JES Szymanowski, and J Converse. 2008a. "Solubility Measurements of the Uranyl Oxide Hydrate Phases Metaschoepite, Compreignacite, Na-Compreignacite, Becquerelite, and Clarkeite." *Journal of Chemical Thermodynamics* 40:980-990.

Gorman-Lewis D, PC Burns, and JB Fein. 2008b. "Review of Uranyl Mineral Solubility Measurements." *Journal of Chemical Thermodynamics* 40:335-352.

Gray WJ and RE Einziger. 1998. *Initial Results from Dissolution Rate Testing of N Reactor Spent Fuel Over a Range of Potential Geologic Repository Aqueous Condition*. DOE/SNF/REP-022, PNNL-11894, Pacific Northwest National Laboratory, Richland, Washington.

Greenwood H. 1942. *Interim Report on Mechanical and Corrosion Tests on 'X' Metal*. BR-78, Imperial Chemical Industries Limited, United Kingdom.

Greenwood NN and A Earnshaw. 1984. *Chemistry of the Elements*. Pergamon Press, Oxford, United Kingdom.

Gresky AT. 1952. *Recovery of Nitrogen Oxides and Rare Gas Fission Products from the Dissolution of Irradiated Uranium*, ORNL-1208, Oak Ridge National Laboratory, Oak Ridge, Tennessee. Available at: <http://www.osti.gov/energycitations/servlets/purl/4116841-PInUGn/4116841.PDF>.

Hansen TC. 1986. "Physical Structure of Hardened Cement Paste. A Classical Approach." *Materials and Structures* 19(6):423-436.

Hanson CE and MC Brouns. 1980. *Fuel Encapsulation Program Design Analysis Report*. UNI-1511, UNC Nuclear Industries, Richland, Washington.

Hayon E and M Moreau. 1965. "Reaction Mechanisms Leading to the Formation of Molecular Hydrogen in the Radiation Chemistry of Water." *Journal of Physical Chemistry* 69(12):4058-4062.

Hilton BA. 2000. *Review of Oxidation Rates of DOE Spent Nuclear Fuel Part 1: Metallic Fuel*. ANL-00/24, Argonne National Laboratory, Idaho Falls, Idaho. Available at: http://www.osti.gov/bridge/product.biblio.jsp?osti_id=775264.

Hinton ER Jr, HL Tucker, and WL Asbury. 1986. "Investigation of an Anion Exchange Resin for Cleanup of a Coolant Used to Machine Nuclear Materials." *Analytical Letters* 19(21-22):2121-2129.

IAEA. 1998. *Durability of Spent Nuclear Fuels and Facility Components in Wet Storage*. IAEA-TECDOC-1012, International Atomic Energy Agency, Vienna. Available at: http://www-pub.iaea.org/MTCD/publications/PDF/te_1012_prn.pdf.

Jambor JL and JE Dutrizac. 1998. "Occurrence and Constitution of Natural and Synthetic Ferrihydrite, a Widespread Iron Oxyhydroxide." *Chemical Reviews* 98:2549-2585.

Johnson AB Jr and SP Burke. 1995. *K Basin Corrosion Program Report*. WHC-EP-0877, Westinghouse Hanford Company, Richland, Washington.

Johnson AB, RG Ballinger, and KA Simpson. 1994. *Kinetic and Thermodynamic Bases to Resolve Issues Regarding Conditioning of Uranium Metal Fuels*. PNL-SA-24458, Pacific Northwest Laboratory, Richland, Washington.

Keeling RF, SC Piper, AF Bollenbacher, and JS Walker. 2008. "Atmospheric CO₂ Records from Sites in the SIO Air Sampling Network." In *Trends: A Compendium of Data on Global Change. Carbon Dioxide Information Analysis Center*, Oak Ridge National Laboratory, Oak Ridge, Tennessee. Available at: <http://cdiac.ornl.gov/trends/co2/sio-ljo.html>.

Kumar M and S Chakraborty. 2006. "Chemical Denitrification of Water by Zero-Valent Magnesium Powder." *Journal of Hazardous Materials* 135(1-3):112-121.

Laborda F, E Bolea, MT Baranguan, and JR Castillo. 2002. "Hydride Generation in Analytical Chemistry and Nascent Hydrogen: When Is it Going to be Over?" *Spectrochimica Acta Part B* 57:797-802.

Lacher JR, JD Salzmman, and JD Park. 1961. "Dissolving Uranium in Nitric Acid." *Industrial and Engineering Chemistry* 53(4):282-284.

Makenas BJ, TL Welsh, RB Baker, DR Hansen, and GR Golcar. 1996. *Analysis of Sludge from Hanford K East Basin Floor and Weasel Pit*. WHC-SP-1182 Rev. 0, Westinghouse Hanford Company, Richland, Washington.

Makenas BJ, TL Welsh, RB Baker, EW Hoppe, AJ Schmidt, J Abrefah, JM Tingey, PR Bredt, and GR Golcar. 1997. *Analysis of Sludge from Hanford K East Basin Canisters*. HNF-SP-1201 Rev. 0, Duke Engineering & Services Hanford, Inc., Richland, Washington.

Makenas BJ, TL Welsh, RB Baker, GR Golcar, PR Bredt, AJ Schmidt, and JM Tingey. 1998. *Analysis of Sludge from Hanford K West Basin Canisters*. HNF-1728 Rev. 0, Fluor Daniel Hanford, Richland, Washington.

Makenas BJ, TL Welsh, PR Bredt, GR Golcar, AJ Schmidt, KL Silvers, JM Tingey, AH Zacher, and RB Baker. 1999. *Analysis of Internal Sludge and Cladding Coatings from N-Reactor Fuel Stored in Hanford K Basins*. HNF-3589 Rev. 0, Fluor Daniel Hanford, Inc., Richland, Washington.

Marchesini FA, S Irusta, C Querini, and E Miró. 2008. "Spectroscopic and Catalytic Characterization of Pd-In and Pt-In Supported on Al₂O₃ and SiO₂, Active Catalysts for Nitrate Hydrogenation." *Applied Catalysts A: General* 348:60-70.

Meija J and A D'Ulivo. 2008. "Solution to Nascent Hydrogen Challenge." *Analytical and Bioanalytical Chemistry* 392:771-772.

Meinrath G. 1998. "Direct Spectroscopic Speciation of Schoepite-Aqueous Phase Equilibria." *Journal of Radioanalytical and Nuclear Chemistry* 232(1-2):179-188.

Meisel D, H Diamond, EP Horwitz, CD Jonah, MS Matheson, MC Sauer Jr, and JC Sullivan. 1991. *Radiation Chemistry of Synthetic Waste*. ANL-91/40, Argonne National Laboratory, Argonne, Illinois.

Mellinger GB, CH Delegard, MA Gerber, BN Naft, AJ Schmidt, and TL Walton. 2004. *Disposition Options for Hanford Site K-Basin Spent Nuclear Fuel Sludge*. PNNL-14729, Pacific Northwest National Laboratory, Richland, Washington. Available at:
http://www.pnl.gov/main/publications/external/technical_reports/PNNL-14729.pdf.

Mezyk SP and DM Bartels. 1997. "Temperature Dependence of Hydrogen Atom Reaction with Nitrate and Nitrite Species in Aqueous Solution." *Journal of Physical Chemistry A* 101:6233-6237.

Moore FW and DR Duncan. 2005. *K Basin Closure Project KW Sludge Containerization System, "Calculation to Determine Flocculent Concentrations in KW Containers."* KBC-27977, Rev. 0, Fluor Hanford, Richland, Washington.

Moore JD, RL Walser, and JJ Fritch. 1980. *Purex Technical Manual*, p. 5-7. RHO-MA-116, Rockwell Hanford Operations, Richland, Washington.

NOAA. 1976. *U.S. Standard Atmosphere, 1976*. NOAA-S/T 76-1562. Table 3, p. 3, and Table 15, p. 33. U.S. Government Printing Office, Washington, D.C.

Perkins KT. 1943. *Oxidation Rates of Tuballoy Metal*. CT-1008, University of Chicago, Chicago, IL. Figure 38, page 380, and citation 52, page 851, of WD Wilkinson. 1962. *Uranium Metallurgy*, Interscience Publishers, New York, NY.

Plys MG and AJ Schmidt. 2006. "Updated Evaluation of Uranium Metal Reaction Rates in Oxygen-Free Liquid Water." *Supporting Basis for SNF Project Sludge Technical Data Book*. SNF-7765 Rev. 3b, Fluor Hanford, Inc., Richland, Washington.

Poskrebyshev GA, V Shafirovich, and SV Lyman. 2004. "Hyponitrite Radical, a Stable Adduct of Nitric Oxide and Nitroxyl." *Journal of the American Chemical Society* 126(3):891-899.

Pourbaix, M. 1966. *Atlas of Electrochemical Equilibria in Aqueous Solutions*, p. 501. Pergamon Press, Oxford, United Kingdom.

Powers TC. 1958. "Structure and Physical Properties of Hardened Portland Cement Paste." *Journal of the American Ceramic Society* 41(1):1-6.

Price CC, WG Jackson, and A Pohland. 1948. "The Radiation-Induced Fluorescence and Fluorescence Spectra of Certain Quinoline Derivatives." *Journal of the American Chemical Society* 70(9):2983-2988.

Purolite. 2007. "Product Data Sheets for NRW37, NRW100, and NRW400." The Purolite Company, Bala Cynwyd, Pennsylvania. Available at:
http://www.purolite.com/library/products/pdf_files/productdata161.pdf (NRW37, mixed bed)
http://www.purolite.com/library/products/pdf_files/productdata49.pdf (NRW100, cation)
http://www.purolite.com/library/products/pdf_files/productdata44.pdf (NRW400, anion).

Ramachandran CE, BA Williams, JA van Bokhoven, and JT Miller. 2005. Observation of a Compensation Relation for *n*-hexane Adsorption in Zeolites with Different Structures: Implications for Catalytic Activity." *Journal of Catalysis* 233:100-108.

- Schmidt AJ. 2006. *Spent Nuclear Fuel Project Databook, Sludge*. HNF-SD-SNF-TI-015, Vol. 2, Rev. 13A, Fluor Hanford, Inc., Richland, Washington.
- Schmidt AJ, KL Silvers, PR Bredt, CH Delegard, EW Hoppe, JM Tingey, AH Zacher, TL Welsh, and RB Baker. 1999. *Supplementary Information on K-Basin Sludges*. HNF-2367, Rev. 0, Fluor Daniel Hanford, Richland, Washington.
- Schmidt AJ, CH Delegard, SA Bryan, MR Elmore, RL Sell, KL Silvers, SR Gano, and BM Thornton. 2003. *Gas Generation from K East Basin Sludges and Irradiated Metallic Uranium Fuel Particles—Series III Testing*. PNNL-14346, Pacific Northwest National Laboratory, Richland, Washington. Available at: http://www.pnl.gov/main/publications/external/technical_reports/PNNL-14346.pdf.
- Senko JM, JD Istok, JM Suflita, and LR Krumholz. 2002. “In-situ Evidence for Uranium Immobilization and Remobilization.” *Environmental Science and Technology* 36:1491-1496.
- Senko JM, Y Mohamed, TA Dewers, and LR Krumholz. 2005. “Role for Fe(III) Minerals in Nitrate-Dependent Microbial U(IV) Oxidation.” *Environmental Science and Technology* 39:2529-2536.
- Serne RJ, BN Bjornstad, HT Schaef, BA Williams, DC Lanigan, DG Horton, RE Clayton, AV Mitroshkov, VL Legore, MJ O'Hara, CF Brown, KE Parker, IV Kutnyakov, JN Serne, GV Last, SC Smith, CW Lindenmeier, JM Zachara, and D Burke. 2002. *Characterization of Vadose Zone Sediment: Uncontaminated RCRA Borehole Core Samples and Composite Samples*. PNNL-13757-1, Pacific Northwest National Laboratory, Richland, Washington. Available at: http://www.pnl.gov/main/publications/external/technical_reports/pnnl-13757-1.pdf.
- Simpson DR. 1980. *Desiccant Materials Screening for Backfill in a Salt Repository*. ONWI-214, Lehigh University, Bethlehem, Pennsylvania, and Battelle Office of Nuclear Waste Isolation, Columbus, Ohio. Available at: <http://www.osti.gov/energycitations/servlets/purl/6444184-j9DOsk/6444184.PDF>.
- Sinkov SI, CH Delegard, and AJ Schmidt. 2008. *Preparation and Characterization of Uranium Oxides in Support of the Sludge Treatment Project*. PNNL-17678, Pacific Northwest National Laboratory, Richland, Washington. Available at: http://www.pnl.gov/main/publications/external/technical_reports/PNNL-17678.pdf.
- Speight JG. 2005. *Lange's Handbook of Chemistry*, 16th Edition, Table 2.91, McGraw-Hill, New York, New York.
- Sprague TP, JM Googin, and LR Phillips. 1964. *Chemical Coolants for Machining Uranium in the Presence of Trace Amounts of Chloride*. Y-1475, Y-12 Plant, Oak Ridge, Tennessee. Available at: <http://www.osti.gov/bridge/servlets/purl/4656648-ujbD6m/4656648.PDF>.
- Stedman G. 1979. “Reaction Mechanisms of Inorganic Nitrogen Compounds.” *Advances in Inorganic Chemistry and Radiochemistry*, Vol. 22, p. 122, HJ Emeléus, and AG Sharpe, editors. Academic Press, New York, New York.
- Swanson JL. 1958. “The Zirflex Process.” *Proceedings of the Second International Conference on the Peaceful Uses of Atomic Energy*, A/CONF.15/P/2429. Geneva, Switzerland.

Thompson A, OA Chadwick, DG Rancourt, and J Chorover. 2006. "Iron Oxide Crystallinity Increases During Soil Redox Oscillations." *Geochimica et Cosmochimica Acta* 70:1710-1727. Accessible at: http://ag.arizona.edu/swes/chorover_lab/pdf_papers/Thompson_etal_2006.pdf.

Totemeier TC, RG Pahl, SL Hayes, and SM Frank. 1998. "Characterization of Corroded Metallic Uranium Fuel Plates." *Journal of Nuclear Materials* 256:87-95.

Trimble DJ. 1996. "Corrosion Inhibitor in K West Basin Fuel Storage Containers." Appendix E in *Data Analysis of Gas and Liquid from K West Basin Fuel Canisters; 1995 Samples*. WHC-SD-SNF-ANAL-008 Rev. 0, Westinghouse Hanford Company, Richland, Washington.

Waber JT. 1956. *A Review of the Corrosion Behavior of Uranium*. LA-2035, Los Alamos Scientific Laboratory, Los Alamos, New Mexico. Available at: <http://library.lanl.gov/cgi-bin/getfile?00320781.pdf>.

Wagman DD, WH Evans, VB Parker, RH Schumm, I Halow, SM Bailey, KL Churney, and RL Nuttall. 1982. "The NBS Tables of Chemical Thermodynamic Properties—Selected Values for Inorganic and C₁ and C₂ Organic Substances in SI Units." *Journal of Physical and Chemical Reference Data* 11 (Supp. 2). Available at: <http://www.nist.gov/srd/PDFfiles/jpcrdS2Vol11.pdf>.

Wetters JH and KL Uglum. 1970. "Direct Spectrophotometric Simultaneous Determination of Nitrite and Nitrate in the Ultraviolet." *Analytical Chemistry* 42(3):335-340.

Wiberg N. 2001. *Holleman-Wiberg Inorganic Chemistry*, 1st English edition. Academic Press, San Diego, California.

Wood DH, SA Snowden, HJ Howe, Jr., LL Thomas, DW Moon, HR Gregg, and PE Miller. 1994. "Regarding the Chemistry of Metallic Uranium Stored in Steel Drums." *Journal of Nuclear Materials* 209:113-115.

Zachara JM, SC Smith, C Liu, JP McKinley, RJ Serne, and PL Gassman. 2002. "Sorption of Cs⁺ to Micaceous Subsurface Sediments from the Hanford Site, USA." *Geochimica et Cosmochimica Acta* 66(2):193-211.

Appendix A

XRD Analyses of Hanford (ALE) Soil and Ferrihydrite

Appendix A

XRD Analyses of Hanford (ALE) Soil and Ferrihydrite

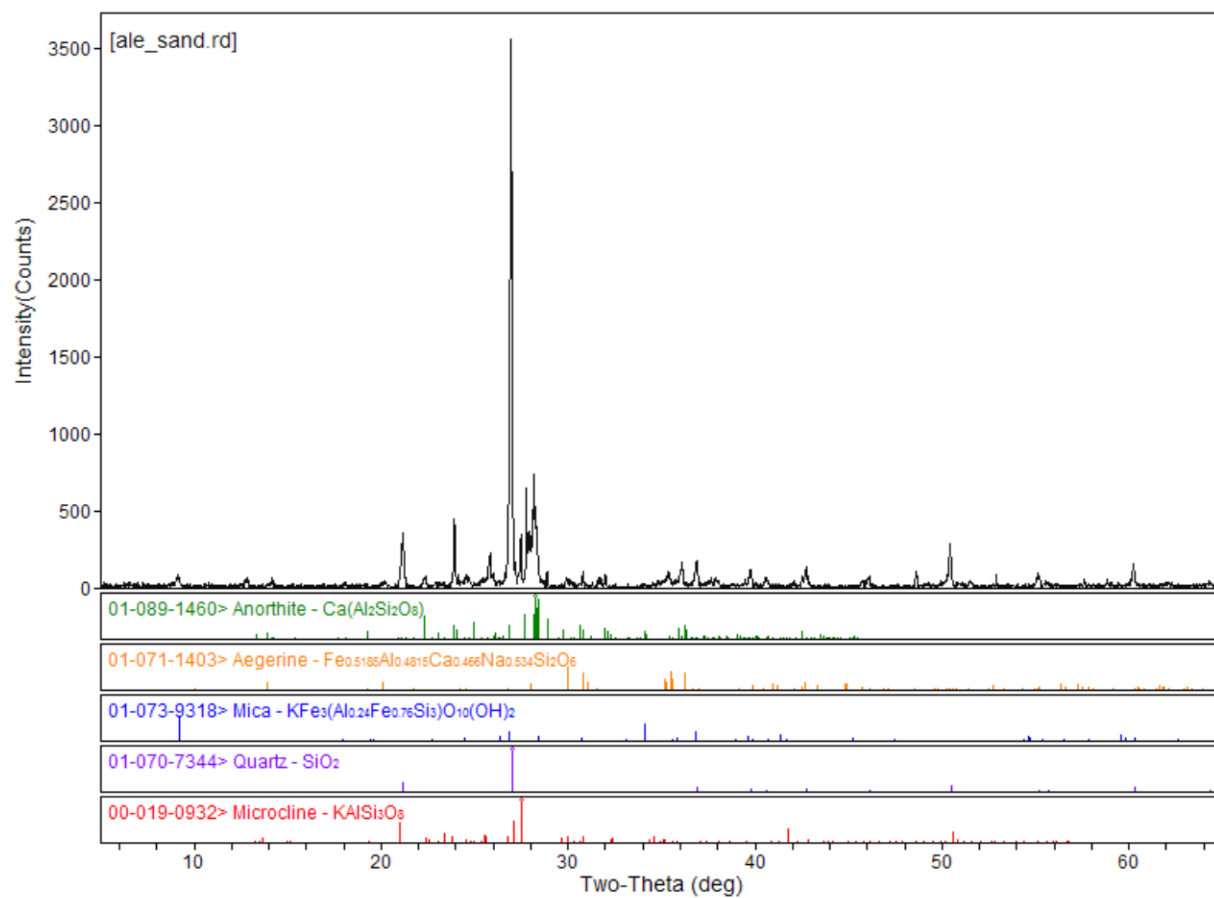


Figure A.1. XRD Pattern and Peak Assignment for Hanford (ALE) Soil

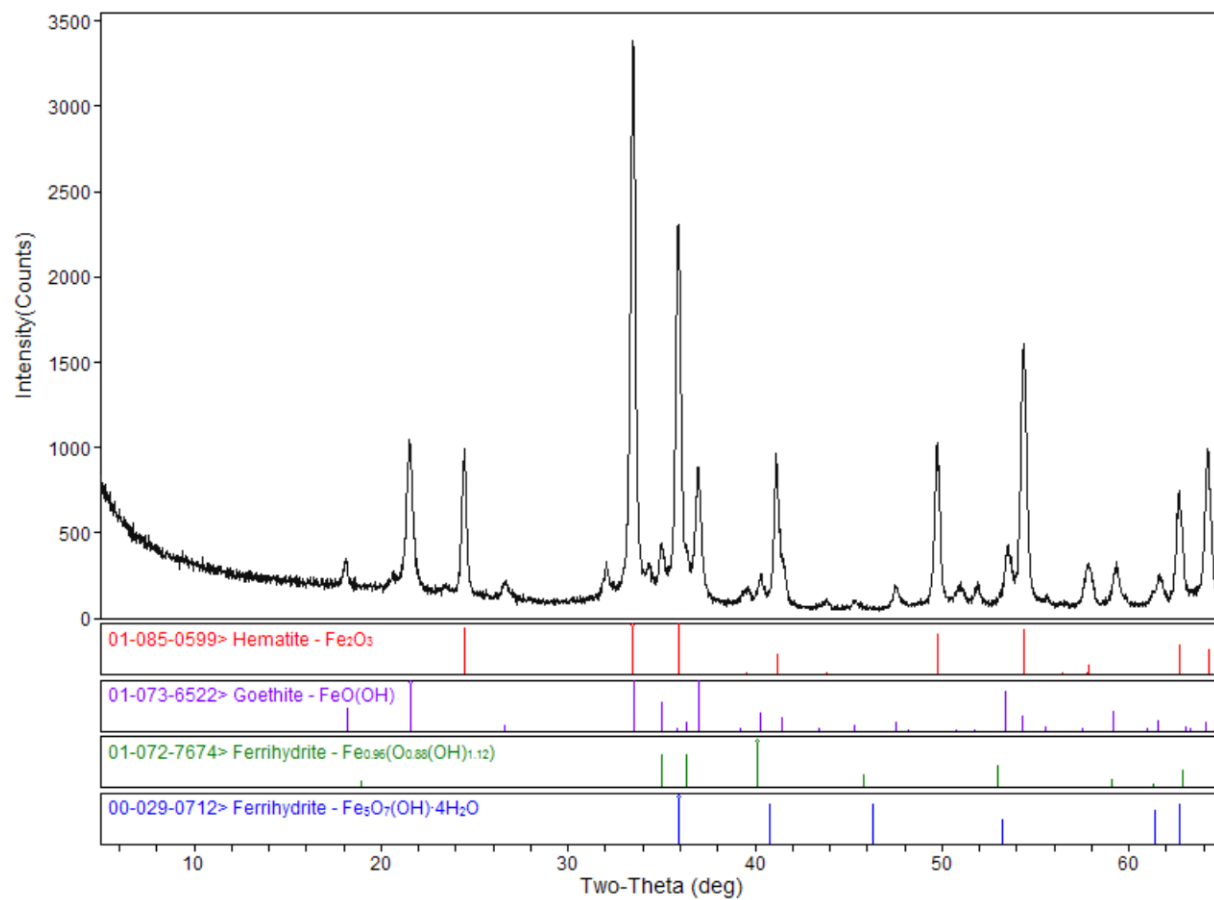


Figure A.2. XRD Pattern and Peak Assignment for Ferrihydrate Material Used in Testing

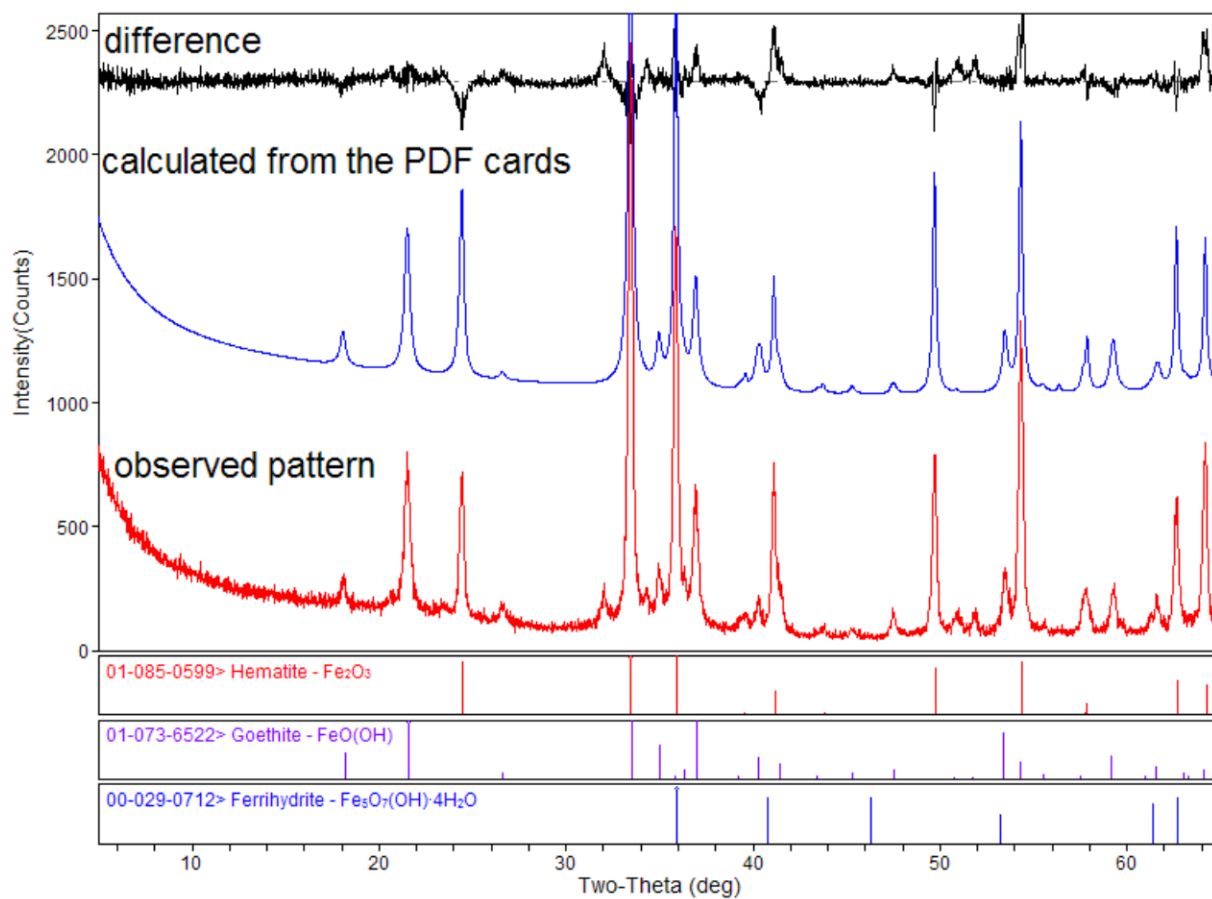


Figure A.3. Rietveld Fitting of XRD Pattern and Peak Assignment for Ferrihydrate Used in Testing

The XRD analyses presented in figures A.1, A.2, and A.3 were performed on pressed powder samples in depression mounts using copper $K\alpha$ radiation. Rietveld analysis of the XRD pattern in Figure A.3 shows that hematite comprises 64.3% of the material in the ferrihydrate sample, that goethite comprises ~35.7%, and that ferrihydrate accounts for none of the pattern.

Appendix B

Initial and Final Gas Volumes and Gas Compositions for Test Series 3, 4, 5, 6, and 7

Appendix B

Initial and Final Gas Volumes and Gas Compositions for Test Series 3, 4, 5, 6, and 7

Test	[NaNO ₃]/ [NaNO ₂], M	Other Materials	Gas Vol., mL		Gas Concentrations, mole percent									
			Initial	Final	Ar	CO ₂	N ₂	O ₂	H ₂	CH ₄	C ₂ H _x	N ₂ O	NO _x ^(a)	Ne
Air ^(b)	–	–	–	–	0.934	0.0385	78.079	20.946	0.00005	0.0002	–	0.00003	–	0.001818
<i>Test Series 3</i>														
1	0.0/0.0	None	13.15	20.25	0.70	0.172	56.8	9.4	32.9	0.019	0.004	<0.005	<0.005	NA
2	0.0/0.0	0.2 g Nochar/g solution	11.20	17.45	0.78	0.231	63.5	8.2	27.2	0.017	<0.001	<0.005	<0.005	NA
3	0.0/0.0	0.2 g Nochar/g solution	11.00	17.10	0.76	0.241	62.0	6.4	30.7	0.019	0.005	<0.005	<0.005	NA
4	0.0/0.0	0.5 g Nochar/g solution	9.60	13.65	0.83	0.086	68.0	8.7	22.3	0.016	0.004	<0.005	<0.005	NA
5 ^(c)	0.0/0.0	0.5 g Nochar/g solution	9.30	11.80	0.83	0.136	69.1	8.60	21.3	0.014	<0.001	<0.005	<0.005	NA
5	Total observed pressure of 113 Torr should have been 70 Torr. Thus, 43 Torr air in-leakage occurred.				0.87	0.099	72.5	13.3	13.2	0.009	<0.001	<0.005	<0.005	NA
6	0.0/0.0	1.0 g Nochar/g solution	8.35	11.90	0.77	0.423	64.3	4.04	30.5	0.020	<0.001	<0.005	<0.005	NA
7	0.1/0.0	None	13.00	14.80	0.90	0.023	74.0	11.1	14.0	0.015	<0.001	<0.005	<0.005	NA
8 ^(c)	0.0/1.0	None	13.05	10.50	1.01	0.053	86.8	12.2	0.011	0.002	<0.001	<0.005	<0.005	NA
8	Total observed pressure of 155 Torr should have been 70 Torr. Thus, 85 Torr air in-leakage occurred.				0.97	0.045	82.0	17.0	0.005	0.001	<0.001	<0.005	<0.005	NA
9	0.0/0.1	None	13.20	11.70	0.98	0.026	83.5	14.1	1.37	0.004	<0.001	<0.005	<0.005	NA
10	0.1/0.0	0.2 g Nochar/g solution	12.20	12.25	0.99	0.355	83.1	7.2	8.3	0.016	<0.001	<0.005	0.007	NA
11	0.0/1.0	0.2 g Nochar/g solution	Test not performed.											
12	0.0/0.1	0.2 g Nochar/g solution	10.90	18.00	0.51	0.650	95.2	1.97	0.009	0.026	0.045	1.64	0.80	NA
<i>Test Series 4</i>														
1	0.0/0.0	None	9.20	13.90	0.61	0.239	47.9	2.48	48.7	0.044	0.005	0.009	<0.005	NA
2	0.2/0.0	None	8.25	8.75	0.91	0.039	75.6	10.4	13.0	0.018	<0.001	0.033	<0.005	NA
3	0.5/0.0	None	8.80	7.65	1.04	0.016	86.5	8.6	3.69	0.019	0.004	0.158	<0.005	NA
4	1.0/0.0	None	9.60	7.90	1.05	0.006	90.6	8.1	0.127	0.002	<0.001	0.100	<0.005	NA
5	2.0/0.0	None	9.45	7.90	1.06	0.022	91.9	6.9	0.002	0.002	<0.001	0.092	<0.005	NA
6	0.0/0.2	None	8.60	7.15	1.08	0.032	91.3	7.0	0.005	0.002	<0.001	0.51	<0.005	NA
7	0.0/0.5	None	8.90	7.40	1.06	0.048	90.5	7.5	0.002	0.002	<0.001	0.84	<0.005	NA
8	0.0/0.75	None	8.50	7.05	1.11	<0.005	95.9	1.25	0.004	0.002	0.009	1.67	<0.005	NA
9	0.0/1.0	None	8.20	6.60	1.02	0.080	87.5	10.9	0.003	0.002	<0.001	0.48	0.03	NA
10	0.5/0.0	UO ₂	7.60	5.55	1.09	<0.005	96.2	1.99	0.444	0.004	<0.001	0.298	0.01	NA
11	0.0/0.5	UO ₂	7.60	5.95	1.08	<0.005	95.4	1.59	0.85	0.004	<0.001	1.10	0.01	NA
12	0.0/0.0	0.07 M Na ₂ HPO ₄	8.25	18.90	0.368	<0.005	28.4	3.45	67.7	0.045	0.005	0.032	<0.005	NA

PNNL-19135

Test	[NaNO ₃]/ [NaNO ₂], M	Other Materials	Gas Vol., mL		Gas Concentrations, mole percent									
			Initial	Final	Ar	CO ₂	N ₂	O ₂	H ₂	CH ₄	C ₂ H _x	N ₂ O	NO _x ^(a)	Ne
<i>Test Series 5</i>														
1	0.0/0.0	None	8.45	11.45	0.594	0.18	48.2	2.97	48	0.049	<0.001	<0.005	0.005	NA
2	0.0/0.2	None	9.70	8.80	0.98	0.236	82.2	16.6	0.021	<0.001	<0.001	<0.005	0.004	NA
3	0.0/0.5	None	10.15	9.05	1.01	0.219	84.3	14.4	0.004	0.001	0.005	0.028	0.01	NA
4	0.0/0.75	None	10.10	8.95	Sample lost; no assay.									
5	0.5/0.0	None	9.60	7.95	1.00	0.037	84.2	14.0	0.75	0.013	<0.001	0.021	<0.005	NA
6	1.0/0.0	None	9.75	8.20	0.99	0.055	82.5	16.4	0.017	0.003	<0.001	0.064	0.005	NA
7	0.0/0.5	UO ₂	8.70	6.85	1.07	0.076	95.4	0.372	1.03	0.003	0.004	1.8	0.208	NA
8	0.5/0.0	UO ₂	8.85	7.40	1.01	0.67	85.7	7.9	0.92	0.007	<0.001	3.68	0.145	NA
9	0.0/0.5	0.01 g Nochar	10.00	8.65	0.96	0.015	80.2	18.6	0.002	0.002	<0.001	0.172	<0.005	NA
10	0.0/0.5	0.0087 g Optimer 7194 Plus	10.30	8.90	1.02	0.427	86.1	12.4	<0.001	0.001	0.005	<0.005	0.01	NA
11	0.0/0.5	3.264 mL sim. sludge	8.39	7.79	0.96	0.67	82.9	0.023	0.044	0.004	0.012	5.4	10	NA
12	0.5/0.0	3.264 mL sim. sludge	8.54	6.24	1.10	2.3	93.4	2.64	0.085	0.027	<0.001	0.48	0.047	NA
<i>Test Series 6</i>														
1	0.0/0.0	None	12.73	16.83	0.87	0.074	57.6	14.8	6.8	0.005	<0.001	0.032	<0.005	20.0
2	0.5/0.0	None	13.91	16.16	0.86	0.047	52.8	14.9	0.061	0.004	<0.001	0.060	<0.005	31.4
3	0.0/0.5	None	15.00	17.55	0.82	0.052	51.0	17.0	0.001	0.0005	<0.001	0.057	<0.005	31.1
4	0.0/0.0	~0.5 mL KE Floc Comp	12.94	19.49	0.86	0.083	57.4	16.8	2.92	0.003	<0.001	0.021	<0.005	21.9
5	0.5/0.0	~1.2 mL KE Floc Comp	15.14	18.84	0.85	0.067	56.5	17.6	0.033	0.001	<0.001	0.047	<0.005	25.0
6	0.0/0.5	~1.5 mL KE Floc Comp	12.38	16.08	0.89	0.077	60.8	18.1	0.004	0.0005	<0.001	0.066	<0.005	20.2
7	0.0/0.0	~2.0 mL KC-2/3 Comp	10.04	13.04	0.92	0.099	61.2	17.2	0.0025	0.001	<0.001	0.016	<0.005	20.7
8	0.5/0.0	~1.8 mL KC-2/3 Comp	11.20	14.10	0.87	0.020	64.2	18.1	0.013	0.001	<0.001	0.127	<0.005	16.8
9	0.0/0.5	~1.8 mL KC-2/3 Comp	11.81	13.01	0.98	0.094	68.5	6.0	0.052	0.001	<0.001	0.035	<0.005	24.4
<i>Test Series 7</i>														
1	0.0/0.0	None	20.45	31.45	0.71	0.086	58.4	13.9	27	0.0135	<0.001	0.004	<0.001	NA
2	0.0/0.0	0.05 M NaCl	20.68	33.28	0.66	0.035	53.6	12.4	33.3	0.0165	<0.001	0.005	<0.001	NA
3	0.0/0.0	2 mL MS ^(d) ; pH 6.9	19.50	30.10	0.67	0.227	54.5	12.2	32.45	0.0185	0.002	0.0065	<0.001	NA
4	0.0/0.0	2 mL MS; pH 5.1	19.00	23.20	0.82	0.329	68.5	16.3	14.05	0.0105	0.004	0.009	<0.001	NA
5	0.0/0.0	2 mL MS; pH 4.3	19.50	20.50	0.87	0.158	71.9	17.3	9.8	0.0075	0.0025	0.0085	<0.001	NA
6	0.0/0.0	0.6 mM UO ₂ Cl ₂	21.82	23.12	Gas not analyzed.									
<p>(a) NO_x analyzed as NO in Series 5.</p> <p>(b) Air composition from NOAA (1976) was adjusted for current atmospheric CO₂ concentration (Keeling et al. 2008) and renormalized.</p> <p>(c) Gas compositions in Tests 5 and 8 of Series 3 were altered by air in-leakage that occurred during sample introduction to the mass spectrometer. The as-analyzed gas compositions were adjusted by the quantity of air in-leakage that is indicated by the difference between the observed sample pressure and the 70-Torr sample pressure that should have been observed. The amount of air contribution was deducted based on the contribution of leaked air to the total pressure and the nominal air composition (e.g., air is 20.946 mole percent O₂).</p> <p>(d) MS is settled metaschoepite aqueous slurry.</p>														



Pacific Northwest
NATIONAL LABORATORY

*Proudly Operated by **Battelle** Since 1965*

902 Battelle Boulevard
P.O. Box 999
Richland, WA 99352
1-888-375-PNNL (7665)

www.pnl.gov



U.S. DEPARTMENT OF
ENERGY